



Slim-Floor Beams

Preparation of Application rules in view of improved safety, functionality and LCA

(SlimAPP)

A large, abstract graphic at the bottom of the page features blue and white wavy lines that resemble water or energy flow. In the center, there is a faint watermark-like image of a globe with a grid pattern.

EUR 30845 EN

Slim-Floor Beams Preparation of Application rules in view of improved safety, functionality and LCA (SlimAPP)

European Commission

Directorate-General for Research and Innovation

Directorate – Clean Planet

Unit C.3 — Low Emission Future Industries

Contact Andrea Gentili

E-mail RTD-STEEL-COAL@ec.europa.eu

RTD-PUBLICATIONS@ec.europa.eu

European Commission

B-1049 Brussels

Manuscript completed in 2020.

This document has been prepared for the European Commission however it reflects the views only of the authors, and the Commission cannot be held responsible for any use which may be made of the information contained therein.

More information on the European Union is available on the internet (<http://europa.eu>).

Luxembourg: Publications Office of the European Union, 2020

PDF

ISBN 978-92-76-42012-5

ISSN 1831-9424

doi: 10.2777/23964

KI-NA-30-845-EN-N

© European Union, 2021.

Reuse is authorised provided the source is acknowledged. The reuse policy of European Commission documents is regulated by Decision 2011/833/EU (OJ L 330, 14.12.2011, p. 39).

For any use or reproduction of photos or other material that is not under the EU copyright, permission must be sought directly from the copyright holders.

All pictures, figures and graphs © University of Stuttgart, RFSR-CT-2015-00020 **SlimAPP**

Research Fund for Coal and Steel

Slim-Floor Beams Preparation of Application rules in view of improved safety, functionality and LCA (SlimAPP)

University of Stuttgart
Pfaffenwaldring 7, 70569 Stuttgart, Germany

The Steel Construction Institute
Silwood Park, Ascot, Berks, SL5 7QN, United Kingdom

ArcelorMittal Belval and Differdange S.A.
L-4008 Esch-Belval and L-4503 Differdange, Luxembourg

University of Bradford
Richmond Road, BD7 1DP Bradford, United Kingdom

University of Trento
Via Calepina 14, 38122 Trento, Italy

LINDAB SA
Route d Ettelbruck, 9230, Diekirch, Luxembourg

Grant Agreement RFSR-CT-2015-00020

1 July 2015 to 31 December 2018

Final Report

TABLE OF CONTENTS

TABLE OF CONTENTS	3
FINAL SUMMARY	7
PUBLICATIONS	10
SCIENTIFIC AND TECHNICAL DESCRIPTION OF RESULTS	13
1 IDENTIFICATION OF APPLICATION RANGE, DEFINITION OF “PILOT PROJECTS”	13
1.1 GENERAL	13
1.2 NEW DEVELOPMENTS IN LONG SPAN SLIM-FLOOR SYSTEMS	13
1.2.1 <i>Limiting criteria for long span slim-floor systems</i>	13
1.2.2 <i>Strategies for long span slim-floor beams</i>	14
1.2.3 <i>New forms of long span slim-floor beams</i>	15
1.2.4 <i>Span capabilities of the long span options</i>	17
1.3 COMPILE THE NEEDS OF AUTHORITIES, DESIGNERS AND THE INDUSTRY	17
1.3.1 <i>Critique of Benefits of Slim-floor Construction</i>	17
1.3.2 <i>Applications</i>	18
1.4 IDENTIFICATION AND ANALYSIS OF “PILOT PROJECTS”	20
1.4.1 <i>Selected case studies and design assumptions</i>	20
1.5 CONCLUSIONS	22
2 PUSH-OUT AND SHEAR BEAM TESTS WITH INNOVATIVE SHEAR CONNECTORS IN SLIM-FLOOR BEAMS	23
2.1 GENERAL	23
2.2 PUSH-OUT TESTS FOR EVALUATION OF CHARACTERISTIC BEHAVIOUR OF CONCRETE DOWELS	23
2.2.1 <i>General</i>	23
2.2.2 <i>Methodology</i>	23
2.2.3 <i>Results & tendencies</i>	24
2.2.4 <i>Numerical investigations</i>	25
2.2.5 <i>Conclusions</i>	26
2.3 SHEAR BEAM TESTS FOR EVALUATION OF CHARACTERISTIC BEHAVIOUR	27
2.3.1 <i>Introduction</i>	27
2.3.2 <i>Test specimens</i>	27
2.3.3 <i>Test set-up and instrumentation</i>	27
2.3.4 <i>Load-deflection response</i>	28
2.3.5 <i>Concrete cracking</i>	29
2.3.6 <i>Measured strains</i>	30
2.3.7 <i>Conclusions</i>	31
2.4 NUMERICAL INVESTIGATIONS	31
2.4.1 <i>Introduction</i>	31
2.4.2 <i>Brief description of FE model</i>	32
2.4.3 <i>Material Properties</i>	32
2.4.4 <i>FE model validation</i>	33

2.4.5	<i>Parametric study</i>	34
2.4.6	<i>Load-bearing behaviour</i>	37
2.4.7	<i>Conclusions</i>	38
2.5	INFLUENCE OF THE SHEAR CONNECTORS ON THE LOAD-BEARING BEHAVIOUR OF SLIM-FLOORS	38
2.5.1	<i>Comparison between push-out and shear beam tests</i>	38
2.5.2	<i>Influence of flexibility of shear connectors</i>	39
2.6	CONCLUSIONS.....	40
3	FLEXURAL BEHAVIOUR OF SLIM-FLOOR BEAMS WITH INNOVATIVE SHEAR CONNECTORS.	41
3.1	GENERAL	41
3.2	EXPERIMENTAL INVESTIGATIONS ON FLEXURAL BEAMS.....	41
3.2.1	<i>Introduction</i>	41
3.2.2	<i>Test specimens</i>	41
3.2.3	<i>Test set-up and instrumentation</i>	42
3.2.4	<i>Load-deflection response</i>	42
3.2.5	<i>End-slip</i>	44
3.2.6	<i>Measured strains</i>	45
3.2.7	<i>Shear connectors</i>	46
3.2.8	<i>Degree of shear connection</i>	46
3.2.9	<i>Conclusions</i>	46
3.3	NUMERICAL INVESTIGATIONS ON FLEXURAL BEAMS	47
3.3.1	<i>Introduction</i>	47
3.3.2	<i>Modelling</i>	47
3.3.3	<i>Validation</i>	48
3.3.4	<i>Analysis of the load-bearing behaviour</i>	49
3.3.5	<i>Parameter studies</i>	51
3.4	CONCLUSION.....	51
4	DEFLECTION AND VIBRATION BEHAVIOUR OF SLIM-FLOOR SYSTEMS WITH INNOVATIVE SHEAR CONNECTORS.	53
4.1	GENERAL	53
4.2	DEFLECTION BEHAVIOUR.....	53
4.2.1	<i>Introduction</i>	53
4.2.2	<i>Full-scale long-term beam tests</i>	53
4.2.3	<i>Beams failure tests</i>	58
4.3	VIBRATION TESTS	59
4.4	CONCLUSIONS.....	61
5	LIFE CYCLE ASSESSMENT AND DEVELOPMENT OF OPTIMIZED SLIM-FLOOR SOLUTIONS IN VIEW OF LCA ASPECTS	63
5.1	GENERAL	63
5.2	LCA - VALIDATION OF THE METHODOLOGY.....	64
5.3	LCA - ADAPTATION OF AMECO SOFTWARE.....	65
5.4	LIFE CYCLE ANALYSIS OF SLIM-FLOOR SYSTEMS, EXAMPLES OF APPLICATION – COMPARISON.....	66
5.4.1	<i>Introduction</i>	66

5.4.2	<i>LCA - analysis</i>	66
5.4.3	<i>Conclusion of the LCA - analysis</i>	74
5.4.4	<i>LCP - Life cycle performance analysis of slim-floors systems</i>	74
6	DEVELOPMENT OF APPLICATION RULES IN EUROCODES	79
6.1	GENERAL	79
6.2	RULES FOR THE ULTIMATE LIMIT STATE (ULS)	79
6.2.1	<i>Construction stage</i>	79
6.2.2	<i>Normal stage</i>	83
6.3	RULES FOR THE SERVICEABILITY LIMIT STATE (SLS)	88
6.3.1	<i>Serviceability limit state – construction stage</i>	89
6.3.2	<i>Serviceability limit state – in-service stage</i>	89
6.4	ADDITIONAL RULES FOR WEB OPENINGS IN SLIM-FLOOR BEAMS	90
6.4.1	<i>General</i>	90
6.4.2	<i>Design verifications</i>	90
6.4.3	<i>Section classification</i>	91
6.4.4	<i>Shear resistance at web opening positions</i>	91
6.4.5	<i>Bending resistance of beam with web openings</i>	91
6.4.6	<i>Resistance of the Tees in Vierendeel bending</i>	92
6.4.7	<i>Web buckling next to openings</i>	92
6.4.8	<i>Alternative method for Vierendeel bending (circular openings)</i>	94
7	DESIGN RECOMMENDATIONS FOR EC4 AND GUIDELINES FOR PRACTICE	95
7.1	RECOMMENDATIONS FOR EUROCODE 4	95
7.1.1	<i>Introduction</i>	95
7.1.2	<i>Ultimate Limit state</i>	95
7.1.3	<i>Serviceability limit state</i>	95
7.2	DESIGN RULES AND GUIDELINES FOR THE PRACTICE	95
7.3	WORKSHOP AND DISSEMINATION	95
8	SUMMARY & OUTLOOK	95
8.1	SUMMARY & CONCLUSIONS	95
8.2	OUTLOOK	95
8.3	ACKNOWLEDGEMENT	95
ABBREVIATIONS	95
LIST OF FIGURES	95
LIST OF TABLES	95
LIST OF REFERENCES	95

FINAL SUMMARY

I. Objectives of SlimAPP

"Slim-Floor Beams - Preparation of Application rules in view of improved safety, functionality and LCA (SlimAPP)" aimed to increase the competitiveness of steel in buildings by developing a holistic approach for slim-floor systems, considering all aspects of efficient design, in view of sustainable constructions. The shear connection between steel beam and concrete floor slab in normal conditions in particular, was accounted for. Focus was on application rules for slim-floor solutions which are currently not covered explicitly by Eurocode 4 in order to achieve improved behaviour in view of safety (ULS), functionality (SLS) and Lifecycle assessment.

III. Description of activities, discussion and conclusions

The interrelation between the work packages is given by Fig. I.

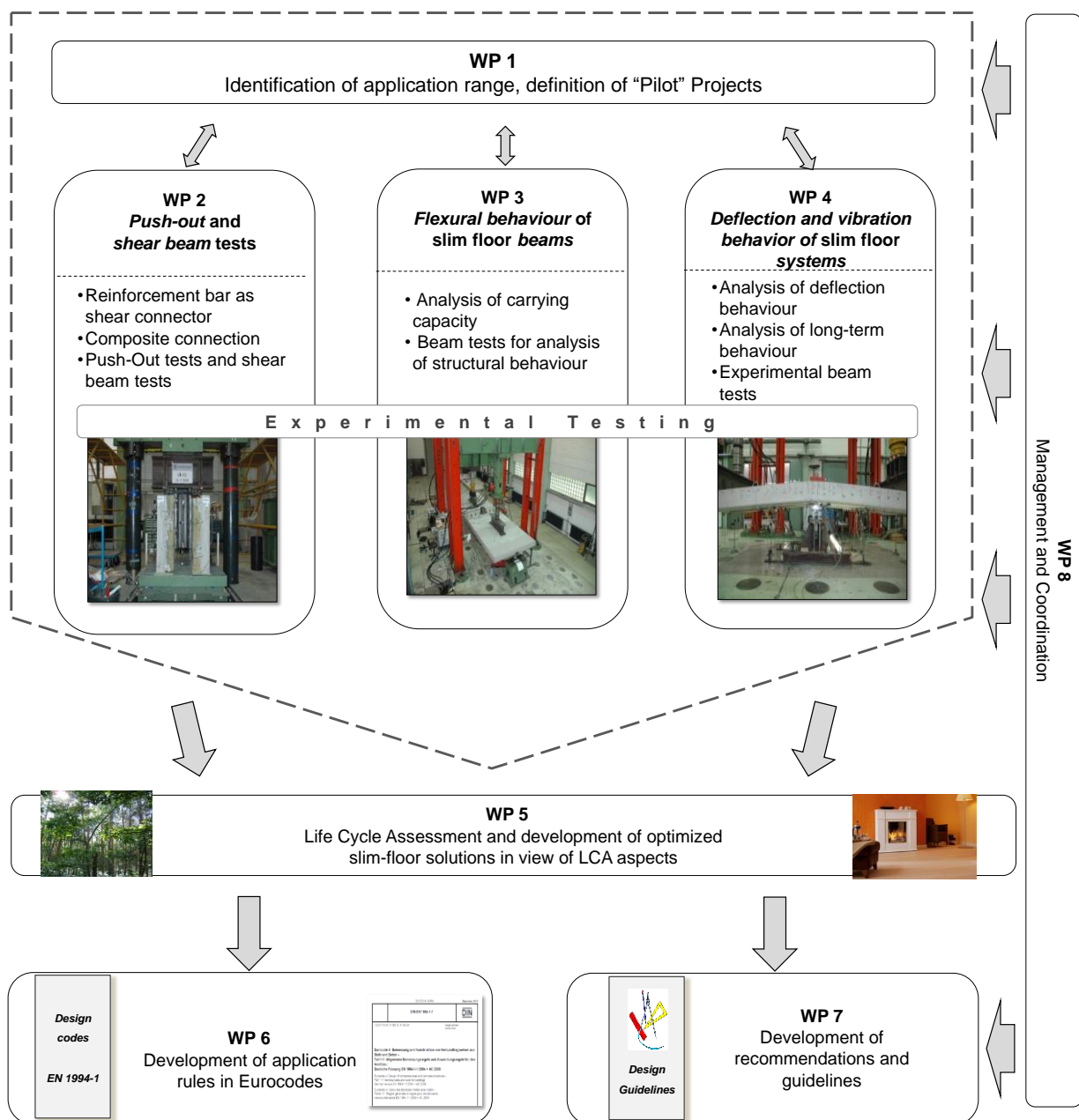


Fig. I: Interrelation of work-packages

Typical pilot projects were chosen to demonstrate the practical application of the research. Three cases have been defined in the scope of WP1, consisting of car parks (2 layouts) and residential and commercial buildings. These examples serve as the basis for the development of rules and recommendations and also for the LCA calculations conducted within the scope of WP5. The benefits of slim-floor construction as well as the application possibilities have been compiled to define the needs by authorities, designers and the industry. Enlarging the application range new forms of slim-floor constructions have been developed achieving spans up to 16 m by combining superior structural behaviour with lightweight flooring systems.

Work packages 2-4 focused on experimental and numerical investigations to obtain more knowledge on the load-bearing behaviour of slim-floor beams. To ensure optimal comparability between different test set-ups, as closely matching as possible geometrical as well as material parameters were chosen.

WP 2 focused on the longitudinal shear forces and their effect on the load-bearing behaviour. 30 push-out tests were conducted investigating the load transfer achieved with the concrete dowel shear connector system CoSFB [63]. The composite slim-floor beam system consists of a standard hot-rolled steel profile with holes in the web of the profile. Reinforcing bars introduced in those holes ensure composite action and a ductile behaviour combined with good load-bearing properties. In particular, parameters such as concrete grade, the diameter of reinforcing bars and the diameter of the hole in the steel profile were investigated, showing dependency on the diameter of the reinforcement in combination with its ratio to the concrete grade. Comparison to tests without shear connectors (only with holes) or with headed studs allowed to identify the individual contributions to the shear connection capacity.

Shear beam tests served to investigate the load-bearing behaviour of shear connectors in a slim-floor beam situation. Investigated parameters were the type of shear connector, the loading arrangement as well as the concrete cover over the steel profile. All beams behaved in a ductile manner. Even without mechanical shear connectors a notable degree of shear connection could be achieved due to clamping action and friction. Shear connectors have an effect on the maximum load as well as the stiffness of the beams. Concrete cover above the top-flange of the steel beam plays a role in providing shear connection by clamping and by friction.

Finite Element calculations allowed deeper insight into the load-bearing-behaviour of the shear connector CoSFB as well as the behaviour of corresponding shear beams. Extensive studies identified further parameters which affect the load-bearing behaviour.

WP 3 focused on the flexural load-bearing behaviour of slim-floor beams. 9 tests on slim-floor beams of 6 m length were conducted focusing on the degree of shear connection, type of shear connector and loading arrangement.

As in the shear beam tests all tests behaved in a ductile manner. The degree of shear connection has a major effect on end-slip, the moment resistance, as well as on the initial stiffness. The shear connector type and subsequently its load-bearing behaviour also influences the structural behaviour of the beam. Numerical investigations using springs as shear connectors provided deeper insight into the load-bearing behaviour of flexural beams. In order to describe this, the load-bearing behaviour was split into characteristic points: cracking of concrete, yielding of the steel profile.

Long-term behaviour of slim-floor beams was investigated within work package 4. Four long term beam tests were conducted over a period of up to 10 months including testing of the residual load carrying capacity after this period. Effects of creep and shrinkage and usage of shear connectors were quantified.

Time-dependent effects of concrete influence the deflections of slim-floor beams and cannot be neglected. However, no significant slip could be detected under the sustained load. Vibration tests

showed the natural frequency of the beams is sufficient high to cause any uncomfortable interference with pedestrian walking.

In WP5 a LCA-evaluation of the defined “pilot” floor systems was realized, including identification of the main environmental impacts for flooring systems as well as the cost calculation for the construction. Evaluation according to LCA calculation methods was performed considering the environmental impact of the products and technology, including raw material, production, use and final disposal but also the transport between the different phases and results regarding energy efficiency.

Based on the presented developments and evaluations, application rules for the ultimate limit state were developed. These rules consider the construction as well as the normal stage, and both edge and internal beams. Rules for terming the moment resistance, resistance against combined bending and torsion, local transverse bending and transverse shear resistance were proposed. Additionally , special rules for web openings in beams are presented.

The defined rules are given in a format ready for transfer into Eurocode 4 (WP6) and recommendations and guidelines for the improved use of slim-floor beams in buildings (WP7) are published in the form of a handbook.

IV. Exploitation and impact of research results

Resulting from the research work a design guide for composite slim-floor beams as handbook was created, addressing “connections design”, “ultimate limit state”, “serviceability design”, “fire design” and “joint design”.

Within SlimAPP 26 deliverables were developed, adding substantial knowledge to the results presented in the Final report. Tab. II presents a list of these deliverables. These deliverables also form the background for a possible transfer of the application rules for slim-floor beams.

Several papers and presentations resulted from the work conducted within the scope of the project. A corresponding list can be found under Publications and in the Reference list. Also a number of bachelor and master theses promoted the knowledge and application of slim-floor beams to the next generation.

At the end of the project (June 2018) a Workshop was organized in Valencia, Spain during the international conference “Advances in Steel-Concrete Composite Structures (ASCCS 2018)”. Thereby practitioners as well as experts in composite structures have been addressed successfully.

PUBLICATIONS

The following publications resulted from the project in chronological order:

Schorr, Johannes; Kuhlmann, Ulrike; Hauf, Gunter: Slim-Floor Constructions - Deformation and Load Carrying Behaviour, In: 8th International Conference on Composite Construction in Steel and Concrete, Jackson Hole, Wyoming, USA, 30.07.2017-02.08.2017

Sheehan, Therese; Lam, Dennis; Dai, Xianghe: Experimental studies of composite slim-floor beams, In: 8th International Conference on Composite Construction in Steel and Concrete, Jackson Hole, Wyoming, USA, 30.07.2017-02.08.2017

Schorr, Johannes; Kuhlmann, Ulrike: Slim-Floor Deckenkonstruktionen. In: Wolfgang Breit, Wolfgang Kurz, Matthias Pahn, Hamid Sadegh-Azar, Jürgen Schnell und Catherina Thiele (Hg.): Beiträge zur 5. DAfStb-Jahrestagung mit 58. Forschungskolloquium. 58. Forschungskolloquium. Kaiserslautern, Deutschland, 20.09.2017-21.09.2017, S. 259-270.

Sheehan, T., Dai, X, Yang, J., Zhou, K and Lam D. (2018) Flexural behaviour of composite slim floor beams. Extended paper, submitted to Structures. Under review

Schorr, Johannes: Push-Out Tests and Analysis on CoSFB Shear Connector, IABSE Young Engineers Colloquium Munich 2018, 2018

Kuhlmann, Ulrike; Eggert, Florian; Schorr, Johannes: Einfluss der Verdübelung auf das Tragverhalten von Verbundträgern unter Berücksichtigung unterschiedlicher Bauweisen, In: Festschrift Prof. Jörg Lange, 2018

Sheehan, T., Dai, X, Yang, J., Zhou, K and Lam D. (2018) Flexural behaviour of composite slim floor beams. Proceedings of the 12th International Conference on Advances in Steel-Concrete Composite Structures, Valencia, Spain 27th – 29th June, pp 137-144.

Schorr, Johannes: Influence of shear-connector-behaviour on load-carrying of slim-floors beams, IABSE Future of Design Conference 2018, 19th of November 2018, London, UK

Lam. D, Sheehan, T. and Dai, X. (2018) Innovative flooring system for steel-concrete composite construction, Keynote paper for 13th International Conference on Steel, Space and Composite Structures, Perth, Australia, 31st Jan – 2nd Feburary.

Baldassino, N.; Roverso, G.; Ranzi, G.; Zandonini, R.: Service and Ultimate Behaviour of Slim Floor Beams: An Experimental Study, Structures, Volume 17, February 2019, Pages 74-86

Kuhlmann, Ulrike; Lam, Dennis; Zandonini, Riccardo; Aggelopoulos, Eleftherios; Tibolt, Mike; Sheehan, Therese; Baldassino, Nadia; Labory, Francoise; Schorr, Johannes; Anwendungsregeln für Slim-Floor-Träger unter Berücksichtigung von Sicherheit, Funktionalität und Nachhaltigkeit, Stahlbau - Special Issue: Slim-Floor, 2019

Kuhlmann, U.; Lam, D.; Zandonini, R.; Sheehan, T.; Baldassino, N.; Schorr, J. Experimentelle Untersuchungen an Slim-Floor-Trägern, Stahlbau - Special Issue: Slim-Floor, 2019

Schorr, Johannes; Kuhlmann, Ulrike: Design of slim-floors and their connections between steel and concrete, The 14th Nordic Steel Construction Conference, September 18-20, 2019, Copenhagen, Denmark

Dai, X., Lam, D., Sheehan, T., Yang, J. and Zhou, K. (2019) Numerical modelling analysis and parametric study of slim-floor composite shear beams (in progress)

Sheehan, T., Dai, X., Yang, J., Zhou, K. and Lam, D. (2019) Shear behaviour of slim floor composite beams (in progress)

Following Bachelor- and Master-Thesis resulted:

Braghini, Matteo: Analisi e progetto di travi tipo slim floor in condizioni ultime, University of Trento, AY 2016-2017 (tutors: Nadia Baldassino and Riccardo Zandonini, in Italian).

Martinelli, Matteo: Analisi e progetto di travi tipo slim floor in condizioni esercizio, University of Trento, AY 2016-2017 (tutors: Nadia Baldassino and Riccardo Zandonini), in Italian

Sigler, Sebastian: Advancement of an FE-Model for Push-out tests of CoSFB slim-floor beams and investigations on the shear connection behaviour, as well as subsequent parameter studies, Master-Thesis, Institute of Structural Design, University of Stuttgart, No. 2017-1X, 2017

Rovere, Paolo: Risposta di sistemi Slim Floor: analisi sperimentale e numerica, University of Trento, AY 2017-2018 (tutors: Nadia Baldassino and Riccardo Zandonini), in Italian.

Fritsch, Daniel: Development of an Excel-Tool for Slim-Floor-constructions and subsequent parametrical studies, Bachelor-Thesis, Institute of Structural Design, University of Stuttgart, No.2018-11X, 2018

Knecht, Wigand: Development of a numerical model for the representation of the load capacity of slim-floor beams, Master-Thesis, Institute of Structural Design, University of Stuttgart, 2019 (ongoing)

Guhl, Felix: Comparative calculation and limit analysis of slim-floor-constructions with and without composite action, Bachelor-Thesis, Institute of Structural Design, University of Stuttgart, 2019 (ongoing)

Rinke, Felix: Recalculation of Slim-Floor-Girders with the model of the M- κ -line taking partial interaction into account, Bachelor-Thesis, Institute of Structural Design, University of Stuttgart, 2019 (ongoing)

SCIENTIFIC AND TECHNICAL DESCRIPTION OF RESULTS

1 IDENTIFICATION OF APPLICATION RANGE, DEFINITION OF “PILOT PROJECTS”

1.1 General

The limiting criteria for long span slim-floor systems have been identified. It was concluded that the limiting span for conventional slim-floor solutions is about 11 m. Based on the limiting criteria, basic strategies for the application of long span slim-floor systems have been developed.

Different benefits of slim-floor construction are identified, together with their implications for design. In addition, the needs of the different players in the building sector are described for the different building types (e.g. residential and office buildings, car parks, hospitals, etc.).

Different floor designs have been selected and are serving as case studies throughout the whole project for the investigation of the innovative use of slim-floor systems. The floor designs cover medium and long span slim-floor beam systems for application in residential/commercial buildings and free-standing and below ground car parks. In addition, consistent loads and design criteria to be applied in the case studies have been defined.

1.2 New developments in long span slim-floor systems

1.2.1 Limiting criteria for long span slim-floor systems

Slim-floor beams are designed efficiently for spans of 5 to 9 m in which the beam and slab occupy the same overall floor depth. For longer span beams, the depth of the beam increases and so does the slab depth. The thicker slab means that the beam has to support higher loads, due to self-weight and so the span capabilities of the beam are reduced. Often, long span beams require temporary propping during construction and then the limiting design criterion tends to be the control of perceptible vibrations. Also, beams may be delivered with a pre-camber (pre-deflection) to offset part of the deflections, due to permanent loads.

Therefore, it is advantageous to consider options in which the slim-floor beam is designed to be deeper than the slab without changing the basic slim-floor concept. An efficient floor slab depth would be 280 to 300 mm for a 5.4 m span slab and 350 mm for 8.1 m span, whereas the span to depth ratio of the beam would be in the range of 25 to 27 for long span applications.

Typical spans of slim-floor beams using HEB sections with a welded bottom plate are shown in Tab. 1-1. For a HEB 400 section, the maximum span of about 11 m is limited by the high loading due to the self-weight of the slab. In this case, allowing for concrete cover to the beam, the self-weight of a 440 mm deep slab with deep decking is 6.5 kN/m², which represents 70 % of the applied loading.

Tab. 1-1: Typical slim-floor beam spans for three HEB sections with welded bottom plate

Slim-floor beam	Slab depth	Maximum span of beam for beam spacing	
		B = 5.4 m	B = 8.1 m
HEB 260 plus 450 mm x 15 mm bottom plate	300 mm	7.8 m	6.5 m
HEB 300 plus 500 mm x 15 mm bottom plate	340 mm	9 m	7.8 m
HEB 400 plus 600 mm x 15 mm bottom plate	440 mm	11 m	9.5 m

1.2.2 Strategies for long span slim-floor beams

Long span slim-floor beams may be considered to be in the span range of 11 to 16 m, which is outside their normal efficient range of application.

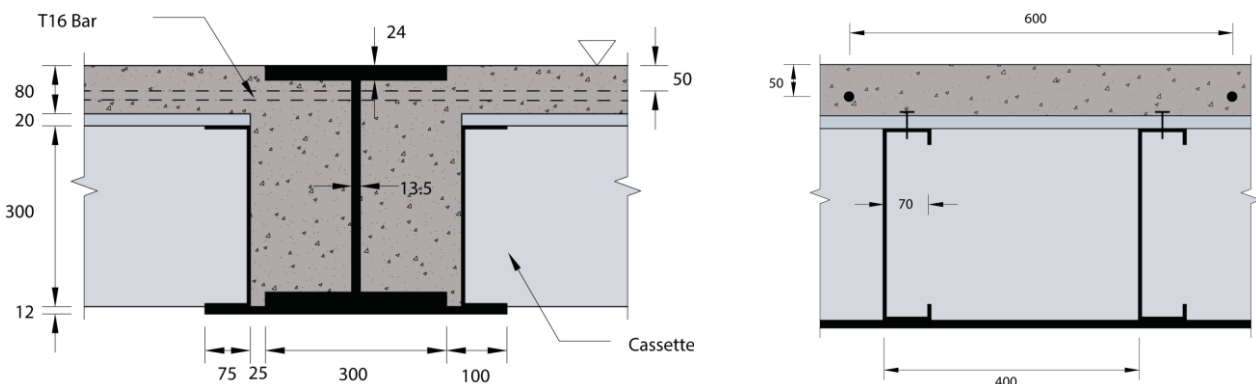
Therefore, one strategy is to reduce the weight of the slab in long span slim-floor construction by using:

- A deeper steel decking system (300 mm typically), or
- A light steel pre-fabricated cassette using 300 mm or 350 mm deep C sections - see Fig. 1-1
- Light weight concrete (density circa 1800 kg/m³)
- Use of new flooring systems such as a deeper *Cofradal* floor slab
- Use of a pre-fabricated composite floor system consisting of Z sections supporting shallow decking-see Fig. 1-4.

In the most efficient form of long span slim-floor construction, the slab depth is 300 to 350 mm and so the topping depth is in the range of 75 to 125 mm. Therefore, the self-weight of the concrete and beam is in the range of 3 to 4 kN/m².

Design studies were carried out using the pre-fabricated cassette system in Fig. 1-1 and it was found that the 300 mm deep x 2 mm thick C sections placed at 400 mm spacing are able to support a slab topping of 120 mm for beams at 5.4 m spacing. The width of the cassette was chosen as 2.4 m to be suitable for transportation to site and lifting into place. However, this system is not practical for slab spans of more than 6 m.

The advantage of the system is that the concrete slab can be designed to be fire resistant by placing 12 mm diameter bars in the concrete ribs. The floor system is also very stiff and services can be routed between the concrete ribs. Again, this system is not practical for slab spans of more than 6 m unless a line of temporary props is introduced at mid-span of the floor cassette.



(a) Cross-section through HEB 400 beam

(b) Cross-section through floor cassette

Fig. 1-1: Prefabricated floor cassettes using C sections supported on the bottom plate

A second strategy would be to provide partial fixity at the beam to column connections to reduce deflections and to increase the natural frequency of the beam. Ways of providing fixity are:

- Full depth end plate connections with a minimum of 4 bolts, for which a deflection coefficient of 4/384 (reduction of 20%) may be used. This type of end plate is required to resist torsional effects applied to the beam. This leads to a round 7 % increase in the beam span (say 0.6 m) and so has limited benefit.
- Extended depth end plate above and below the beam that is designed for a minimum of 30 % of the bending resistance of the slim-floor beam. In this case, the bending moment acting on the beam is reduced and a deflection coefficient of 3.5/384 (reduction of 3%) may be used at the serviceability limit state. This leads to an 11 % increase in the beam span and so has useful benefit.
- Haunched connection in which the beam is deepened by about 300 mm. The disadvantage is that the connection projects below the beam. This may be acceptable in some highly serviced buildings where a deep zone is allowed below the slab for services. A haunch can lead to a 15

% increase in the beam span assuming also that the columns are of equivalent stiffness to the beam.

1.2.3 New forms of long span slim-floor beams

Various new forms of long span slim-floor beams were investigated in this research project. Some kept to the same beam configuration but reduced the slab depth and weight whereas others projected below or above the floor zone. They are described as follows:

Slim-floor beams with welded UPN sections to the bottom plate

UPN sections of 100 to 150 mm depth may be welded to the ends of the bottom plate to provide support to a shallower floor slab (300 to 330 mm depth). The beam may be a HEB 400 section and so it projects 135 mm below the beam in the example shown in Fig. 1-2. Although the stiffness of the beam is increased slightly, the main benefit is the reduction in self-weight of the floor slab. The increase in span of the HEB 400 section is estimated to be 12 to 15 % in this case, depending on the depth of the UPN.

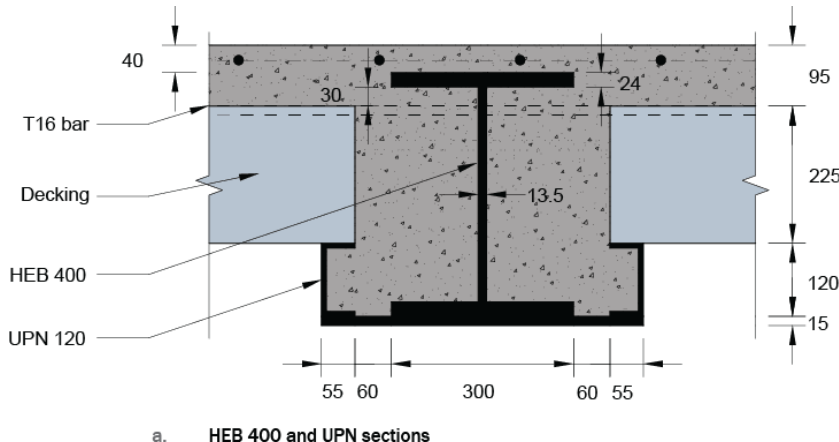


Fig. 1-2: Slab supported by UPN sections welded to the bottom plate

Slim-floor beams with welded profiled bottom plate

A steel plate may be bent to the required profile to support the decking at 80 to 120 mm above the bottom of the beam, as shown in Fig. 1-3. In this system the maximum bend angle is taken as 60° to the horizontal. This leads to a relatively wide plate (700 to 800 mm), which adds to the stiffness of the beam but also to its fabrication cost. The plate thickness may be reduced from 20 mm to 12 mm for shorter span slabs.

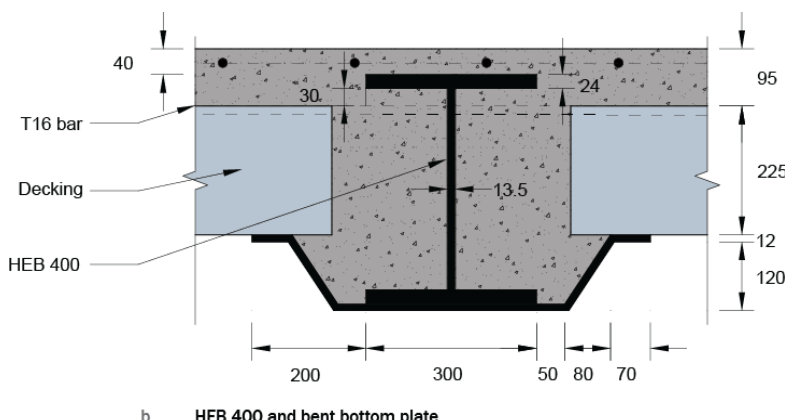


Fig. 1-3: Slab supported by profiled bottom plate

Slim-floor beams with angles welded to bottom flange

An HEB 400 or HEB 450 beam may be fabricated with angles welded to its bottom flange to support the deep decking as shown in Fig. 1-4. The angle size is 100x100x10 mm for an HEB 400 section and 150x100x10 mm for a HEB 450 section. The angle supports the weight of the decking and slab and the angles and their welds are designed for the eccentric load acting on them. Because of this eccentric loading, it is proposed that this system is not used for a beam spacing more than 5.4 m. Fig. 1-4 shows the use of an IPE 450 beam with 150 mmx100 mm angles. It does not require the use of a bottom plate and composite action with the slab is achieved in the same way as the previous systems. It is relatively efficient in fabrication although the welds may have to be partial penetration to be sufficiently strong in bending. The angles may also be held in place by straps connected to the beam web. The angles may be welded in short lengths of 2 to 3 m, but they should be placed against each other in longitudinal direction to avoid loss of concrete.

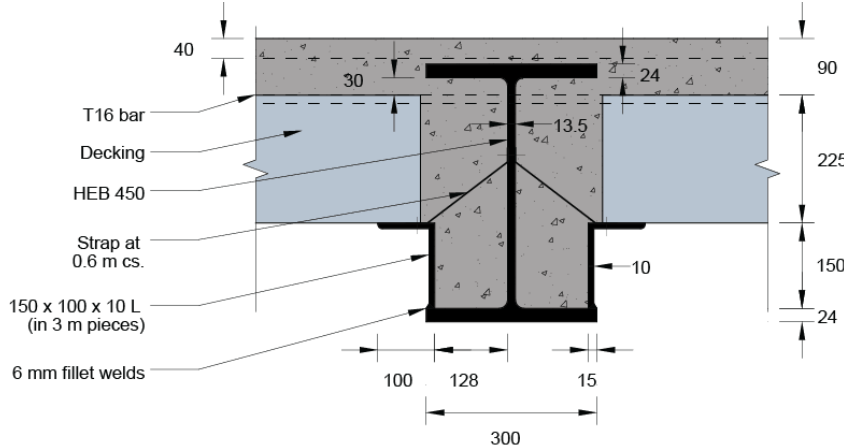


Fig. 1-4: Slab supported by angles welded to the bottom flange of HEB 450

Hybrid slim-floor beams with welded half cell

A conventional slim-floor beam may be stiffened by welding a half cellular beam section, as shown in Fig. 1-5. In this example, a 350 mm deep section is cut from an IPE 400 section with half cells of 500 mm diameter. The slim-floor beam may be formed by welding half an IPE 400 or IPE 500 section to a 400 mm wide x 15 mm or 20 mm thick plate. The overall depth of the beam and slab of Fig. 1-5 is now 600 mm.

The advantage of this hybrid form of construction is that the size and depth of the bottom Tee profile can be chosen for the required span and loading without modifying the upper section or plate.

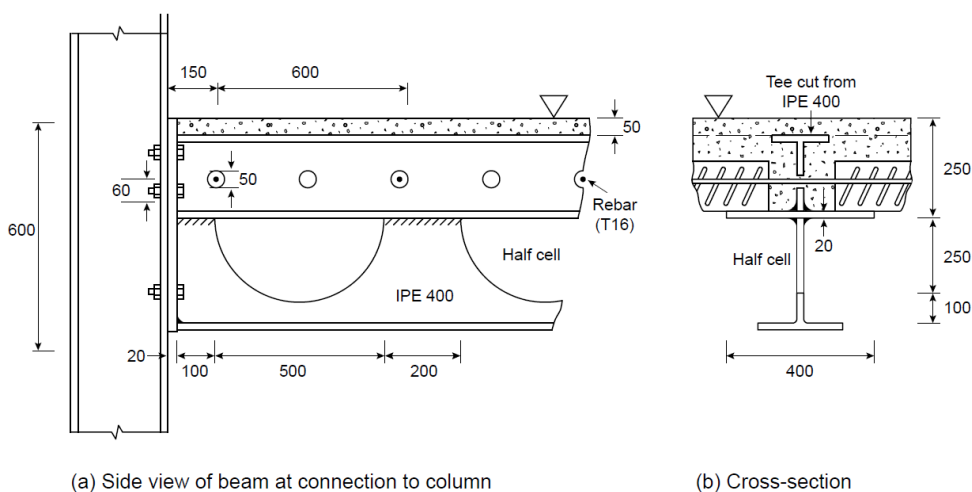


Fig. 1-5: Hybrid slim-floor concept using a welded half cell

Bars are passed through the upper Tee section to achieve high degree of composite action. Partial fixity can be provided by the deep end plate connection.

Design studies have shown that this hybrid slim-floor beam system can achieve spans of 14 to 16 m with a half cell projecting of 300 to 400mm below the floor slab.

1.2.4 Span capabilities of the long span options

The span capabilities of the various long span options together with their slab depths are presented in Tab. 1-2.

Tab. 1-2: Typical long span slim-floor beam configurations and their span capabilities for offices

Long span slim-floor beam option	Option	Slab and beam depth	Maximum span of beam for beam spacing of:	
			B = 5.4 m	B = 8.1 m
HEB 400 slim-floor beam plus 500 mm x 15 mm plate	Light weight concrete slab	440 mm	12 m	10.3m
	Floor cassette with 300mm deep C-sections	440 mm	12.5 m	Not applicable
		400 mm	13.2 m	
	With 120UPN edge sections	440 mm	12.3 m	10.5m
		400 mm	12.8 m	10.9m
HEB 400 plus bent bottom plate	With 800mm x12mm bent bottom plate	440 mm	12.5 m	10.8m
		400 mm	13 m	11.2m
HEB 400/450 plus welded angles	HEB 400 plus 100x100 angles	440 mm	12 m	Not applicable
	HEB 450 plus 150x100 angles	490 mm	13.5 m	
HEB 220 plus IPE400 half cell	Hybrid cellular slim-floor beam	300 mm plus 350 mm deep half cell	15 m	13m

1.3 Compiling the needs of authorities, designers and the industry

1.3.1 Critique of Benefits of Slim-floor Construction

Slim-floor construction has many variants but its primary feature is that it offers the minimum structural depth, which is directly comparable with reinforced concrete flat slabs in the span range of 5 to 9 m. Slim-floor beams may be combined with pre-cast concrete hollow core units or deep steel decking with in-situ concrete.

The precast concrete system tends to be preferred in residential buildings or hotels where the floor slab is directly exposed to the room. The deep deck system is lighter and is preferred in cases where there is a suspended ceiling and opportunity for service integration between the ribs of the deep decking.

The following benefits of slim-floor construction are identified, together with their implications for design:

- Minimum floor depth
 - Floor depths of 270 to 350 mm are achieved by all slim-floor systems.
 - Competes with RC flat slabs in 6 to 9 m span range.
 - Overall building heights are potentially reduced by 10% relative to beam and slab construction (equivalent to one floor in 10).
 - Span: depth ratio of slim-floor beams is typically 27 to 30.
 - The limiting design criteria tend to be control of total deflection or natural frequency.

- Construction process
 - All forms of steel construction are fast to construct and slim-floors are equally fast, and faster than concrete construction.
 - Propping should be avoided where speed of construction is important.
 - Deck spans are limited to 6m to avoid propping but can be longer if temporary props are introduced.
 - Hollow-core units are lifted into place rapidly and supported on the bottom plate. On site concrete is required to form the final slab surface.
 - Hollow- core units require broken out ends to be able to anchor rebars in the cores for fire resistance.
- Implications for design
 - Slim-floor systems weigh less than half of the equivalent reinforced concrete flat slab (350 kg/m² typically)
 - Combined bending and torsion has to be considered in the beam design during construction (reduced by propping).
 - Connections of slim-floor beams to columns should consider torsional effects (full depth and plates are preferred).
 - Partial fixity may be provided by the semi-rigid connections to reduce deflections.
 - Tie beams may be used to connect the columns orthogonal to the slim-floor beams.
 - Excellent acoustic insulation is provided with a suitable resilient floor covering.
- Service integration
 - All slim-floor systems provide an un-interrupted service zone under the floor.
 - Deep decking provides space for pipes and small ducts that can be suspended from the decking.
 - Circular holes can be cut (by diamond drilling) between the deck ribs on site.
- Fire resistance
 - The embedment of the steel beam in the floor slab provides 60 minutes fire resistance without protection.
 - The bottom flange or plate of the beam can be protected for 90/120 minutes fire resistance.
 - Reinforcing bars may be added to eliminate the need for further fire protection.
 - Edge beams with an exposed face on one side need further protection.
- Façade attachments
 - Rectangular hollow sections (RHS) may be used as slim-floor edge beams to provide a clean edge to the building.
 - Brickwork support brackets may be connected to the edge of the 300mm deep slab.
 - H-profile edge beams can be provided with welded side plates to connect the brickwork support brackets

1.3.2 Applications

- Residential buildings
 - Floor to floor heights are limited to a maximum of 3m for which structural zone plus ceiling and floor finishes is 500mm. This is achieved by slim-floor construction.
 - Slim-floor beams are often combined with hollow core slabs in this sector.

- Spans of 5 to 7.5 m are typical of the residential sector. Small columns can be located in the separating walls.
 - Freedom in planning of the rooms is provided.
 - Excellent acoustic insulation is provided.
 - Foundation costs are reduced for taller buildings.

- Hotels
 - Floor to floor heights are limited in hotels and this is achieved by slim-floor construction.
 - Slim-floor beams are often combined with hollow core slabs in which the concrete is exposed to the room below.
 - For hotels, freedom in planning of the rooms is provided by beams spanning from the façade to the corridor.

- Medical buildings
 - Uninterrupted distribution of complex services is the key to the use of slim-floor construction in this sector.
 - The two-way spanning action of the floor ‘system’ means that response to impulsive actions is low, making it suitable for wards and theatres.

- Educational buildings
 - Deep decking is preferred in schools and colleges and it is often semi-exposed to the room (decking can be painted).
 - The deep deck system enhances the daily thermal capacity of the floor system.
 - Spans of 8 to 10m are preferred for this sector (the beam span the longer distance in the ‘grid’)

- Car parks
 - Car parks often have floor grids of 5m/7m/5m across the building and 5.5m or 8m along the building.
 - This is within the economic span range of slim-floor construction.
 - Car parks have minimum floor to floor zones.
 - Car parks are often located in basements below offices etc.
 - Deep decking spans 5.5m across 2 car park spaces. Hollow-core units span 8m across 3 car park spaces.
 - Decking can be painted for durability.

- Basements
 - Below ground structures require the minimum depth to minimise excavation costs and slim-floor construction is preferred.
 - Car parks are often designed to be accommodated in basement levels for which slim-floor construction is beneficial.
 - Slim-floor beams resist high compression forces where they act as struts between retaining walls.

- Building extensions
 - Where existing facades are retained, it is often necessary to minimise the floor zone, for which slim-floors are preferred.
 - Deep decking systems are often preferred to minimise loads on the supporting structures and foundations.

1.4 Identification and analysis of “pilot projects”

1.4.1 Selected case studies and design assumptions

In order to identify its application and competitiveness limits, different case studies are defined and analysed. A description of the floor layouts, the loads and the design criteria is given below. The case studies are grouped into 3 cases in function of the building type and span (Fig. 1-6 to Fig. 1-9)

The calculation of the case studies will be limited to one floor level for each floor layout only.

To fix the dimensions of the columns, two different numbers of floors will be considered for each layout:

- Building with 3 floors (R+2) and a constant column cross section along the height.
- Building with 6 floors (R+5) and varying column cross sections over the height.

The height h of the columns (= buckling length) is defined as follows:

- Commercial/residential buildings: $h = 3.50 \text{ m}$
- Car parks: $h = 2.80 \text{ m}$

The following loads and design criteria are considered for the case studies:

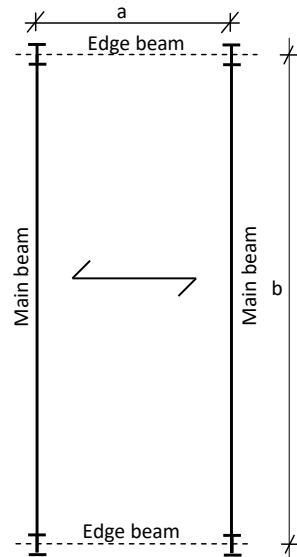
- Dead load: Depends on slab system
- Additional dead load: Concrete screed:
 - Raised floor and ceiling: $g_i = 1.5 \text{ kN/m}^2$
 - Car parks: $g_i = 0.7 \text{ kN/m}^2$
- Imposed loading:
 - Commercial/residential buildings: $q_i = 2.5 \text{ kN/m}^2 + 1 \text{ kN/m}^2$
 - Car parks: $q_i = 2.5 \text{ kN/m}^2$
- Façade:
 - Without façade: $q_i = 0 \text{ kN/m}$
 - With façade: $q_i = 3.0 \text{ kN/m}$
- Deflection criteria:
 - Total deflection: $L/200$
 - Imposed load deflection: $L/300$
- Vibration criteria:
 - (100% Dead load + 20% Live load)
 - Commercial/residential buildings: $f = 3.0 \text{ Hz}$
 - Car parks: $f = 2.3 \text{ Hz}$
- Fire resistance:
 - 3 storey buildings: REI 60
 - 6 storey buildings: REI 90

Different floor systems have been selected for analysis throughout the case studies:

- Cofradal 200 & Cofradal 260
- Inodek & Monodek
- ComFlor

The calculations are carried out in accordance to EN 1994-1-1:2006 [40], EN 1993-1-1:2005 [42] and the approval of the CoSFB-dowel Z-26.4-59 [63].

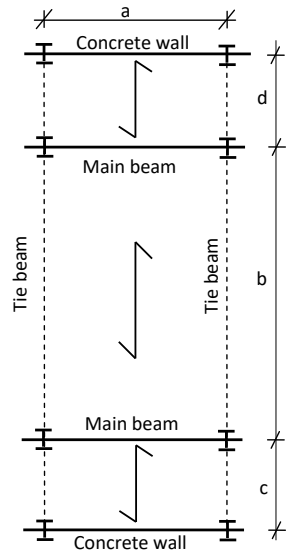
Car parks - Case 1:



$$a = 5.0 \text{ m}$$

$$b = 16.0 \text{ m}$$

Fig. 1-6: Slim-floor beams in free-standing car park

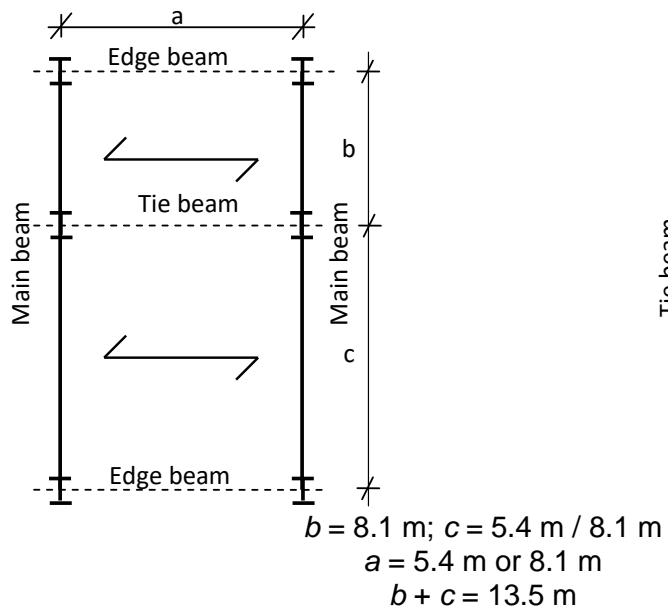


$$a = 5.4 \text{ m} / 8.1 \text{ m}$$

$$c = d = 4.05 \text{ m}; b = 8.1 \text{ m}$$

Fig. 1-7: Slim-floor beams in below ground car park

Residential/Commercial buildings - Case 2:

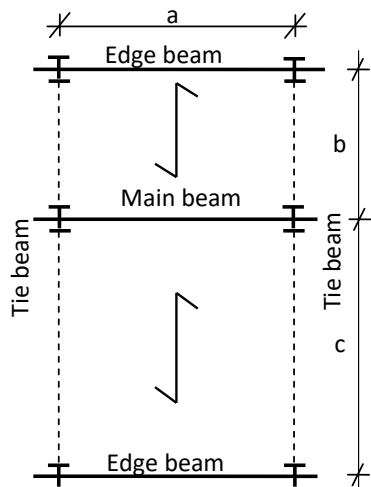


$$b = 8.1 \text{ m}; c = 5.4 \text{ m} / 8.1 \text{ m}$$

$$a = 5.4 \text{ m or } 8.1 \text{ m}$$

$$b + c = 13.5 \text{ m}$$

Fig. 1-8: Slim-floor beams spanning along and across the building - medium spans



Residential/Commercial buildings - Case 3:

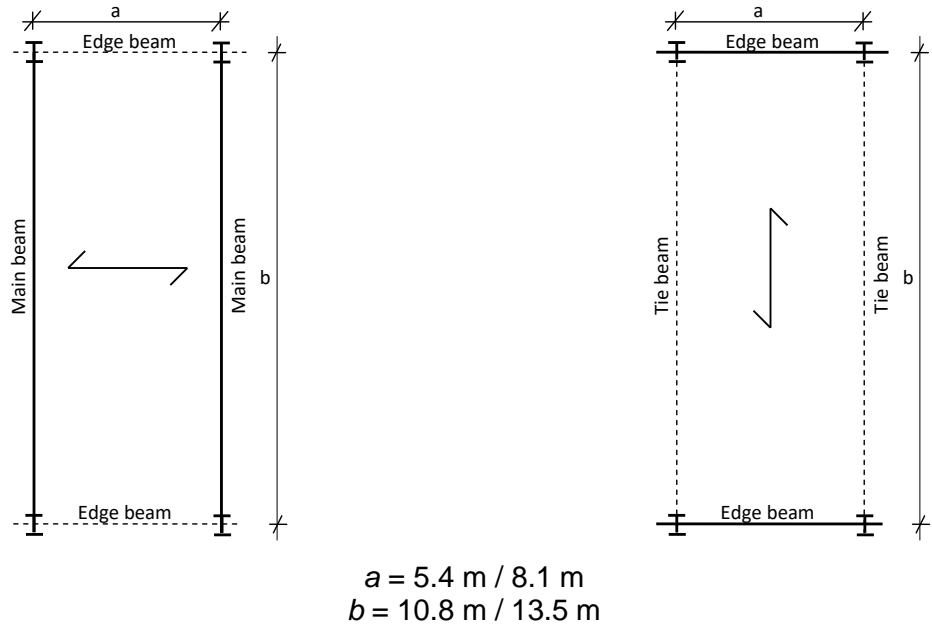


Fig. 1-9: Slim-floor beams spanning along and across the building - long spans

1.5 Conclusions

Conventional slim-floor beams are limited to spans of about 11 m even with measures to reduce the self-weight of the floor slab. Floor cassettes are useful as they minimise the weight of the floor slab and they are prefabricated to speed up the construction process [1].

The most efficient long span options are the welded side angles to the HE beam, which eliminate the bottom plate and minimises the slab depth and weight. The use of hybrid beams consisting of a welded half-cell section below the slim-floor beam or a welded bottom chord using a RHS section are also efficient, but they depart from the principles of slim-floor construction, where the steel section is fully contained within the slab depth [1].

The systems also benefit from partial fixity at the connections. The target design of the long span systems is 13.5 m for naturally ventilated offices and 16.2 m for car parks (in both cases less 0.4 m for the column dimensions). An intermediate span of 10.8 m was also designed which is the limit of conventional slim-floor construction. It was found that the steel intensity of the 13.5 m span using HEB 550 section with welded side angles is similar to that of a more conventional 8.1 m span slim-floor beam [1].

The advantages and the applications of slim-floors have been highlighted [1].

Finally, different case studies have been defined and designed according to the European standards for composite structures and technical approvals. The case studies represent commonly used floor layouts for slim-floor solutions and they were used throughout the project [1].

2 PUSH-OUT AND SHEAR BEAM TESTS WITH INNOVATIVE SHEAR CONNECTORS IN SLIM-FLOOR BEAMS

2.1 General

The objectives of these investigations are to evaluate the performance of slim-floor beams with a wide range of shear connection systems, based on existing test data and new tests as well as numerical calculations. The structural behaviour of the methods of shear connection in slim-floor beam systems, and in particular the use of reinforcing bars placed through holes in the beam web were investigated. Reinforcing bars used as shear connectors are the most efficient and practical way of achieving composite action for slim-floor beam solutions with shallow composite slabs.

An optimal arrangement of shear connectors in slim-floor beams reduces their overall height and therefore becomes a decisive factor in the economic use of slim-floor construction.

2.2 Push-Out tests for evaluation of characteristic behaviour of concrete dowels

2.2.1 General

Ten Push-Out test series were conducted on concrete dowel shear connector system "Composite Slim-Floor Beam System" (CoSFB, [63]) - 30 tests in total. The influence of parameters, such as the concrete grade, reinforcing bar diameter and diameter of the hole in the web of the steel profile have been investigated [2].

2.2.2 Methodology

The geometry was kept the same for all specimens. Therefore, the concrete slab and the steel profile had identical dimensions for all specimens. Within each test ten shear connectors, five per side, were tested. To reduce effects due to eccentric loading the two halves of each specimen with five shear connectors each were welded together at the bottom flanges to achieve a symmetric geometry. To reduce deviations in the material between all test set-ups the HEB 200 steel profiles and reinforcing bars were ordered from one batch. Same procedure was chosen for the production of the concrete slab. Therefore, each test series was produced with concrete from one batch.

All push-out tests were conducted at the testing laboratory of the University of Stuttgart (Materialprüfungsanstalt Universität Stuttgart - MPA). Each test was equipped with extensometers, measuring the slip of the machine, the slip on top of the specimen, the vertical and horizontal displacements of the concrete slab and the slip at the bottom of the specimen, as shown in Fig. 2-1 and Fig. 2-2. Furthermore, one test of each series was equipped with strain gauges on the reinforcement bars.

All tests were conducted according to Eurocode 4, Annex B2.5 [40]. Data from the extensometers and from the strain gauges, as well as the force applied by the machine were recorded. All tests were evaluated according to EN 1994-1-1 [40], Annex B2.5. Therefore, the following values were measured and calculated:

P_e maximum achieved load by one shear connector

P_{Rk} characteristic load achieved by one shear connector $P_{Rk} = 0.9 \times P_e$

δ_u deformation capacity

δ_{uk} characteristic deformation capacity $\delta_{uk} = 0.9 \times \delta_u$

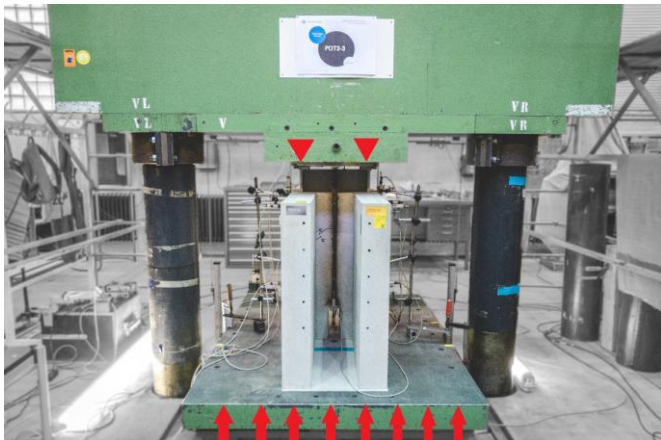


Fig. 2-1: Push-out tests - Test setup

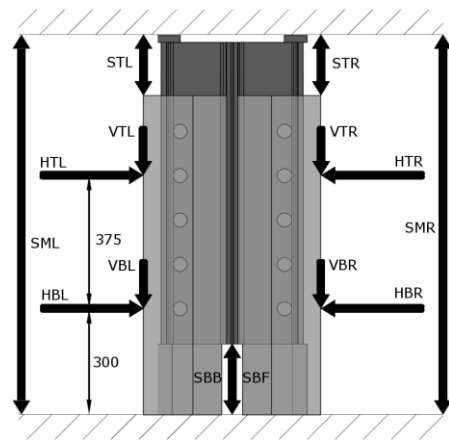


Fig. 2-2: Extensometers

The listed values were evaluated for dynamic loading and for loading under respect of the short time relaxation. The "relaxed" values were measured by stopping the machine until the relaxation process was completed. To evaluate the deformation capacity, the minimum slip of the system from the beginning of the loading phase was calculated. Slip during preloading phase was not considered.

2.2.3 Results & tendencies

The role of concrete grade, reinforcing bar diameter and hole diameter in the web of the steel beam was investigated. In Tab. 2-1 the corresponding results are shown.

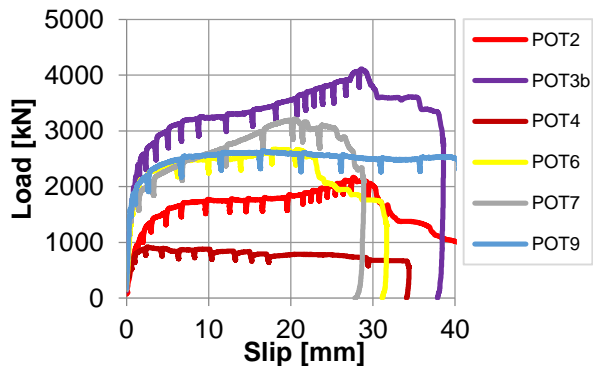
Two types of failure were monitored - failure of the shear connector and failure of the concrete support. Failure of the shear connector was the target failure mode. In case of concrete failure the full potential of the particular shear connection configuration had not been exploited.

Fig. 2-3 shows load-slip curves of the push-out tests to present relations and tendencies between the tests (results of one specimen are given from each series of 3 tests). All tests showed a ductile behaviour including POT 4 without rebars. The "6 mm" ductility criterion given for headed studs by Eurocode 4 [40] to ensure plastic redundancies for design has been achieved by far. Therefore, the CoSFB concrete dowel can provide sufficient deformation capacity retaining a high level of load at the same time.

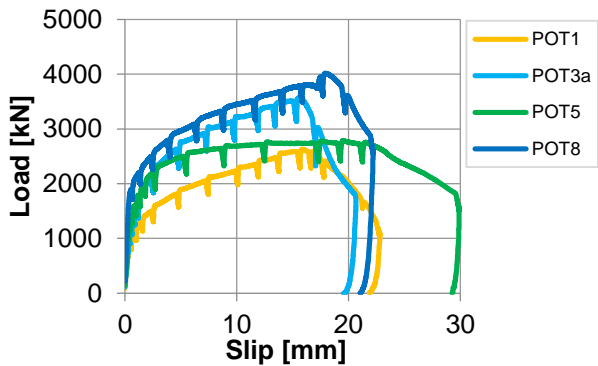
Diameters 12, 16 and 20 mm of the reinforcing bars were tested combined with various concrete grades. Fig. 2-4 shows the characteristic load P_{Rk} for different concrete grades depending on the tested reinforcing bar diameters.

Tab. 2-1: Overview of the conducted push-out testing programme

Series	Reinf. Ø	Hole Ø	Concrete	P_{Rk}	δ_{uk}	Failure
[-]	[mm]	[mm]		[kN]	[mm]	[]
POT 1	16	40	C25/30	220	21.2	Support
POT 2	12	40	C25/30	180	23.5	Shear connector
POT 3a	20	40	C25/30	309	17.9	Support
POT 3b	20	40	C50/60	358	24.7	Shear connector
POT 4	X	80	C25/30	75	10.2	Shear connector
POT 5	16	80	C25/30	242	20.5	Support
POT 6	16	40	C50/60	232	19.4	Shear connector
POT 7	16	40	C30/37	276	24.3	Shear connector
POT 8	20	40	C30/37	325	16.9	Support
POT 9	16	80	C30/37	245	39.7	Shear connector



(a) Failure of shear connector



(b) Failure of concrete support

Fig. 2-3: Load-slip curves - One specimen of each series

The maximum load in the tests mainly depends on the reinforcing bar diameter. An increasing diameter results in an increasing maximum load. The diameter of the hole in the web of the profile had minor influence on the maximum achieved load. The influence of the concrete grade depends on the used rebar diameter. Small rebar diameter resulted in a decreasing load with increasing concrete grade. A large diameter resulted in an increasing load with an increasing concrete grade.

Hence rebars are decisive for the CoSFB shear connector system and its load bearing capacity. Other concrete dowel shear connector systems mainly use rebars to ensure ductility.

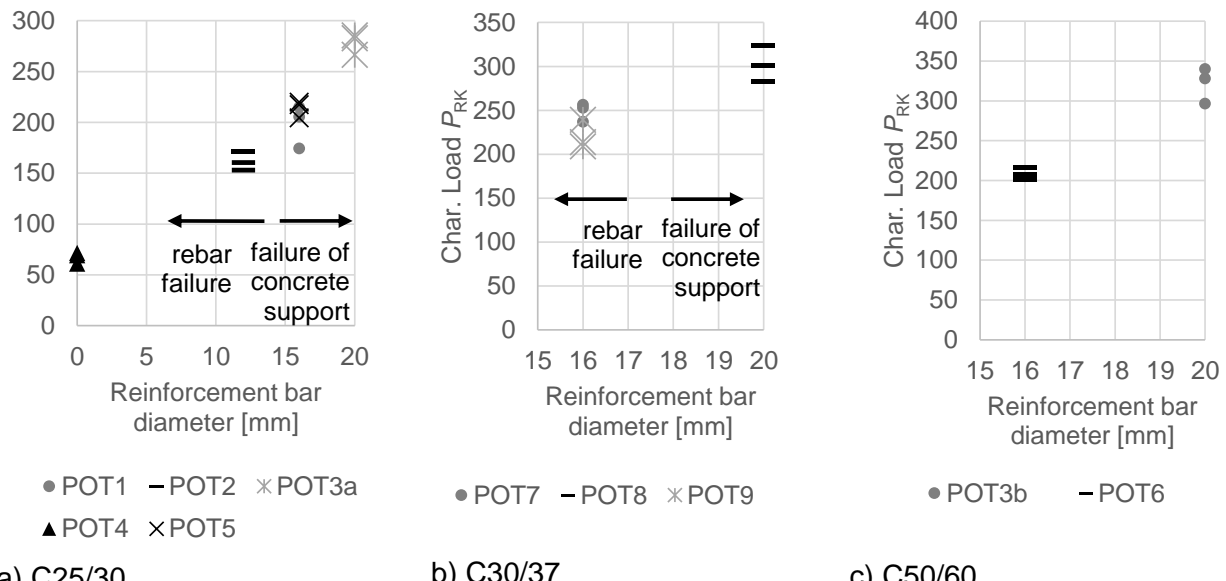


Fig. 2-4: Influence of the rebar diameter on the load-bearing behaviour of the CoSFB dowels depending on concrete grade

2.2.4 Numerical investigations

For the purpose investigating the load-bearing behaviour of the Composite Slim-Floor Beam system [63] a numerical model was developed in ABAQUS [65], based on the numerical investigations by Sigler [37]. The numerical model was also based on conducted push-out tests (see Fig. 2-5) [4].

Relevant material and geometrical parameters were taken into account in the modelling process with as much detail as possible. Therefore, sophisticated material models for concrete (Concrete Damaged Plasticity Model) and for reinforcing steel (Ductile Damage) were introduced. Interfaces between steel and concrete or between reinforcement bars and concrete were modelled using sophisticated contact formulations. Friction coefficients were estimated by experience [71]. The explicit dynamic solver in combination with mass scaling was used.

Push-Out test series 2 (POT 2) with \varnothing 12 mm reinforcement bars and concrete grade C25/30 was recalculated numerically and verified against the tests up to a slip-range of 20 mm, shown in Fig. 2-6. The verified model serves to determine the load-bearing behaviour of the CoSFB-System.

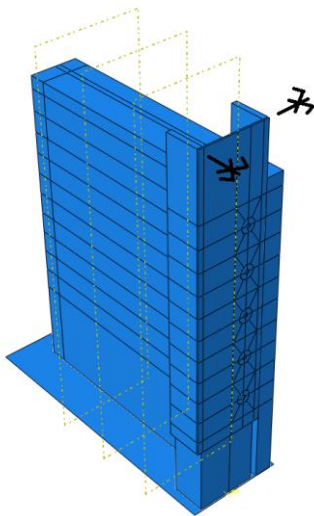


Fig. 2-5: Push-out-test model- led in ABAQUS

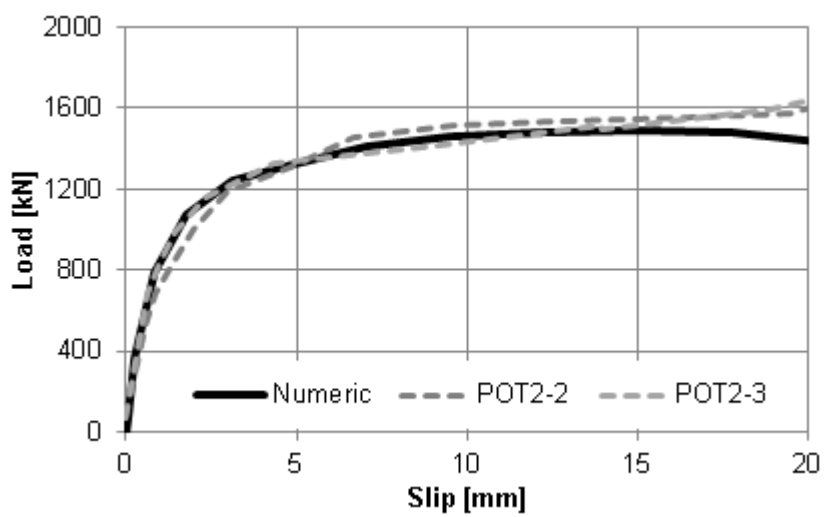


Fig. 2-6: Verification of load-slip-curve

The load-bearing behaviour of the Composite Slim-Floor beam system (CoSFB) comprises different mechanisms:

- a) concrete compression at the rounding of the holes in the steel-profile web
- b) bending of the reinforcement bars and subsequent activation of surrounding concrete
- c) developing concrete strut at the top flange of the steel profile

Furthermore the verified model was used to investigate various parameters and their influence on the load-bearing behaviour. Tendencies could be determined, but due to the uncertainties in concrete modelling, the model was not able to capture the effect of changing concrete grades in a satisfactory manner, regarding failure mode of the specimens.

One parameter at a time was varied and compared with the verified model base case to show its effect on the load-bearing behaviour. The following main conclusions are listed:

Material parameters

- Steel and reinforcement bars: no effect
- Concrete: effects load-bearing behaviour

Geometric parameters

- profile web width: effect is limited and correlates with concrete grade as indicated by [63]
- profile width: effects distribution of concrete strut between rebar and profile flanges
- hole diameter: effects distribution of load in the concrete (increasing diameter leads to wider spreading of loads)

None of the investigated parameters suggests a strong effect on the stiffness of the connection. Maximum load and beginning of the plastic branch of the load-slip curve seemed to be clearly dependent.

2.2.5 Conclusions

Push-out tests on the concrete dowel shear connector system (CoSFB) [63] extended the existing knowledge. Investigated parameters were the rebar diameter, the concrete grade and diameter of the hole in the profile web. The load-bearing behaviour is mainly affected by the rebar diameter. But to reach the full potential of the system, the concrete grade and the rebar diameter must be compatible. Numerical investigations provided further knowledge of the load-bearing mechanisms. Tests and numerical investigations serve as basis for the developed model presented in section 6.2.2.1.

2.3 Shear beam tests for evaluation of characteristic behaviour

2.3.1 Introduction

Following the push-out tests, eight shear beams were tested. The majority of specimens used a novel shear connector, comprising a rebar passing through a hole in the steel section web. The cross-section, loading arrangements and connector details varied between specimens in order to quantify the contributions of different mechanisms towards the shear connection and the overall beam behaviour. Further details are provided in the following sections.

2.3.2 Test specimens

Details of the eight shear beam specimens are as follows:

SBT1a and SBT1b	- 40% shear connection, with and without stirrups, eccentric loading
SBT2	- 40% shear connection, concentric loading, basic case
SBT3	- no shear connectors, eccentric loading
SBT4	- no topping, concentric loading,
SBT5	- larger holes, concentric loading
SBT6	- shear studs, concentric loading
SBT7	- larger holes without transverse bars passing through them, conc. loading

Typical specimen cross-sections under eccentric and concentric loading are presented in Fig. 2-7 and Fig. 2-8.

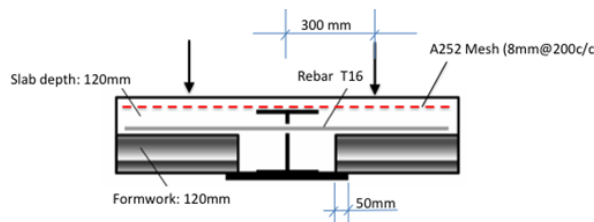


Fig. 2-7: Details of specimen SBT1b

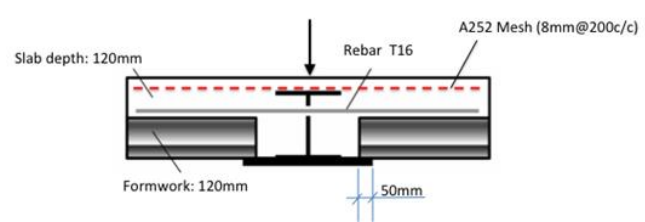


Fig. 2-8: Details of specimen SBT2

All of the specimens comprised a HEB200 steel section welded onto a 400 × 15 mm steel plate, embedded in a 2 m wide concrete slab, with a total depth of 240 mm (above decking depth of 120 mm). A252 mesh reinforcement was placed below the top surface of the concrete slab. Rebars were passed through holes in the HEB section web for most of the specimens, with the web hole-diameter being 40 mm. SBT5 and SBT7 had web hole-diameters of 80 mm. The concrete strength for each specimen was determined on the test date by taking the average results from three compressive cube tests. Specimens SBT4 and SBT6 had the lowest concrete strength of 34.1 N/mm². The concrete strength on the test date for the all of other specimens was in the range of 41.3 N/mm² to 43.9 N/mm².

2.3.3 Test set-up and instrumentation

Each shear beam had a length of 4 m. Load was applied at two locations along the beam length, 1.5 m from the supports, or 1.0 m apart (see Fig. 2-10). During the early stages of the tests load was applied in 20 kN increments. As the load began to reach a plateau this was switched to 5 mm deflection increments. The load/displacement was increased until one of the following occurred: failure of the beam or maximum displacement of test rig reached.

11 LVDTs were employed to measure deflections of the beams. Nine LVDTs were placed underneath the specimens to measure vertical deflection and one LVDT was positioned at each end to measure the end-slip. Strain gauges were used measuring the strains on the top surface of the concrete slab, the top flange of the steel section and the bottom steel plate. For SBT1a and SBT1b, 3 to 4 strain gauges were placed on the transverse bars that were closest to the ends of the beam

(located between the loading point and the support). These bars were expected to be the only bars involved in providing shear connection. For the remaining specimens strain gauges were placed on every bar placed close to the centre of the bar. Here the strains were expected to be the largest.

2.3.4 Load-deflection response

The load-deflection response for each of the shear beam specimens is presented in Fig. 2-9. The graph shows three distinct phases:

1. During initial stage, the response was linear elastic.
2. After reaching a load of approximately 300 kN, at which the first crack and slippage occurred, the stiffness of the load-deflection curve was reduced dramatically.
3. During the final stage, the load plateaued as the displacement increased. All specimens exhibited a ductile response, reaching a mid-span deflection of over 80 mm (span/50) while maintaining this load plateau.

For SBT1a, the maximum load reached was 738 kN (corresponding to a shear force of 369 kN and bending moment of 554 kNm) including the self-weight of the specimen and spreader beams. Only one of the reinforcement bars exceeded the yield strain. The load-slip response was nearly the same at each end, with maximum end-slips of 11.7 mm and 13.4 mm recorded during the test. Similar values of end-slip were recorded for the other test specimens. The recorded slip exceeded the minimum slip requirement of 6 mm specified by Clause 6.6.1.1 in Eurocode 4 for ductile shear connector behaviour. Specimen SBT1b was the same as SBT1a except that it did not use reinforcement stirrups in the slab. SBT1b reached a maximum load of 732 kN including the self-weight, and exhibited a very similar relationship between load and vertical deflection at the mid-span to that of specimen SBT1a. For most of the tests, load was applied until the actuator ran out of travel. For the first test, however, the test was terminated when the loading plates punched through

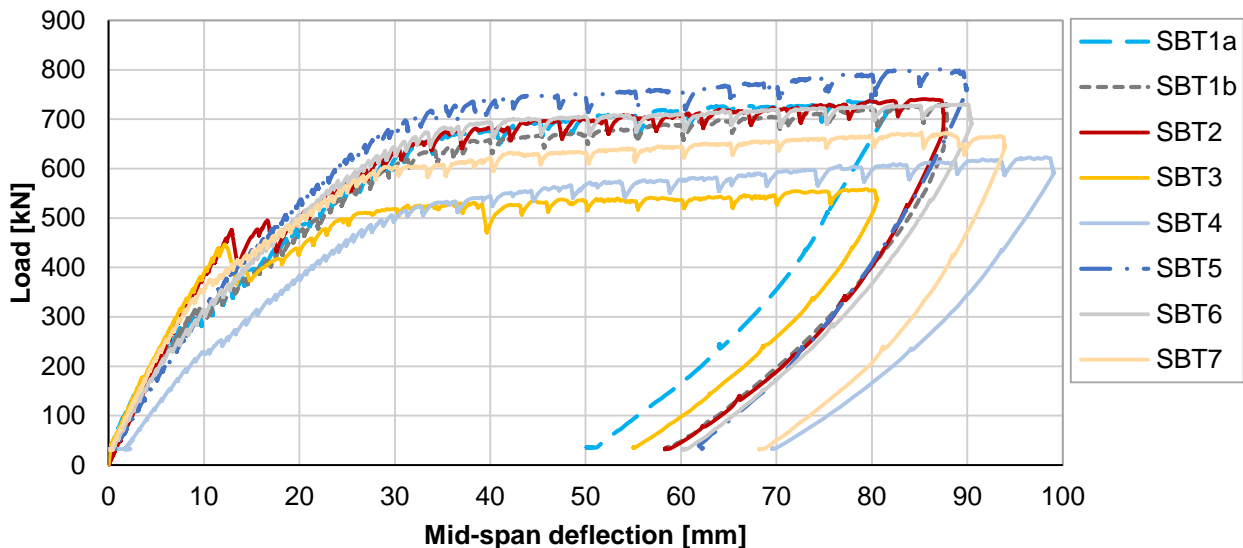


Fig. 2-9: Relationship between load and mid-span deflection for shear beam specimens

the concrete slab. However, since the actuator had nearly run out of travel and the shape of the load-deflection curve was similar to that of the other tests, as can be seen in Fig. 2-9, it was concluded that no further increase in load would have occurred if the test had continued without the occurrence of punching shear. It was concluded that the stirrups did not enhance the performance of the particular specimen type that was considered in this study and hence these were not employed for any of the remaining specimens.

The maximum load for SBT2 (concentric loading) was 741 kN. The load-deflection response was similar to SBT1a and SBT1b and hence it was concluded that the 'clamping' action from the slab did not significantly affect the overall response, although the strains measured in the reinforcement bars were higher than those of SBT1a and SBT1b, which may have been owing to the absence of clamping action. SBT3 reached a maximum load of 559 kN. The transfer of shear between the steel

and concrete for this specimen relied entirely on the friction and clamping action between the steel and concrete, and hence the shear connectors in SBT1a and SBT1b resisted an extra 170 kN in comparison with SBT3. However, SBT3 resisted a higher load than the pure steel section, and further calculations indicated that the clamping and friction action provided a degree of shear connection of 17 %. For both SBT2 and SBT3, the initial phases of the load-deflection curves were slightly different to those of SBT1a or SBT1b, with the curves maintaining their initial stiffness beyond 400 kN. At this stage, a loud sound was heard as cracking occurred in the lower part of the concrete and the load dropped suddenly by approximately 70 kN. The same concrete mix was used for SBT2 and SBT3, and so the difference in behaviour from that of SBT1a and SBT1b was attributed to the concrete.

The maximum load resisted by SBT4 was 623 kN, which lay between the maximum loads of SBT2 and SBT3. The upper concrete slab depth for this specimen was reduced from 120 mm to 80 mm, with no concrete topping above the top flange of the steel section. The specimen was noticeably less stiff than the previous specimens as a result of this concrete depth reduction. All of the transverse bars had yielded by the end of the test. Two longitudinal cracks were observed on the top of the slab, marking the separation between the edges of the steel beam and the concrete.

Specimen SBT5 used wider holes in the steel beam web (80 mm in diameter) than the other specimens (40 mm). This beam reached a maximum load of 804 kN, approximately 60 kN more than SBT2, showing the contribution of the larger concrete dowel to the resistance.

SBT6 utilised headed shear studs, welded onto the HEB-200 web, instead of transverse bars for the shear connectors, and was designed to have the same degree of shear connection as SBT2. The maximum load resisted by SBT6 was 731 kN, which was similar to that of SBT2, and the load-displacement relationship was also similar, showing that in shear beam tests a similar overall response could be achieved with headed shear studs, to that with transverse shear connectors.

SBT7 used large concrete dowels of the same dimensions as those in SBT5, but without any transverse steel bars. SBT7 resisted a maximum load of 673 kN, implying that the steel connectors in SBT5 added an extra 130 kN to the load resistance. The concrete dowels alone provided an impressive degree of shear connection, with the beam resisting 110 kN more than SBT3, which relied on clamping action from eccentric loading.

2.3.5 Concrete cracking

The first concrete cracks appeared as diagonal shear cracks on the edge of the lower portion of concrete slab, between the loading points and supports. With progressing testing procedure cracks developed on the outer edge of the upper slab also.

After initial shear cracking, some flexural cracking was observed closer to the mid-length of the beam and cracks occurred on the top surface of the concrete slab. During the later stages of the tests, these cracks grew in width and depth. Fig. 2-10 and Fig. 2-11 show the specimen in the test rig and the shear cracks in the concrete that occurred after the first phase of the test for specimen SBT1a.



Fig. 2-10: Test specimen in test-rig



Fig. 2-11: Shear cracks in concrete

2.3.6 Measured strains

The relationships between load and strain for each specimen are presented in Fig. 2-12 to Fig. 2-14 for the top flange strain, bottom plate strain and concrete strain respectively.

For most of the tests, the top flange of the steel beam and bottom plate reached the yield strains before the end of the test. The concrete strains were in the range of $1000 \mu\epsilon$ - $1500 \mu\epsilon$. That is lower than the strain value associated with yielding, except for specimen SBT4, in which it exceeded $2000 \mu\epsilon$. Large concrete strains were also observed in SBT3 without shear connectors. The strains measured on the top flange of SBT6 (shear studs) were lower than those in most of the other specimens, and relatively large strains were measured in the concrete slab, indicating that although the shear studs and transverse bars provided similar overall load resistances and deflection behaviour, there were some differences in the strain profiles of the beams for each type of shear connector.

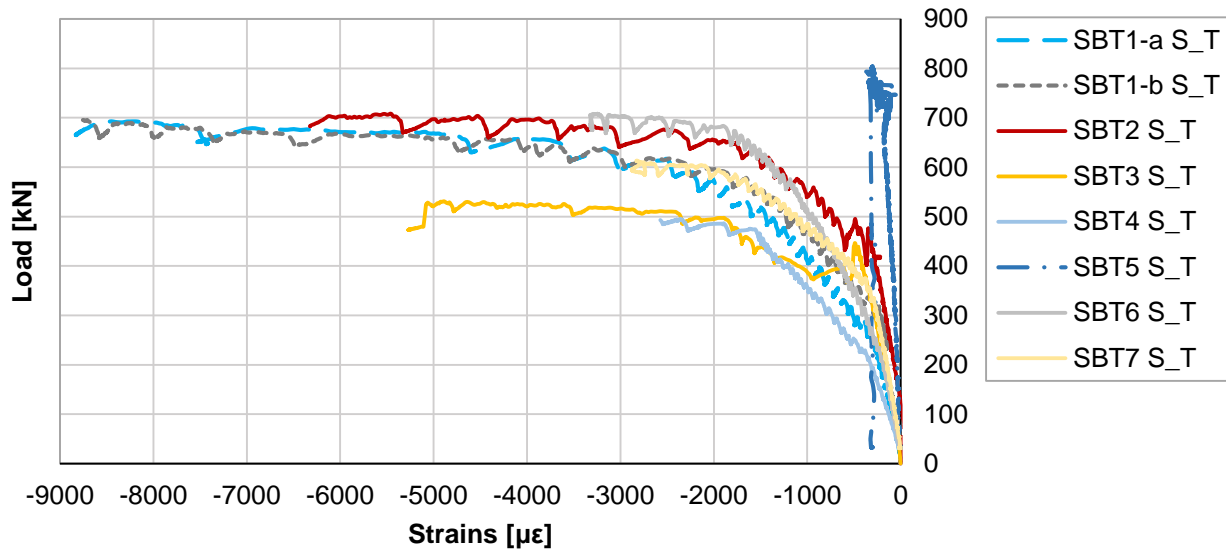


Fig. 2-12: Relationship between load and top flange strain

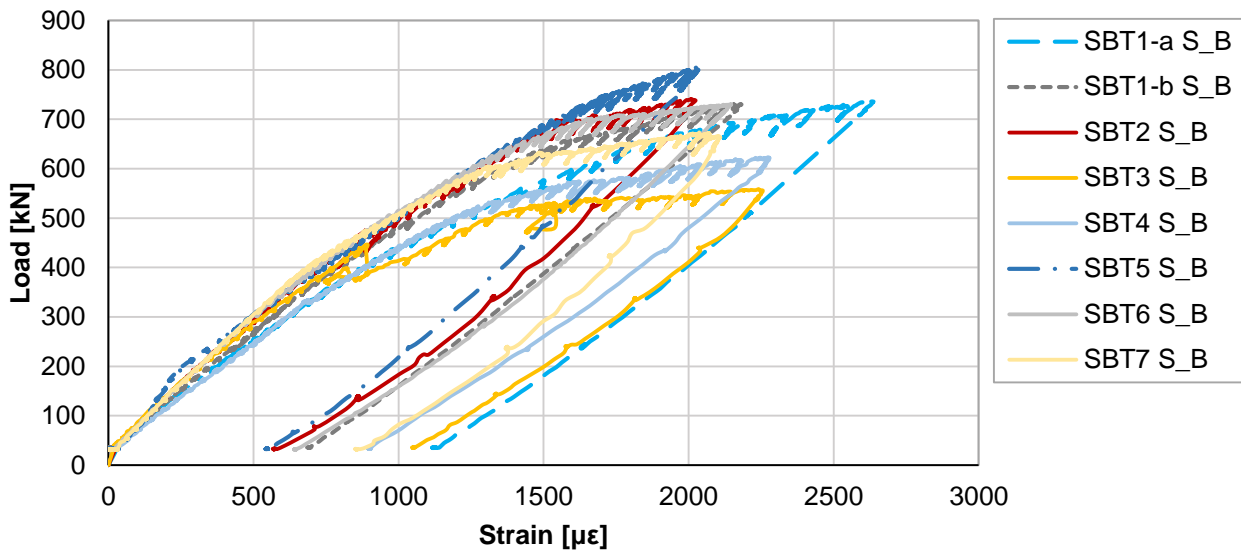


Fig. 2-13: Relationship between load and bottom flange strain

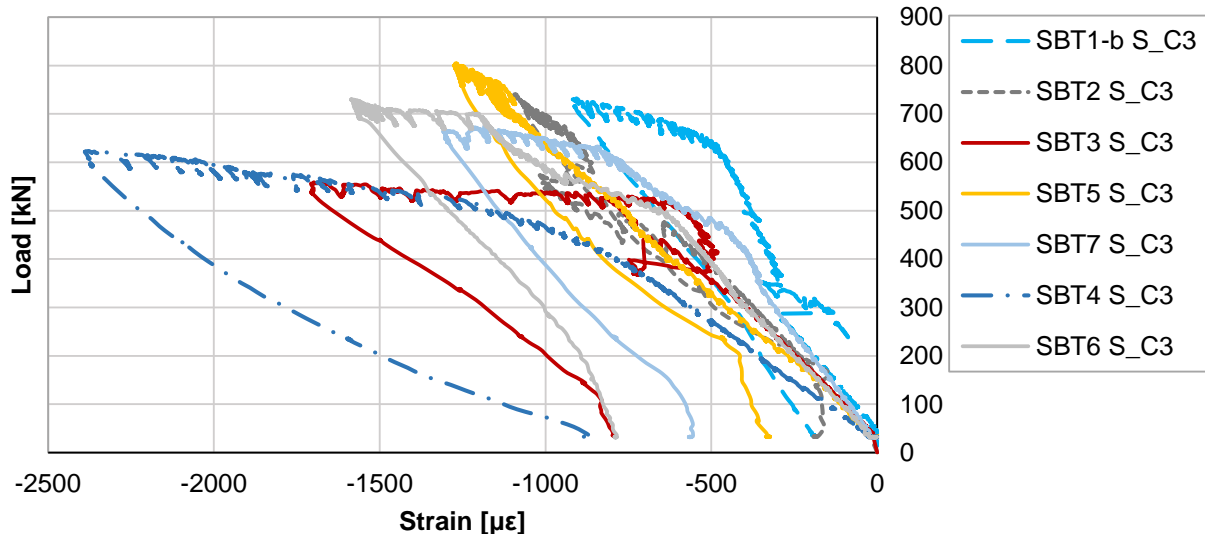


Fig. 2-14: Relationship between load and concrete strain

2.3.7 Conclusions

Eight shear beam tests were conducted at the University of Bradford, United Kingdom, to investigate the performance of slim-floor beams using innovative shear connectors. Different mechanisms contributing to the shear connection were taken into account, including the longitudinal shear resistance of individual connectors, clamping and friction effects. By comparing the results from specimens using different connector and loading arrangements, the contribution of different mechanisms could be assessed. The main conclusions drawn are as follows:

All of the slim-floor beams exhibited a very ductile response, undergoing a mid-span deflection exceeding span/50 despite some of the beams being designed with a comparably low degree of shear connection. Following conclusions have been made:

- Reinforcing stirrups did not make a significant contribution to the longitudinal shear resistance in the tested configuration
- Similar response of specimens under eccentric and concentric loading
- Specimens using transverse bars exhibited a similar load capacity and load-deflection behaviour to specimens using horizontally lying studs, for the shear beams tested in this study. However, differences were noted in the strain distribution, which may have a significant effect if studs are employed for other types of test set-up. It seems that the chamber gives a similar effect to a stirrup for the shear beams that were used in this study
- Pure friction and clamping action without mechanical connection achieved a degree of shear connection around 17 %
- The concrete dowel provides significant contribution to the longitudinal shear resistance, with specimens using larger web openings resisting a greater overall maximum load.
- The concrete cover above the steel top flange plays an important role in providing shear connection through clamping and friction effects.

2.4 Numerical Investigations

2.4.1 Introduction

Following the slim-floor shear beam tests carried out in the University of Bradford, FE models were developed and validated against the experimental observations. ABAQUS software [65] and with the concrete damage plasticity (CDP) material constitutive model have been used. After validation of the modelling method, a comprehensive parametric study was conducted, covering the dowel hole-diameters in the beam web, diameters of the rebar shear connectors and concrete strength grades. The parameter studies highlighted the structural behaviour and performance of the slim-floor composite beam systems [5].

2.4.2 Brief description of FE model

Non-linear finite element software ABAQUS was used to simulate the slim-floor shear beam specimens under applied loading. The ABAQUS general Standard/Riks analysis approach was employed in this modelling. Considering the symmetrical conditions of the tested specimen across the centre lines of the whole composite beam system, only a quarter of the geometry of the specimen was considered in the simulation to save computational time. The main components of the FE model included the concrete slab, steel beam, reinforcement steel mesh, rebar shear connectors passing the dowel holes of the steel beam web, shear studs welded at the steel beam web, additional reinforcement stirrups. All components were created separately and assembled together to form the shear beam, as tested in the University of Bradford. Fig. 2-15 shows a typical FE model.

The three dimensional eight-node solid brick element C3D8R with reduced integration was adopted to mesh the concrete slab, steel beam/bottom plate, shear connector rebar and shear studs (SBT6). The two-noded truss element T3D2 was used for the reinforcement steel mesh and reinforcement steel stirrups in specimen SBT1b. For the main components, the element size of 50 mm in the axial direction and 25 mm in the transverse direction was adopted based on the mesh sensitivity study giving best agreement compared with the experimental observation.

The appropriate contact interactions were defined between interacting surfaces of different components. For contact between the concrete slab and the steel beam section, the normal behaviour was assumed to be “hard”. The “penalty” method was used to define the tangential slip where a friction coefficient of 0.2 was adopted according to a sensitivity study. The reinforcement

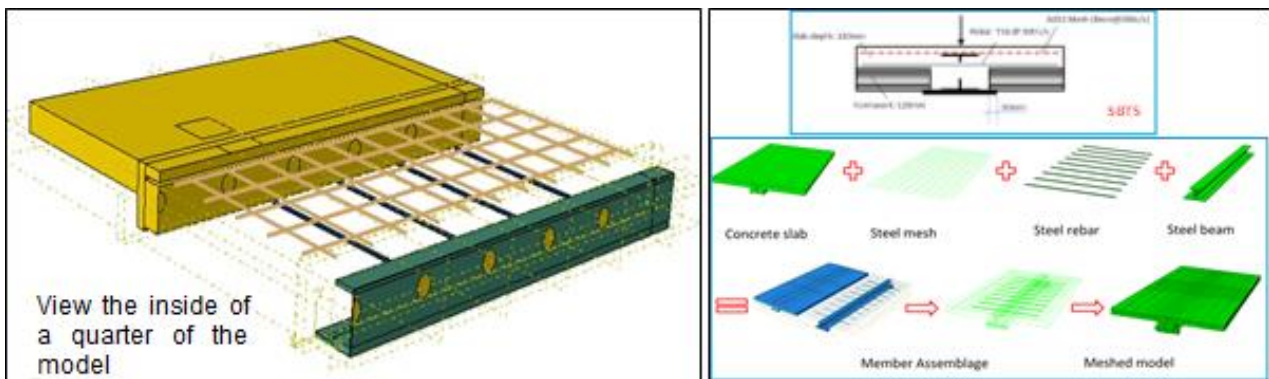


Fig. 2-15: FE model and assembly of a typical tested specimen (SBT5)

steel mesh, rebar shear connector and shear stud were “embedded” into the concrete slab to simplify the modelling. The loading procedure and other boundary conditions were completely based on the experimental programme.

2.4.3 Material Properties

Steel beam section including welded bottom plate was grade of S355 with Young’s modulus of 210 000 N/mm² and Poisson’s ratio 0.3 assumed. For the reinforcement steel mesh/rebar connector/stirrup, both the yield strength and the ultimate strength were assumed to be 500 N/mm², with a Young’s modulus of 210 000 N/mm² and a Poisson’s ratio of 0.3. For the shear studs, a yield strength of 420 N/mm² and ultimate strength of 610 N/mm² were used based on a test carried out in the University of Bradford.

For the concrete, the target grade for the tested specimens should be C25/30. However, the test day measurements showed that for most specimens the average cubic compressive strength was higher with a cubic compressive strength of 41.3-43.9 N/mm². For SBT4 and SBT6 the measured compressive strength was 34.1 N/mm². Therefore, in the FE modelling, average compressive strength of 42.5 N/mm² was adopted for SBT1 (a, b), SBT2, SBT3, SBT5 and SBT7. 34.1 N/mm² was adopted for SBT4 and SBT6. Concrete damage plasticity (CPD) constitutive model was employed and the concrete maximum tensile strength was assumed to be 10% of the maximum compressive strength.

2.4.4 FE model validation

The comparisons between FE predictions and experimental results show very good agreements. Fig. 2-16 compares the predicted mid-span deflection vs load relationships and end-slip vs load relationships with the experimental observations for typical tested specimens SBT5 and SBT7. The FE prediction clearly captured the main load-deflection and load - end-slip behaviour. Fig. 2-17 compares the visible deformation of the slim-floor composite beam system including the mid-span vertical deflection and end-slip between the steel beam section and wrapped concrete, and crack distribution/development. The FE modelling successfully captured these features. The FE model can be used for the simulation of similar composite beam systems and to carry out the parametric study.

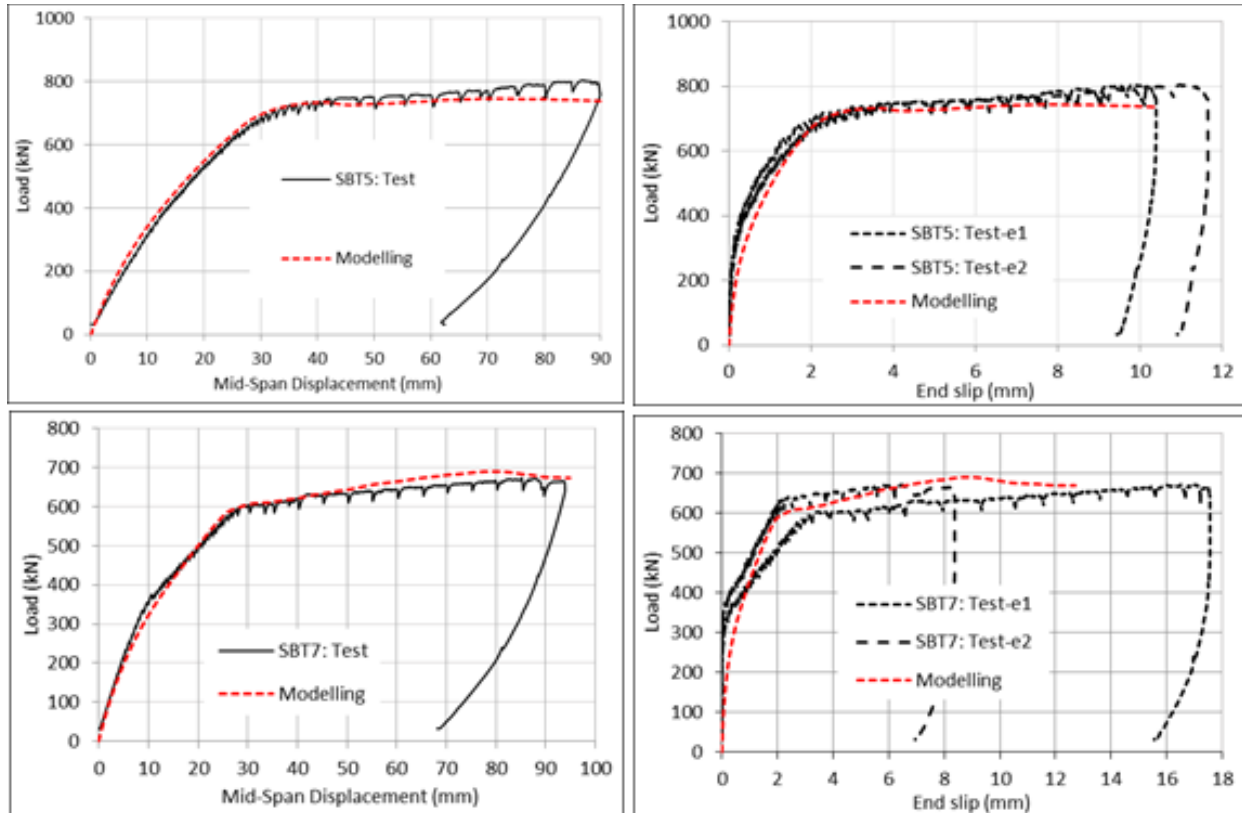


Fig. 2-16: Comparison of end-slips obtained from FE prediction and test observation



Fig. 2-17: Comparing predicted concrete slab crack/damage pattern and composite beam end-slip with those observed

2.4.5 Parametric study

2.4.5.1 Effect of dowel hole-diameter on the load capacity

The difference between SBT1a, SBT1b, SBT2 and SBT5 was the dowel hole-diameter in the steel beam web for the rebar connector being different. The experimental results clearly indicated the higher capacity of SBT5 due to adoption of a bigger dowel hole-diameter. Therefore to investigate the effect of the concrete dowel shear to the loading capacity of the beam system, a parametric study was carried out by FE models on the following dowel hole-diameters: 0 mm (no dowel-hole used and therefore no rebar shear connector in this case), 40 mm, 80 mm, 100 mm, 120 mm and 160 mm. The model feature parameters were completely based on specimen SBT 5, in which the concrete cubic compressive strength employed was 42.5 N/mm² (cubic compressive strength), the rebar diameter was 16 mm and it was centrally loaded.

Fig. 2-18 compares the load to the mid-span deflection curves and load to the end-slip behaviours of slim-floor beam systems with different dowel hole-diameters. Different dowel hole-diameters resulted in different beam performance. The composite beam without dowel holes, thus without rebar connectors, has the lowest load capacity. The beam systems with dowel hole of diameters ranging from 80 to 120 mm have higher load capacities followed by the beam systems with dowel hole-diameters of 40 or 160 mm.

The experimental study also investigated the effect of the rebar connector on the slim-floor beam systems by SBT5 and SBT7. Compared with SBT5, SBT7, without the use of rebar connectors although the dowel hole-diameter the same, had lower capacity.

Another parametric study was carried out considering the effect of the dowel hole-diameter on the beam system without rebar shear connectors. The FE models were completely the same as those FE models for the beam system with rebar shear connectors, except that the rebar shear connectors were removed. The comparison is shown in Fig. 2-19. As expected, different dowel hole-diameters resulted in different composite beam capacities. The composite beam without a dowel hole ($D = 0$ mm) has the lowest load capacity. The beam systems with dowel hole-diameters of 80-120 mm have higher load capacities followed by beam systems with dowel hole-diameters of 40 or 160mm.

Fig. 2-20 compares the load-bearing capacities of composite beams with different dowel hole-diameters at 30 mm and 60 mm mid-span deflections. The use of shear connector bar, the beam systems with dowel holes of 80-120 mm have higher resistance and might be adopted in practice, but 100 mm dowel holes with rebars might be the best. It has been noticed that beam systems using solid steel sections have the lowest load capacity due to lack of dowel shear resistance.

Certainly, besides the concrete dowel action, rebar shear connector provided effective shear resistance. Therefore the load capacity of beam systems with rebar is higher than those without rebar. Clearly, for the beam system with the largest hole of 160 mm, the resistance from shear connector increased while the resistance from the steel section itself reduced. Therefore, the optimum beam system needs to consider both steel section and dowel resistance.

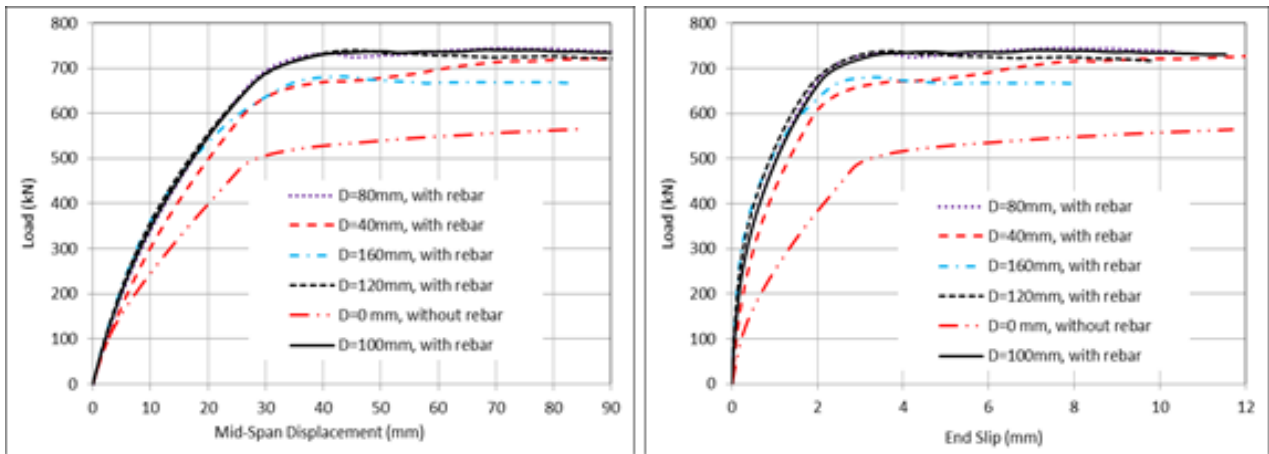


Fig. 2-18: Comparison of shear beam with different web dowel hole-diameter (with rebar T16)

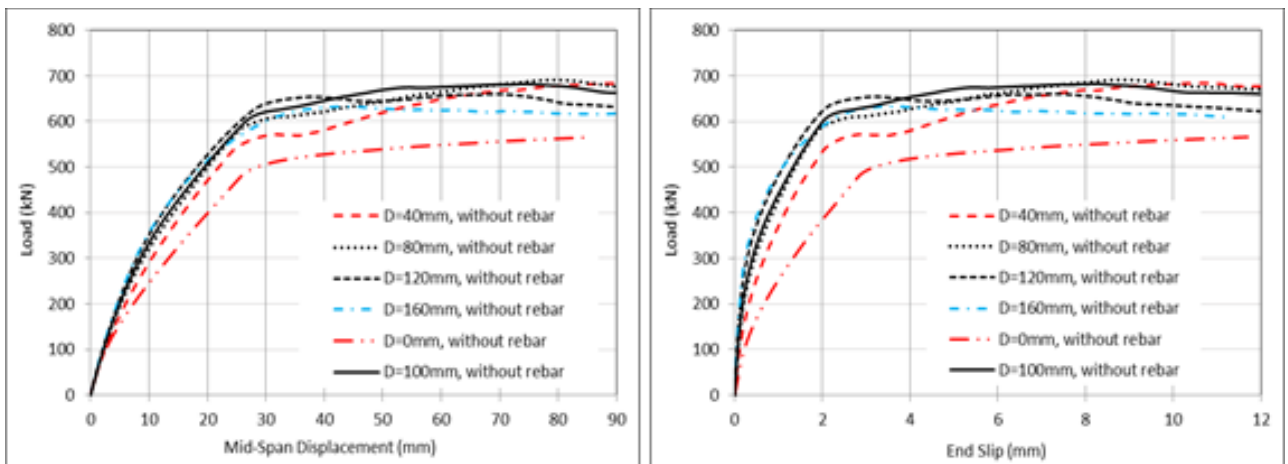


Fig. 2-19: Comparison of shear beam with different web dowel hole-diameter (without rebar)

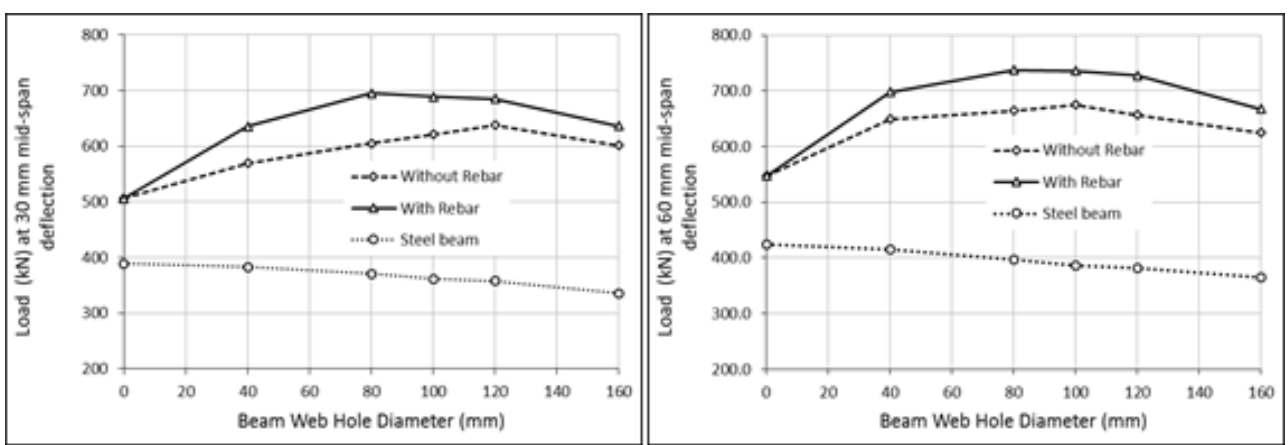


Fig. 2-20: Comparison of loading capacity of composite beam with different dowel hole-diameters at 30/60 mm mid-span deflection

2.4.5.2 Effect of diameter of rebar shear connector to the load capacity

To further investigate the influence of the rebar on the beam behaviour, a parametric study was conducted. The FE models were based on SBT5 and four rebar diameters: 12 mm, 16 mm, 20 mm and 24 mm, were considered.

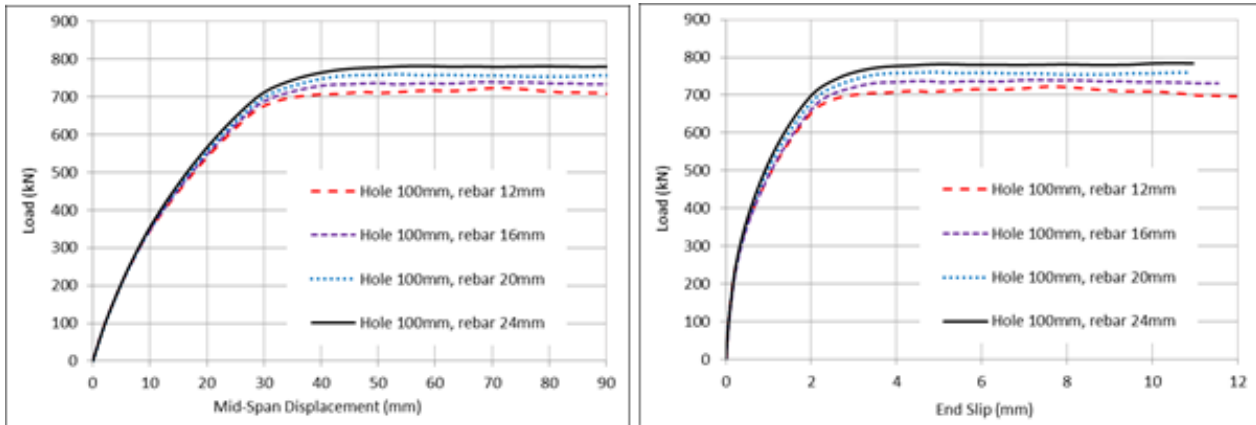


Fig. 2-21: Load vs mid-span deflection and end-slip of beam systems with different rebar diameters (the dowel hole-diameter 100mm)

Fig. 2-21 shows the load vs. mid-span deflection relationship and load vs. end-slip relationship of composite beam systems with 4 different rebar diameters. With increasing rebar diameter the load-bearing capacity increases. Fig. 2-22 further compared the load capacity at 30/60 mm mid-span deflections and 6 mm end-slip. At 30 mm mid-span deflection, the load capacity increased by about 2% for every 4 mm increase in bar diameter. At 60 mm mid-span deflection, the load capacity increased by about 3% when the bar diameter increased by 4 mm.

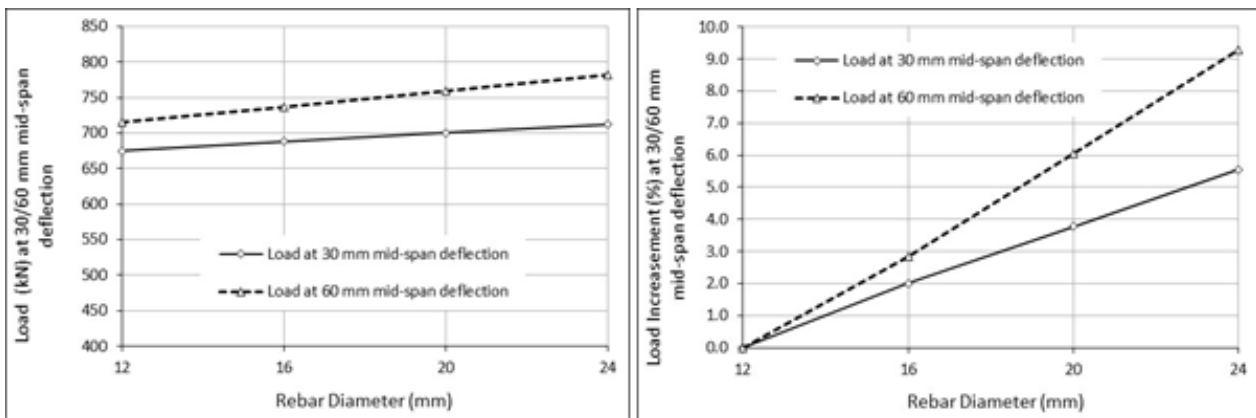


Fig. 2-22: Effect of rebar diameter on the load-bearing capacity (the dowel hole-diameter 100mm)

2.4.5.3 Effect of concrete strength on the load capacity

The experimental programme did not investigate the effect of concrete strength on the composite beam behaviour. Therefore a parameter study, considering only changes in the concrete strength, was performed to investigate the effect of concrete. The FE models were completely based on different tested specimens in the test programme. Four different concrete grades were employed in the parametric study, their cylinder compressive strengths were assumed to be 20 N/mm², 30 N/mm², 40 N/mm² and 50 N/mm².

Fig. 2-23 presents typical load vs. mid-span deflection and load vs. end-slip curves of the composite beam system with different concrete strengths adopted. As expected, the higher the concrete strength, the higher the beam stiffness and the higher the beam load-bearing capacity. Fig. 2-24

further compares the different effects of concrete strength on different composite beams. As observed from the experimental study, regardless of what concrete grade was used, SBT1b, SBT2 and SBT5 possess higher load capacity, followed by SBT6, and then SBT4. SBT3 has the lowest loading capacity. The comparison clearly shows the importance of the rebar shear connector and concrete dowel (cylinder) shear resistance.

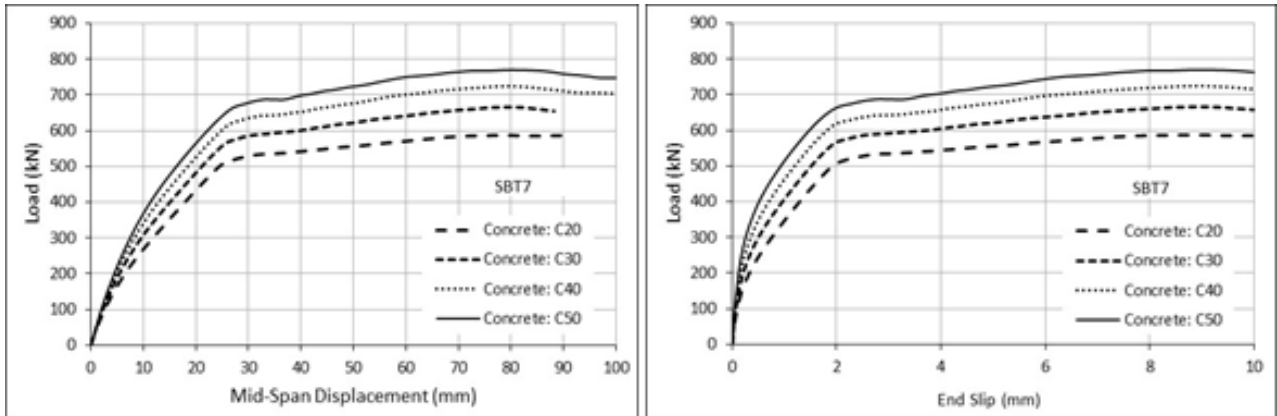


Fig. 2-23: Load-mid span deflection/end-slip curves of SBT5 with varying concrete strength

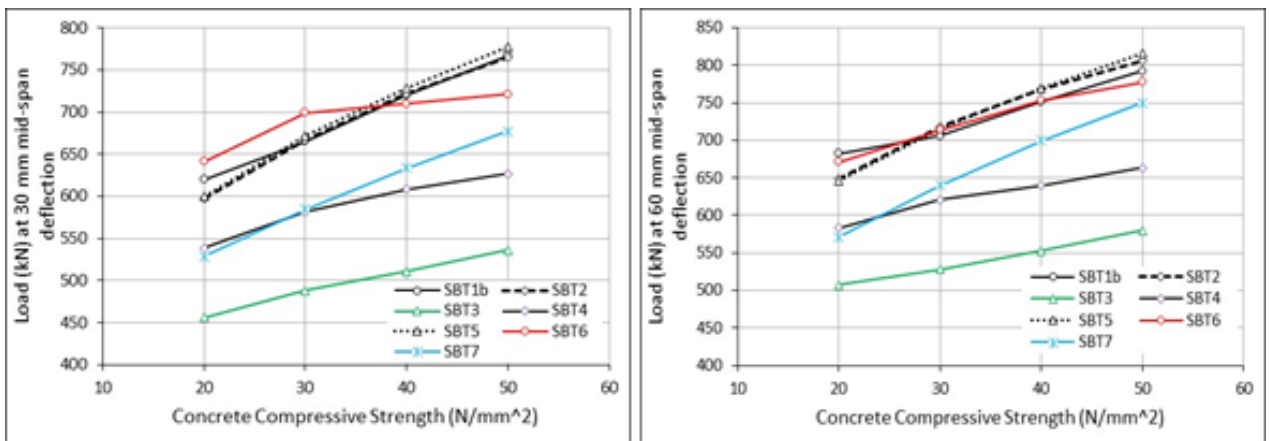


Fig. 2-24: Effect of concrete strength on the load capacity of different specimens at 30mm and 60mm mid-span deflection

2.4.6 Load-bearing behaviour

Based on the numerical simulation, comparison and analysis, the following structural behaviour and performance of slim-floor composite beam systems are highlighted.

- The dowel hole in the steel beam web played an important role in the load-bearing capacity of the slim-floor beam system. The larger the hole, the higher the shear resistance that was provided by the concrete cylinder. However, since the larger hole caused more area reduction to the web of the steel section, it reduced the load-bearing capacity of the steel section, and therefore for the tested slim-floor composite beam system, the optimum hole-diameter is recommended to be from 80 mm to 120 mm based on the limited cases considered in this study. The 100 mm dowel hole might allow the beam system to have the best load-bearing capacity and structural performance regardless of whether rebar shear connectors are adopted or not.
- The diameter of the incorporating rebar shear connector affected the load-bearing capacity. For the tested slim-floor beam system, considering a rebar diameter ranging from 12 mm to 24 mm, the load-bearing capacity increased by 2-3 % if the rebar diameter increased by 4 mm.
- The concrete strength had a significant effect on the load-bearing capacity and slip behaviour. The higher the concrete strength, the higher the load-bearing capacity reached by the composite shear beam system

2.4.7 Conclusions

The Finite-Element-model developed through ABAQUS software could be used to capture the main structural behaviour and failure modes of the slim-floor shear composite beam including load-bearing capacity, deflection, slip behaviour and concrete cracking distribution etc. The effect of the dowel hole, diameter of the rebar and concrete strength on the load-bearing behaviour on shear beams ($L = 4$ m) have been investigated.

2.5 Influence of the shear connectors on the load-bearing behaviour of slim-floors

2.5.1 Comparison between push-out and shear beam tests

The comprehensive testing programme with similar geometric and material parameters allows a direct comparison between push-out- and shear beam tests, especially regarding the shear load-bearing behaviour.

Highlighting the effect of the shear connector capacity on the load-bearing of the shear beams exemplary tests with diameter 40 and 80 mm holes in the web of the steel are presented. Fig. 2-25 shows the load – mid-span deflection of shear beam tests with diameter 40 and 80 mm holes in the web. Bigger holes led to increasing load-bearing capacity. In the corresponding push-out tests the maximum load was achieved by the smaller diameter holes, as indicated by Fig. 2-26. Regarding the maximum loads push-out and shear beam tests differ from each other.

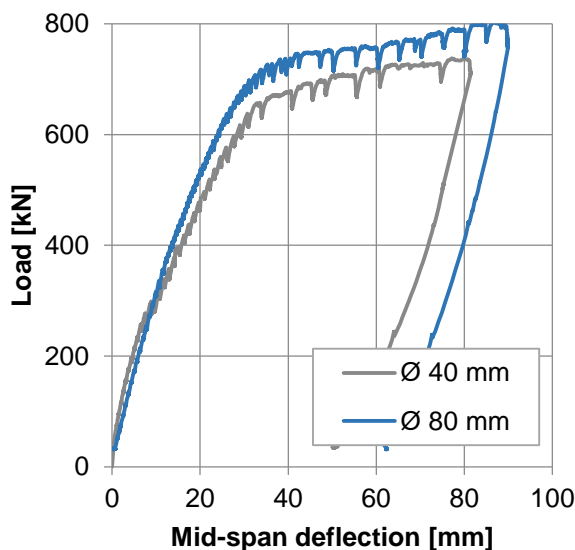


Fig. 2-25: Shear beam tests – Load - Mid-span deflection

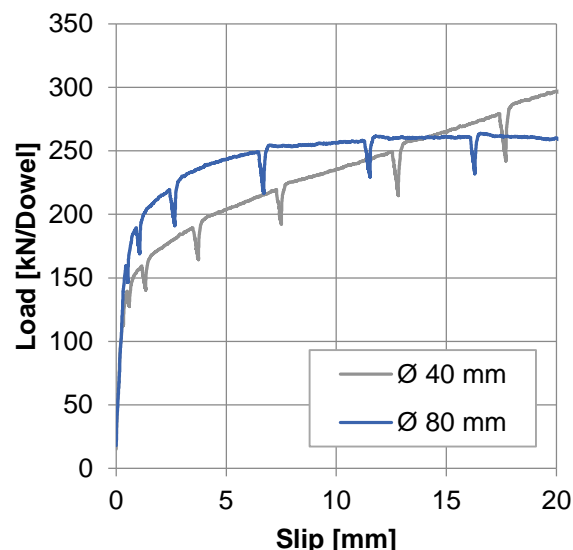


Fig. 2-26: Push-Out tests - Load-slip behaviour

Fig. 2-27 shows the corresponding end-slip to the load – mid-span deflections in Fig. 2-25. For comparison 8 mm are marked. Assuming the end-slip in the shear beam tests introduced the same slip for the connections, 8 mm are marked in Fig. 2-28 showing the load - slip behaviour of the corresponding push-out tests. At slip 8 mm the push-out tests with 80 mm holes reached a higher level of load-bearing than the 40 mm holes.

Therefore, the 80 mm holes activated more shear load in the shear beams at 8 mm slip. Consequently, a higher load capacity can be achieved in a beam test configuration.

Eurocode 4 considers the maximum load of shear connectors. The characteristics of individual connectors are unconsidered, what is a sufficient assumption for composite beams of normal height. Whereas the presented comparisons between the conducted tests show, that the load-slip-behaviour of connectors affects the load-bearing of slim-floor beams.

In a shear beam test configuration additional mechanisms affect the shear transfer, e.g. clamping and friction as shown in section 2.3 and 2.4

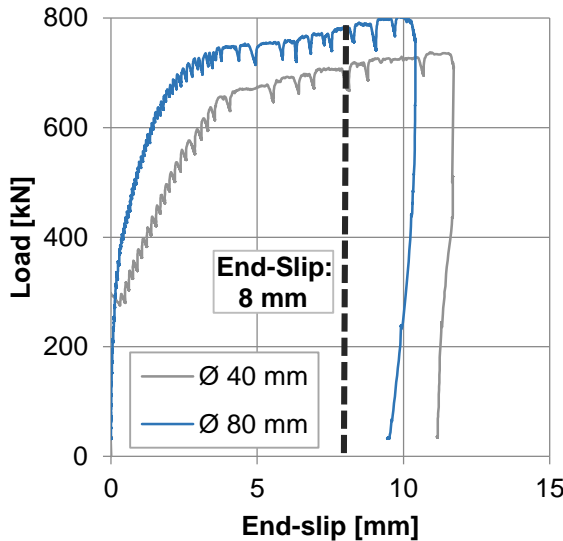


Fig. 2-27: End-slip in shear beam tests

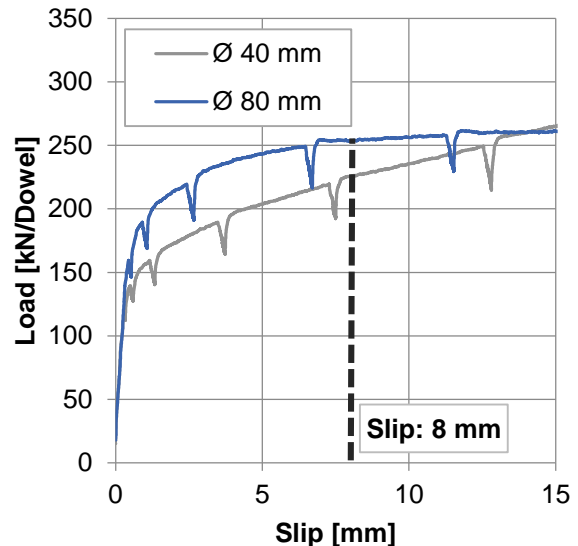


Fig. 2-28: Push-Out tests - Load-slip behaviour

2.5.2 Influence of flexibility of shear connectors

Previous studies on slim-floor constructions have been conducted by Hauf [64]. Based on various beam tests, among others with hat profiles and headed studs as shear connectors an analytical model has been developed to calculate the behaviour of slim-floor construction in serviceability limit state (SLS).

The developed model assumes a rigid shear connection between steel profile and concrete slab. Subsequently a monolithic cross section is assumed, fulfilling the Bernoulli hypothesis. Concrete cracking as well as bending and membrane stiffness of the concrete slab are taken into account (see Fig. 2-29). The beam is split into a number of elements. A $M-\kappa$ -curve is calculated for each element including its position as well as the mentioned effects (see Fig. 2-30 and Fig. 2-31). Using the calculated $M-\kappa$ -curve the deflection of the beams is determined. The presented model showed good accordance with the conducted tests [64].

The load-bearing behaviour of beam test 3 (BT3) has been recalculated by Rinke [36] with the analytical model by Hauf [64] assuming rigid shear connection. BT3 has been designed to 100 % degree of shear connection using transverse reinforcement bars as shear connectors (see sec. 3.2). All shear beam tests have been designed to less than 100 % degree of shear connection.

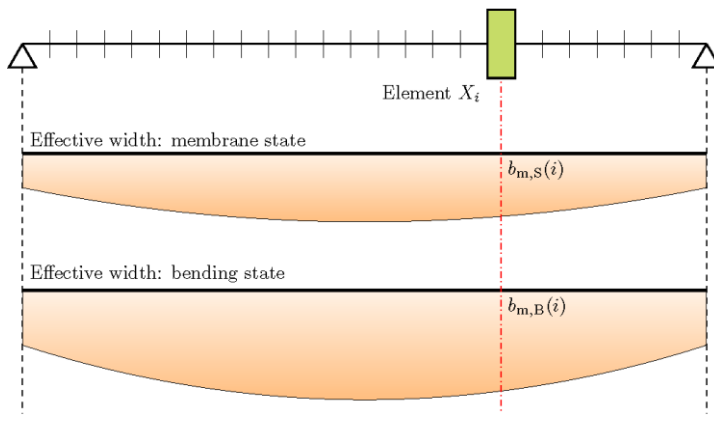


Fig. 2-29: Discretization and distribution of membrane and bending state for a one span girder [64]

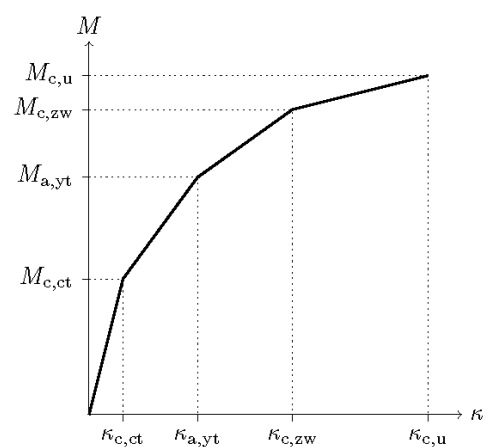


Fig. 2-30: $M-\kappa$ -curve for positive bending [64]

Fig. 2-32 compares the load - mid-span deflection curve of BT3 with the calculated curve by the analytical model. As shown the assumed rigid shear connection for the conducted flexural beam tests is only valid in the initial loading phase. Within this phase a monolithic cross-section can be assumed due to bonding between steel profile and the concrete slab. When adhesive bonding releases and merges to sliding friction the shear connectors are activated. Shear load might be transferred by the developing friction, contributing to the overall load-bearing behaviour of slim-floor beams. Determination of friction is only indirectly possible by experimental investigations. Within the numerical investigations of the shear beams in section 2.4 Coulomb frictional coefficient of 0.2 has been assumed, leading to good accordance with the tests.

Non-rigid or flexible shear connectors influence the load-bearing behaviour of shear beams. They lead to reduced stiffness of slim-floors compared with rigid shear connectors.

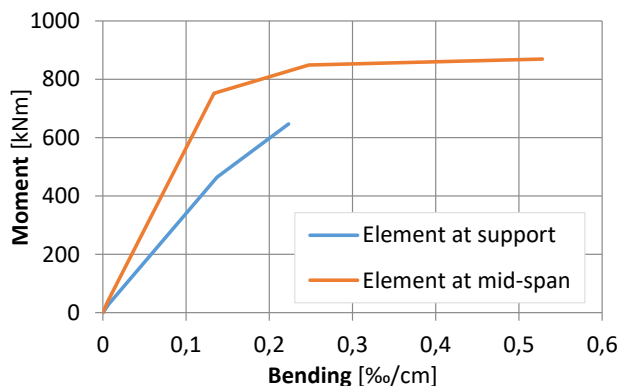


Fig. 2-31: M- κ -curve for different elements according to their position [36]

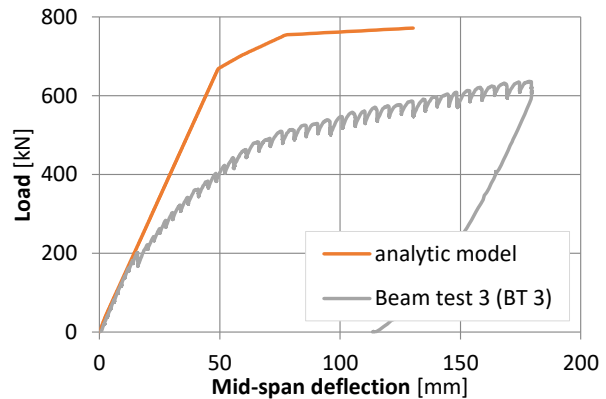


Fig. 2-32: Recalculation of beam test 3 (BT 3) assuming rigid shear connection [36]

2.6 Conclusions

The shear connector behaviour in slim-floor beams has been investigated experimentally, numerically and analytically. 30 push-out tests and 8 shear beam tests have been conducted to determine the load-bearing behaviour of concrete dowel shear connector systems in slim-floor beams. Geometrical and material parameters have been chosen accordingly for comparison reasons.

The load-bearing behaviour of the CoSFB concrete dowel shear connector system depends mainly on the diameter of the reinforcement bars conducted through the holes in the profile web. The concrete grade must be chosen appropriately depending on the rebar diameter to reach bending within the reinforcement bars and prevent excessive concrete cracking or a pure shear failure of the rebars.

Shear beams behave very ductile under loading. The configuration of the shear connection has major effect on the load-bearing, especially in ultimate limit state. The stiffness of the beams is influenced by the flexibility of the shear connectors. Reinforcing stirrups did not seem to make a significant contribution to the behaviour. Additional test series are needed to verify this observation. Friction and clamping action achieved a remarkable degree of shear connection. The size of the concrete dowel provides significant contribution to the longitudinal shear resistance. The concrete cover above the steel top flange plays an important role in providing shear connection through clamping and friction effects.

3 FLEXURAL BEHAVIOUR OF SLIM-FLOOR BEAMS WITH INNOVATIVE SHEAR CONNECTORS

3.1 General

The flexural behaviour of slim-floor beams has been investigated to improve present structural models for composite action. Therefore the design of the pure steel profile according to Eurocode 3 has been evaluated and adapted to slim-floor beams. The validity of plastic stress block design as well as strain based design has been determined. Therefore, various beam tests as well as numerical investigations have been conducted.

3.2 Experimental investigations on flexural beams

3.2.1 Introduction

Work Package 3 comprises flexural tests on a series of slim-floor beams, each with a span of 6 metres. These specimens used similar shear connectors and testing arrangements to the shear beams in Work Package 2, but were designed to fail in flexure. Different degrees of shear connection were explored in addition to variations in the connector type, loading and slab thickness [7].

3.2.2 Test specimens

The specimens tested in flexure were as follows:

- BT1a: basic test configuration (40% Shear connection): This test beam is used for long-term tests, see Work Package 4. The test results will also be used for analysis of the structural behaviour at ULS.
- BT1b: basic test configuration without shear connectors, uniform distributed load (udl)
- BT2: eccentric loading
- BT3: 100% shear connection
- BT4: 25% shear connection
- BT5: no top cover
- BT6: no shear connector
- BT7: horizontal studs as shear connectors
- BT8: large openings, without shear connector

A typical cross-section is presented in Fig. 3-1. All specimens comprised a HEB200 steel section welded onto a 400 × 15 mm steel plate, embedded in a 2 m wide concrete slab, with a total depth of 240 mm (upper portion depth of 120 mm). A252 mesh reinforcement was placed below the top

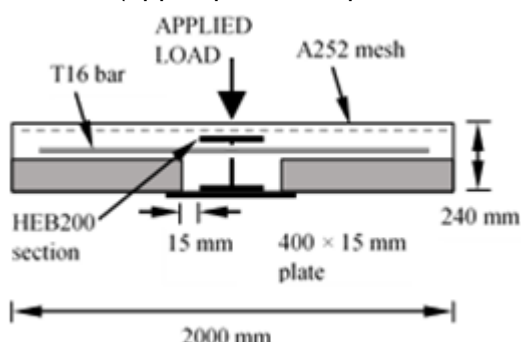


Fig. 3-1: Typical beam cross-section

surface of the concrete slab. All specimens apart from BT1b, BT6 and BT7 had transverse bars passing through holes in the HEB section web, to provide shear connection between the steel and the concrete.

3.2.3 Test set-up and instrumentation

Each specimen had an overall length of 6 m. The specimens were tested in a similar test-rig to the shear beam tests in the previous section. Load was applied at two locations along the beam length, 2.25 m from the supports. Load was applied in 20 kN increments during the early stages of the test, switched to 5 mm deflection increments in the later phases as the load began to reach a plateau. The load/displacement was increased until failure occurred, as evidenced by cracking of the concrete, yielding of the steel, or the inability of the beam to resist any further increase in load. These items will be discussed in subsequent sections.

11 LVDTs were employed to measure deflections of the beams: 9 of these were placed underneath the specimens to measure vertical deflection and one LVDT was positioned at each end to measure the end-slip. Strain gauges were also used to measure the strains in the top flange of the HEB section, the bottom steel plate, the shear connectors, the top surface of the concrete slab, and in some cases, the web of the HEB section. A test specimen and some of the instrumentation used is presented in Fig. 3-2.

For each test specimen, the concrete compressive strength was measured at 28 days and on the test date using 100 mm cube specimens, while the tensile strength was measured on the test date using a split-tensile test. The concrete compressive strengths varied between the specimens, with BT1(b) having the lowest strength, at 27.5 N/mm², following by BT2 at 35.6 N/mm² and BT5 at 38.4 N/mm². The compressive strengths for the other specimens were all between 41.0 and 47.9 N/mm², with BT6 and BT8 having the highest compressive strengths. The tensile strengths ranged from 1.9 N/mm² to 2.7 N/mm².



(a)

(b) & (c)

Fig. 3-2: Specimen BT3 at beginning of test: (a) Test-specimen in rig; (b) LVDT underneath to measure vertical deflection; (c) LVDT to measure end-slip

3.2.4 Load-deflection response

Overall, the nine specimens exhibited fairly similar behaviour during the test. The relationship between moment (total applied load/2 × 2.25m) and mid-span deflection, shown in Fig. 3-3, was initially fairly stiff and linear. At around 200 - 250 kN, depending on the specimen, some initial cracks occurred. A drop in load was noticed in some specimens, which was more pronounced in BT4 than in the other cases. As the applied load increased the stiffness suddenly reduced, to approximately

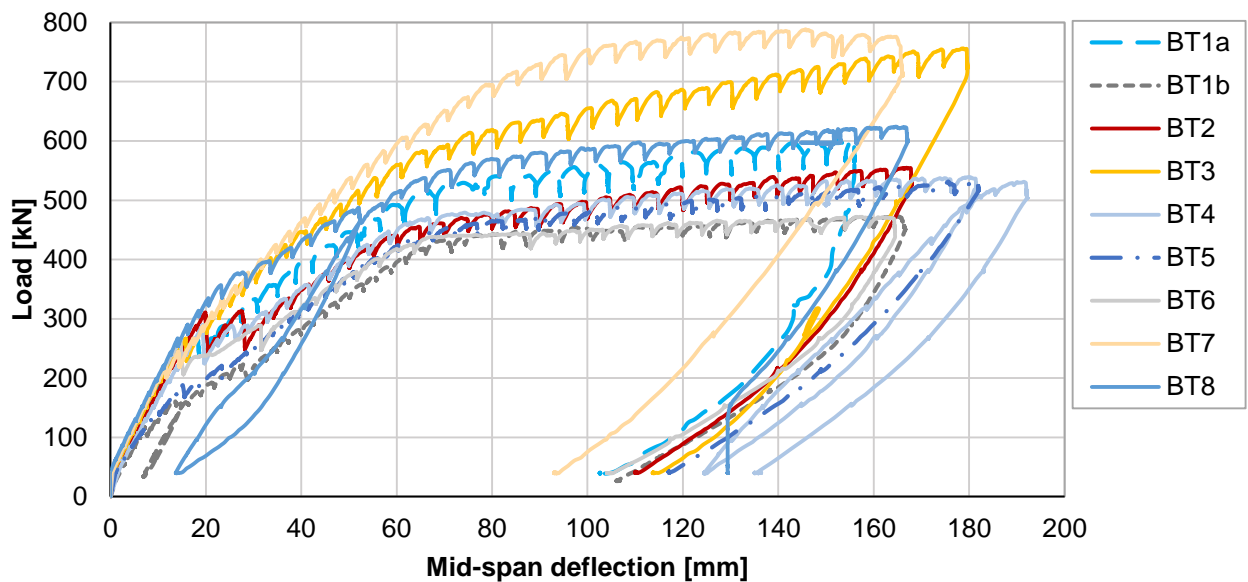


Fig. 3-3: Relationship between moment and mid-span deflection

half of the original stiffness in some cases. As the load was increased further, the mid-span deflection continued to increase, along with the crack widths. Cracks, as seen on the side of the concrete slab, are presented in Fig. 3-4. During the final phase of the test, the stiffness reduced further, as the load reached a plateau, and the test was continued for each of the four specimens until they could withstand no further load. Due to some issues with instrumentation and loading set-up, specimen BT4 was unloaded and reloaded again at the end of the test and BT8 was unloaded and reloaded at an earlier stage of the test. This did not affect the load-deflection relationship and the load returned to the same magnitude upon reloading.

Specimens BT1b and BT6, without any shear connectors, resisted the lowest bending moment. The type of load distribution had some influence on performance, with BT1b (distributed load) appearing to be less stiff and resisting a lower bending moment in the earlier stages of the test than BT6. However, these became more similar during the later stages, when the load resistance in both specimens reached a plateau. Specimen BT5 (no top slab) exhibited a similar response to BT1b in the earlier stages of the test, but reached a higher maximum load at the beginning of the plateau. Specimens BT5, BT4 (25% shear connection) and BT2 (eccentric load) all exhibited similar levels of load resistance. The opportunity to use different degrees of shear connection was exploited for the bending tests and showed that the performance of BT5, with no topping and a 33 % reduction in slab depth was similar to that of a specimen with few transverse bars, designed for 25% shear connection (BT4). The use of eccentric loading instead of concentric loading did not have a noticeable



Fig. 3-4: Cracking in concrete for specimen BT3

effect on the load capacity for shear beam tests in sec. 2.3. But in the bending tests eccentric loading clearly reduced the moment capacity of the beam. BT2, loaded eccentrically and designed for 40 % shear connection, exhibits a similar moment resistance to a concentrically loaded specimen designed for 25% shear connection (BT4).

BT3, designed for 100% shear connection, resisted a significantly higher maximum moment (756 kNm) than the basic specimen BT1a (604 kNm), that was designed for 40% shear connection. BT3 also displayed a steady increase in moment up to the end of the test, while the moment resistance of the other specimens had reached a plateau. Specimen BT8, also exceeded the maximum moment resistance of BT1a, by 20 kNm, demonstrated that using a larger concrete dowel can increase the degree of shear connection and moment resistance of slim-floor specimens. An increase in resistance had also been noted in the previous shear beam tests, when larger concrete dowels had been used. In the shear beam series, using an 80 mm diameter concrete dowel instead of a 40 mm dowel increased the estimated degree of shear connection from 52.3 % to 64.4 %, although it was concluded that this larger dowel may have reduced the extent of friction/clamping action between the steel and concrete in the beam.

Surprisingly, BT7, which was constructed using shear studs instead of transverse bars, resisted a significantly higher moment than BT1a, by over 33%. In the previous shear beam tests, no significant difference was noticed in terms of maximum load between the specimens using transverse bars and the specimens using studs.

3.2.5 End-slip

Fig. 3-5 presents the relationship between moment and end-slip for each of the test specimens. In all cases, the degree of end-slip was very low during the initial phase of the test, and then increased rapidly during the second and third phases. For most specimens, the end-slip was very visible by the end of the test. With the exceptions of BT7 and BT6, in most cases, the maximum end-slip was between 10 and 20 mm, and similar values were measured at each end. These values were significantly larger than the 6 mm value of slippage stipulated by Eurocode 4 for ductile shear connector behaviour. For BT6, with no shear connectors, the measured end-slip appeared to be larger at one end (shown), although the slip measured at the other end was similar to that of the majority of specimens. For BT7, the measured end-slip was much lower than that for the other specimens, suggesting that the studs provided a stronger connection between the steel and concrete than the transverse bars used in the other specimens.

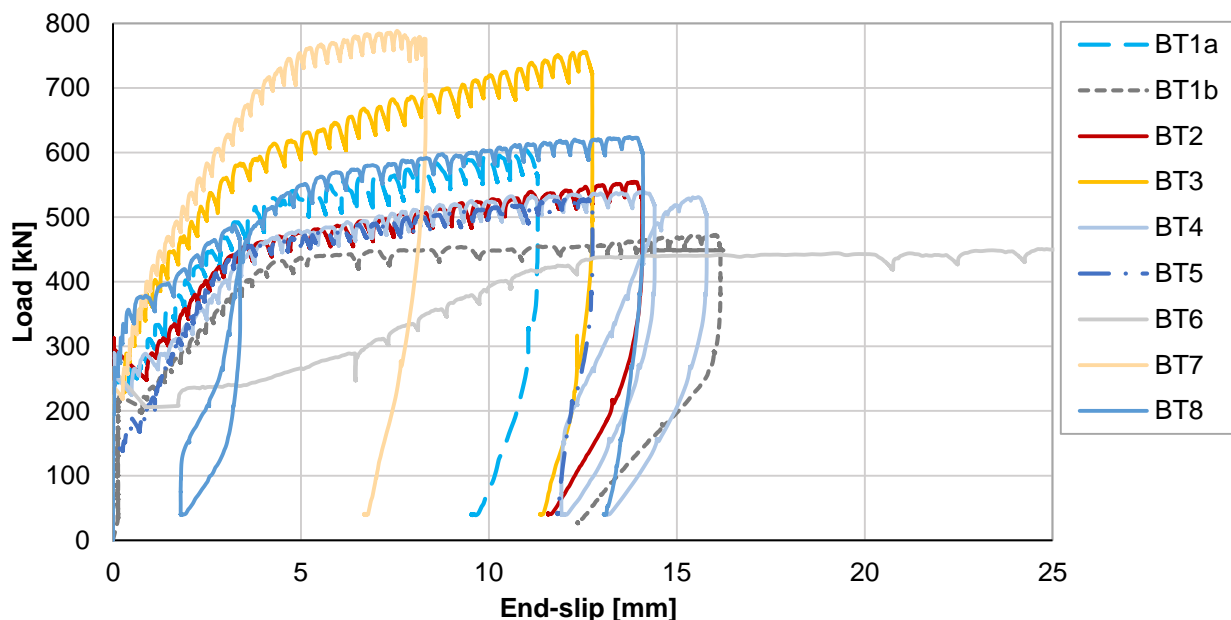


Fig. 3-5: Relationship between moment and end-slip

3.2.6 Measured strains

The strains in the top flange and bottom plate were measured at the mid-span and at the loading points, with slightly larger strains measured at the loading points. The strains measured at the loading points for the top flange and bottom plate are presented in Fig. 3-6 and Fig. 3-7.

In most specimens, the top flange of the beam reached the yield strain in compression before the end of the test. The only exception was BT7, which achieved strains of approximately $1000 \mu\epsilon$ in five of the six monitoring points. The strains in the bottom plate reached or surpassed the value associated with yielding in tension during the later stages of all of the tests, with the largest occurring in BT7. BT3 and BT5 also had large strains in the bottom flange. The strains measured in the web were mainly compressive, and smaller in magnitude than those in the top flange.

For the majority of specimens, the strains measured in the concrete reached a maximum value between 1000 and $1500 \mu\epsilon$, which was lower than the value associated with yielding of the material.

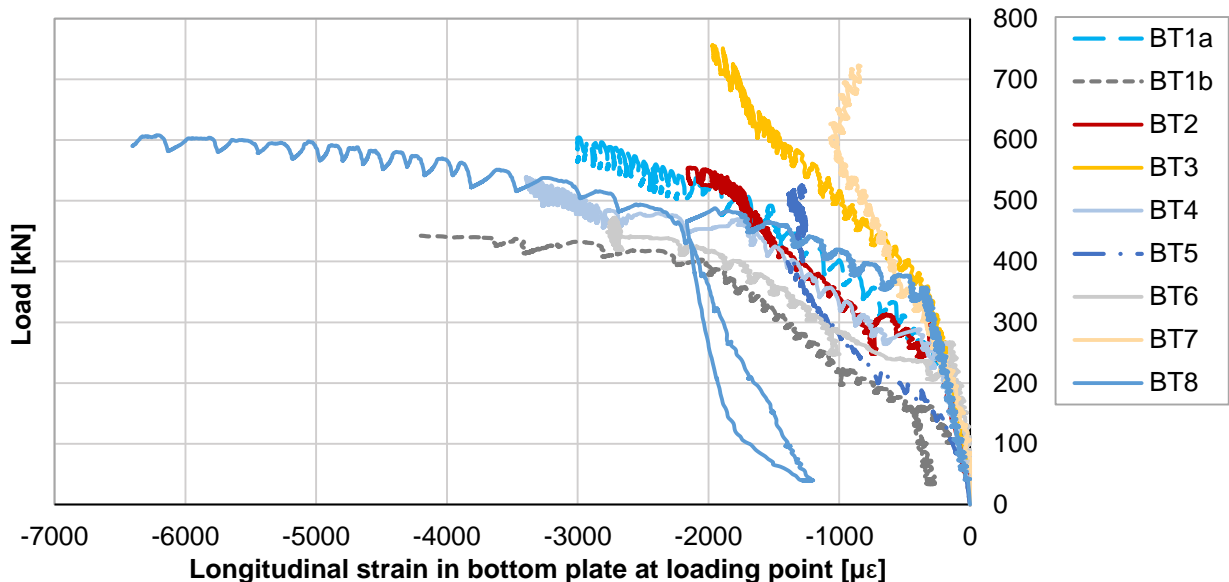


Fig. 3-6: Strains measured in top flange at loading point

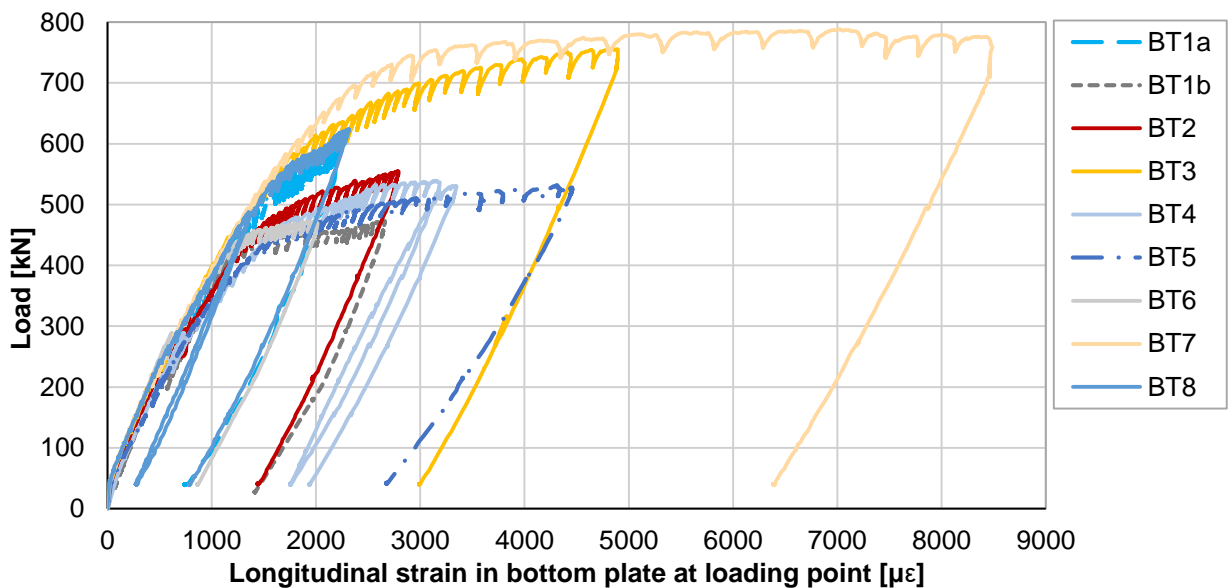


Fig. 3-7: Strains measured in bottom plate at loading point

Specimen BT7 exhibited slightly larger strains, with strains at one of the monitoring points exceeding $2000 \mu\epsilon$ and the strains at the other two monitoring points almost reaching $2000 \mu\epsilon$. The different strain profile in BT7 could be explained by the fact that it employed horizontally lying studs, instead

of transverse bars, as shear connectors. The higher concrete and lower top flange strain suggest that a higher degree of shear connection was attained, with less slippage, which also accounts for the higher moment resistance. However, the response was noticeably less ductile than that of the other specimens, as seen in the end-slips presented in Fig. 3-5. Generally, the beam specimens with the transverse bars performed well, with the strains in the top flange and bottom plate reaching the yield strain before the specimen failed. All specimens achieved a maximum mid-span deflection of span/40 while maintaining the high load plateau.

3.2.7 Shear connectors

For the majority of the specimens, the shear connectors comprised the transverse steel bars and the concrete dowel that surrounded each bar where it passed through the HEB web hole. As the concrete slab began to move relative to the steel beam, the steel bars and the concrete dowel resisted this shearing action and transferred the longitudinal stresses to the steel beam, maintaining composite action between the two components. In all specimens the shear connectors had very low strains during the initial phase of the test, which increased rapidly during the second phase showing that they had been ‘activated’ in transferring stresses between the concrete and steel, as the movement between the components caused the bars to deform. Although the greatest strains tended to occur in the bars closer to the ends of the beam, within the ‘shear-span’, notable strains were also observed in the connectors in the mid-span, suggesting that these also contributed to the shear connection.

3.2.8 Degree of shear connection

Beam specimens with different design degrees of shear connection were considered in this research. Fig. 3-8 (a) and (b) show the trend between the design degree of shear connection and the maximum bending moment and end-slip respectively for specimens BT1a (40% shear connection), BT3 (100 % shear connection), BT4 (25% shear connection) and BT6 (no shear connection). The end-slip decreased with an increase in shear connection while the maximum moment resisted increased almost linearly with an increase in degree of shear connection.

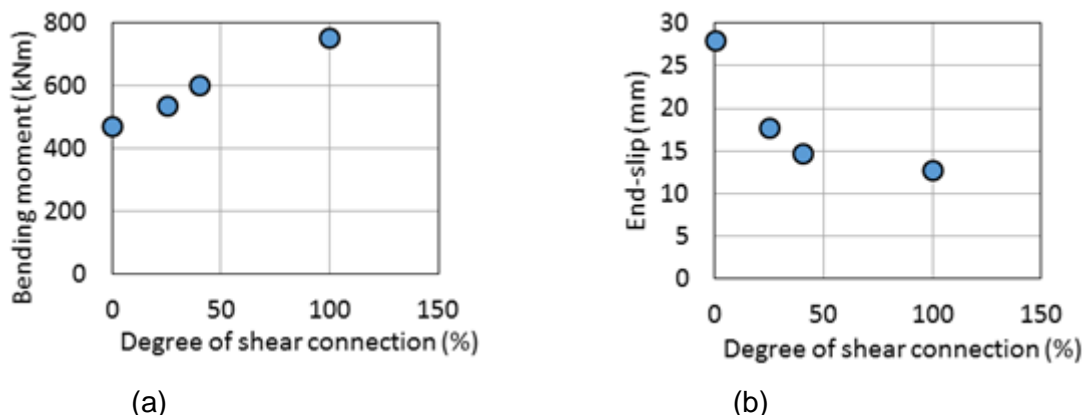


Fig. 3-8: Influence of degree of shear on (a) bending moment; (b) end-slip for slim-floor beams in flexure

3.2.9 Conclusions

This section presented the results of a series of bending tests for slim-floor beams. The main conclusions that were drawn from the tests are as follows:

- The beams behaved in a ductile manner, achieving a total deflection exceeding span/40 and end-slips greater than 6 mm prior to failure.
- Transverse bars passing through holes in the steel beam web proved to be effective shear connectors and the size of the web hole affected the overall resistance.

- Applying the load at an eccentricity from the centre of the cross-section had some effect on the performance, when compared with applying the load concentrically.
- The use of larger concrete dowels clearly enhanced the performance of the slim-floor beams.
- A beam subjected to distribute loading displayed a similar performance and moment resistance to that under point loads, although some differences were observed in the strain profile and slippage.
- Test specimens were designed for four different degrees of shear connection. Clear trends were observed in relationships between degree of shear connection, end-slip and moment resistance.

3.3 Numerical investigations on flexural beams

3.3.1 Introduction

The Finite Element software tool SOFiSTiK [66] is used to investigate the load-bearing behaviour of slim-floor beams numerically. Therefore, shear beam tests [3] as well as flexural beam tests [7] have been modelled, re-calculated and thereby the model has been validated [8][35].

3.3.2 Modelling

The symmetry of the single span beam was applied and only half of the system was illustrated from the support to the middle of the field as shown in Fig. 3-9.

For the modelling of the steel section shell elements are used due to the thin wall thickness of the cross-section. The steel section consists of a steel profile and a welded bottom plate. The welds connecting the bottom plate with the bottom flange of the profile have been taken into account by rigid coupling of the nodes in the longitudinal direction of the beam. Spring elements were used in the joint between the lower flange of the steel profile and the bottom plates to create contact pressure.

The concrete slab was modelled with three-dimensional eight-node volume brick elements in order to assess the spatial load-bearing behaviour of the structure in the calculation. The material behaviour of the concrete is taken into account by an elastic-plastic material model according to Lade [67]. The softening behaviour of the concrete after exceeding the tensile strength f_{ct} is simplified with a linear decreasing end.

The mesh reinforcement influences the bending stiffness of the concrete slab in transverse direction as well as the cracking on the upper side of the concrete slab under transverse tensile stress. In

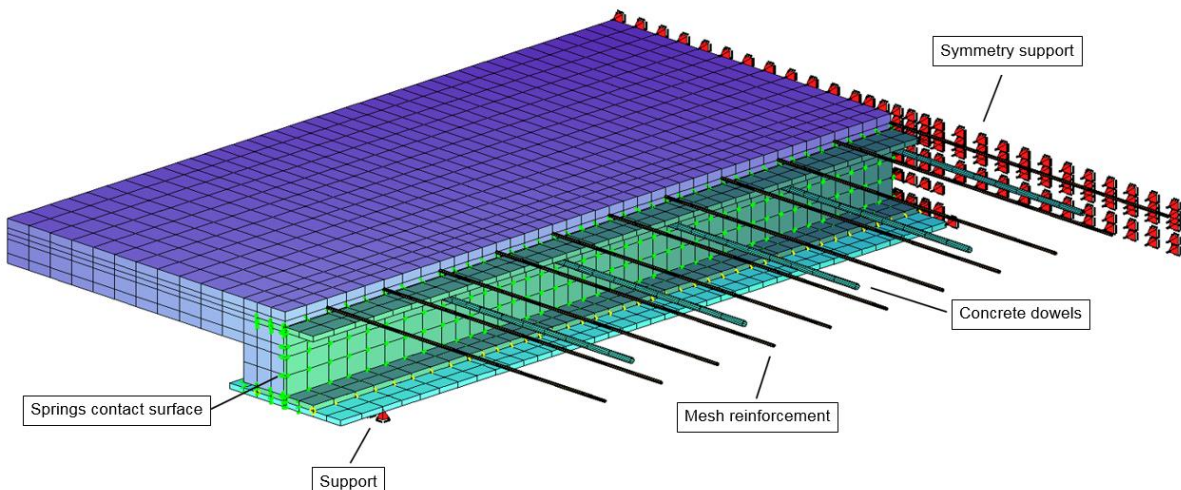


Fig. 3-9: FE-model in SOFiSTiK of slim-floor beam test BT3 [7]

longitudinal direction of the beam, no influence of the mesh reinforcement on the load and deformation behaviour has been determined. Based on this finding the mesh reinforcement is only arranged in transverse direction. The reinforcement elements are modelled by using truss elements connected to the nodes of the volume elements. Truss elements are only able to transfer tensile or compressive forces. The load-slip relationship between concrete and reinforcement is neglected. The nodes of both sectional elements are bonded together. The bond behaviour can be considered by modifying the material characteristics of reinforcing steel.

Following simplifications have been made in the modelling:

- web openings in the steel beam are dispensed
- initially acting adhesive bond is neglected
- bond behaviour between reinforcement and concrete is also neglected

The joint between concrete and steel was modelled by spring elements at the element nodes, consisting of spring in longitudinal and in transverse direction. The friction between steel and concrete is taken into account by transverse springs with bilinear elastic-plastic behaviour. Once the coefficient of friction is reached, no more load can be absorbed. With a coefficient of sliding friction $\mu = 0.25$ very good results had been achieved with the FE simulation of the tests SBT3. In SBT3 no shear connectors have been used. The initially effective adhesive bond in the composite joint (slip $s = 0$) is not reproduced by the spring elements in SOFiSTiK [66]. Therefore, the model is not able to reproduce the initial stiffness induced by adhesive bond. Quantitative determination of the adhesive bond within the tests was not possible.

The shear connectors are modelled using spring elements. Characteristic load - slip curves have been derived from the push-out tests, conducted within the project. The curves are shown in Fig. 3-10. Assuming the shear connectors as springs allows to investigate different types of shear connectors, provided sufficient information on the load-bearing behaviour of these shear connectors is available.

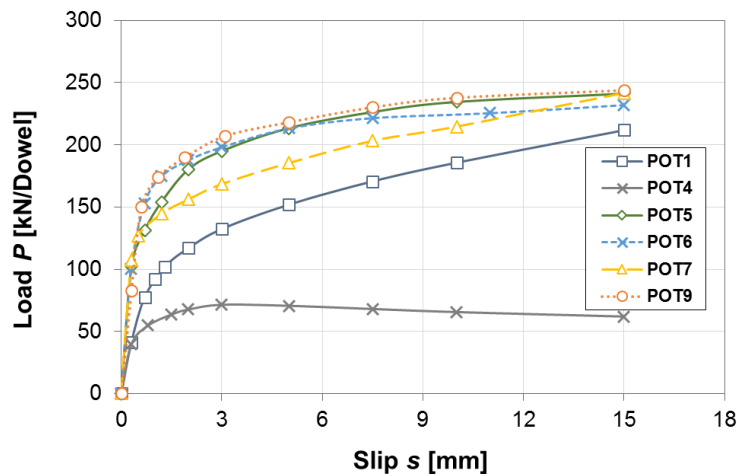


Fig. 3-10: Spring-curves derived from push-out tests

3.3.3 Validation

BT3 has been produced with calculated degree of shear connection of $\eta = 100\%$. CoSFB has been used as shear connection system. POT7 with concrete grade C30/37, rebar diameter 16 mm and diameter of the hole in the profile web 40 mm was taken as basis for the introduced spring curve, based on the measured concrete compressive strengths in the beam test. The load has been applied concentrically.

The load - mid-span curve of the tests and the model is shown in Fig. 3-11. Tab. 3-1 demonstrates the load differences of the load-mid-span curve between the test and numerical model at 3 characteristic points. The maximum load difference is 40.7 kN at $\delta_m = 80$ mm, complying with a difference of 10.8 %.

Fig. 3-12 compares the load-end-slip behaviour of the numerical model and test BT3. The numerical model corresponds well with the test. Good correspondence of the end-slip ensures that the shear connectors are activated realistically.

Due to the good accordance with the tests, the model is assumed as validated.

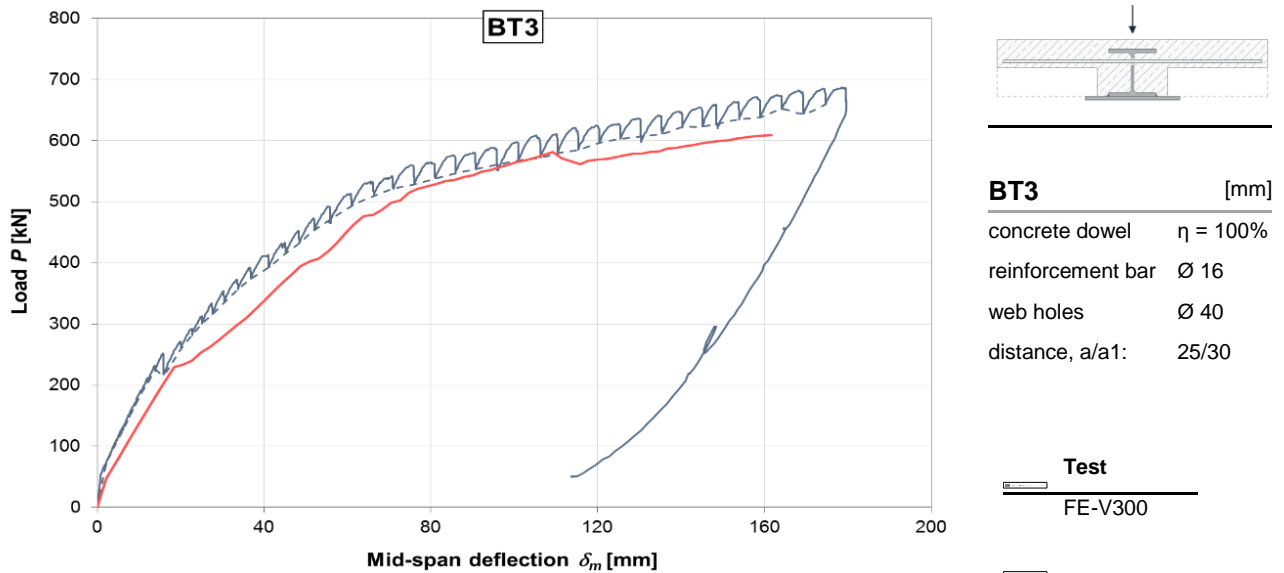


Fig. 3-11: Validation of the load-mid-span deflection of Beam test 3 (BT3)

Tab. 3-1: Differences mid-span deflection between test and FE-model, BT3 [kN, mm]

	$\delta_m = 40$	$\delta_m = 80$	$\delta_m = 160$
P_{static}	378.2	531.8	637.5
P_{FE}	337.5	526.4	608.7
difference	-10.8%	-1.0%	-4.5%

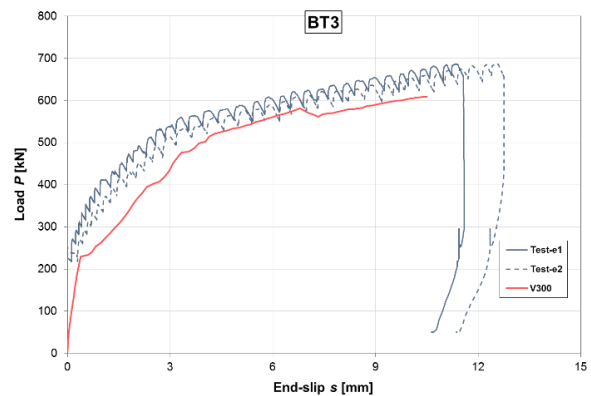


Fig. 3-12: BT3 – Load - end-slip

3.3.4 Analysis of the load-bearing behaviour

The load-bearing behaviour of the Slim-Floor beam test is described using the FE-model, validated on Beam test BT4 [7]. The degree of shear connection of BT4 was $\eta = 25\%$.

To describe the load-bearing behaviour five characteristic points in the load-deflection curve are chosen as indicated in Fig. 3-13. The points and their characteristics are described hereafter.

At point A, the concrete is still in the uncracked state (see Fig. 3-14). Linear-elastic behaviour can be assumed. With increasing load and exceeding the tensile strength, first cracks appear in the lower area of the concrete in the chamber as shown in Fig. 3-15. The “bend” in the load deformation curve between point A to point B is due to the brittle material behaviour of concrete. When cracking happened in the beam, linear-elastic behaviour cannot be assumed anymore. Cracking begins at the load level below self-weight. Therefore, according to the numerical model linear-elastic deformation behaviour cannot be assumed.

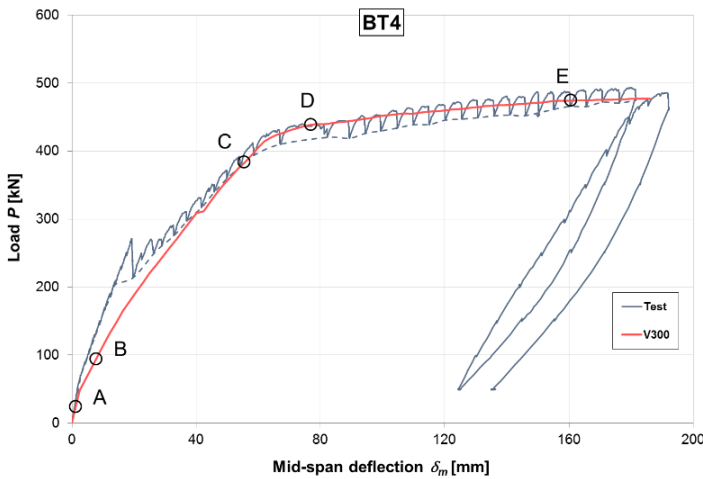


Fig. 3-13: Analysis of the load-bearing behaviour, test BT4

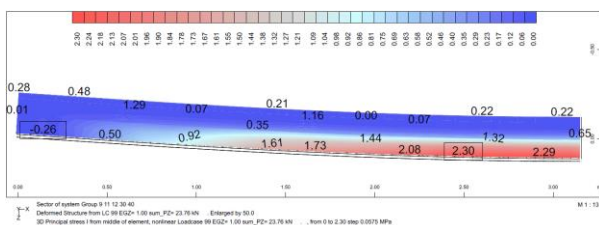


Fig. 3-14: Point A - Concrete uncracked, linear-elastic behaviour of the slim-floor

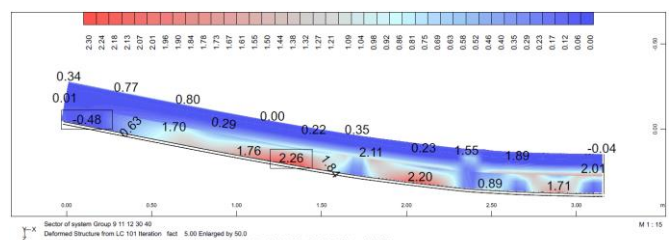


Fig. 3-15: Point B - Concrete started cracking

In Point C the steel section (profile and bottom plate) is still in the linear-elastic state (see Fig. 3-16). Stresses have not reached the measured yield point $f_y = 420 \text{ N/mm}^2$. Between point C and D the transition of the steel from the linear elastic to the plastic area is marked. The yield strength is exceeded in the upper web area of the steel profile as shown in Fig. 3-17. Within the tests a similar behaviour has been observed. Strain gauges at the top flange also exceeded the deformation associated with the yield point of the steel profile.

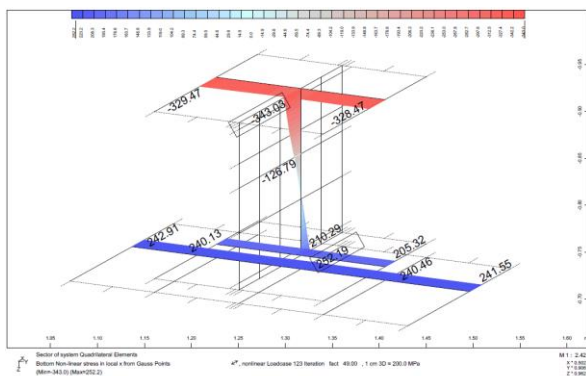


Fig. 3-16: Point C - Linear-elastic material behaviour of the steel section ($f_y < 420 \text{ N/mm}^2$)

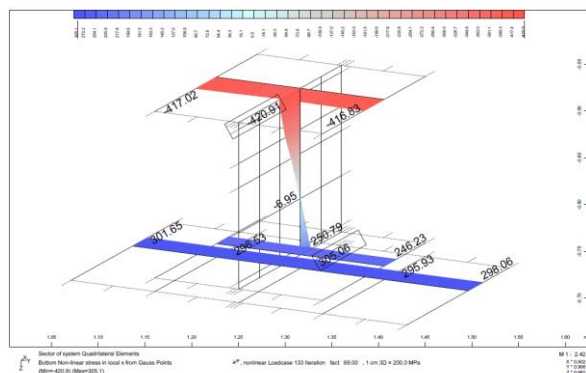


Fig. 3-17: Point D, Transition of the steel section to the plastic range ($f_y > 420 \text{ N/mm}^2$)

With increasing load the steel profile plasticizes (point E). The fully plastic moment capacity of the steel beam is not reached in point E. The bottom plate can still be assumed as linear-elastic. The neutral axis is in the lower part of the steel profile web as shown in Fig. 3-18.

Characteristic points:

- A:** uncracked state
- B:** cracking of concrete
- C:** steel profile before yielding
- D:** steel profile yields
- E:** plasticising of steel profile

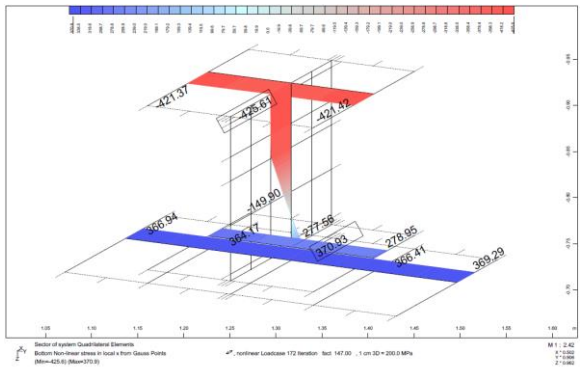


Fig. 3-18: Point D - Plastic load-bearing capacity of the steel section not completely reached

Fig. 3-19 shows the loading in longitudinal direction of the springs used as shear connectors. In accordance to the general theory, the loading at the end of the beam is higher than in the middle of the beam. Increasing mid-span deflection and corresponding increasing load leads to plasticizing of the shear connectors. Shear connectors begin to plasticize from the end of the beam to the middle.

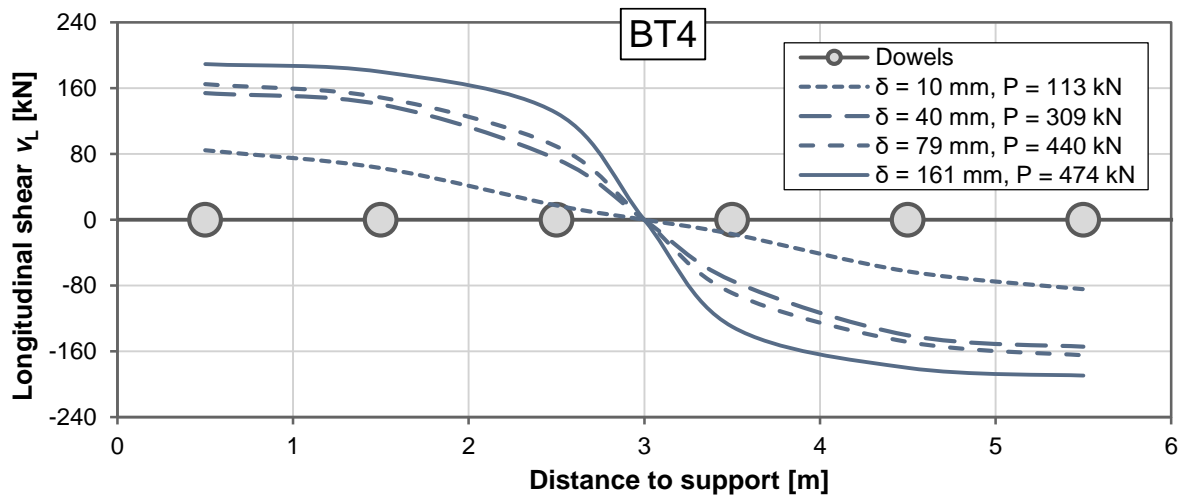


Fig. 3-19: Longitudinal shear force in correspondence with the mid-span deflection

3.3.5 Parameter studies

The verified model is used to recalculate the conducted shear [3]- and flexural beam tests [7]. The listed parameter are furthermore investigated:

- Beam length
- Increase of Degree of shear connection
- Friction

3.4 Conclusion

Due to the proportion of the steel section flexural slim-floor beams behave very ductile, achieving total deflections exceeding span/40 and end-slips greater than 6 mm prior to failure. Effective shear connection can be achieved by using transverse bars passing through holes in the web of a steel profile. The use of larger concrete dowels clearly enhances the performance of the slim-floor beams.

Eccentric loading affects the performance of flexural beams in contrary to shear beam tests. A beam subjected to distribute loading displayed a similar performance and moment resistance to that under point loads, although some differences were observed in the strain profile and slippage. Clear trends were observed in relationships between degree of shear connection, end-slip and moment resistance.

4 DEFLECTION AND VIBRATION BEHAVIOUR OF SLIM-FLOOR SYSTEMS WITH INNOVATIVE SHEAR CONNECTORS

4.1 General

In the following the study to the service behaviour of slim-floor systems is addressed. At this aim, experimental investigations were conducted. The outcomes produce the necessary test measurements for the validation of numerical models.

4.2 Deflection behaviour

4.2.1 Introduction

The service behaviour of slim-floor systems was analysed in the following research. In particular, the investigation concentrates the attention on:

- influence of the partial interaction on both instantaneous deformations and deflections;
- time-dependent response associated with shrinkage and creep of concrete which might be exacerbated by the partial interaction;
- floor dynamic response and how this is affected by concrete time-dependent behaviour and cracking, and by the concrete-steel interface properties;
- shear lag which influence the concrete slab width contributing to the flexural stiffness and how this varies with time.

At this aim, experimental investigations were carried out on both full-scale beam specimens and material samples.

4.2.2 Full-scale long-term beam tests

4.2.2.1 Specimens

The long-term effects induced by creep and shrinkage on the service response of slim-floor beams were the main goal of the study. For this purpose, four slim-floor specimens were tested in simply supported conditions and complementary tests on concrete were carried out to investigate its time properties.

As to the beam tests, a sustained load was applied and the long term deflections and deformations were measured. The total length of the beams was of 6300 mm while the internal span between the supports was of 6000 mm. The specimens had identical concrete and steel geometry. The steel part of the specimens was composed by a HEB200 steel beam and by a 400x15 mm steel plate welded to the lower flange of the steel beam. The steel beam was encased in a T-shaped concrete slab with a flange of width of 2000 mm and thickness of 120 mm. The web of the concrete slab had a width of 300 mm and a height of 120 mm (see Fig. 4-1).

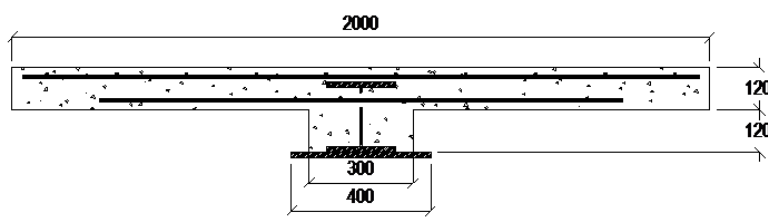


Fig. 4-1: Typical beam cross-section (measures in mm)

The main difference between the specimens refers to the shear connection system. Three different solutions were adopted. In two specimens, the shear connection was provided by concrete dowels (see Fig. 4-1).

- SF1 / SF2 holes in the web of the steel profile were made having a diameter of 40 mm and a spacing of 500 mm. Rebar of diameter 16 mm crossing the hole was added to ensure ductility
- SF3 The third specimen had a web's hole of 80 mm in diameter and no crossing rebar
- SF4 No shear connector. Shear transfer is provided by friction only.

Special formworks allowed casting the specimens in un-propped condition so that the self-weight of the beam was carried only by the steel section during casting. Therefore, once the concrete was hardened, it was assumed to be unloaded and, therefore, subjected to shrinkage only.

At the end of the long-term experiment, the samples were tested to failure aiming at evaluating the influence of the time-dependent concrete behaviour and the possible shear connection degradations (due to long-term deformations) on their ultimate response.

4.2.2.2 Loading and measurement setup

Two different loading conditions were adopted: specimen SF1 was left unloaded, specimens SF2 and SF4 were loaded by a load evenly 'distributed' on the slab (Fig. 4-2), at the last specimen (SF3) the load was applied along two longitudinal lines symmetric with respect to the steel web. The eccentricity of these lines is intended to maximize friction (Fig. 4-3). The total load simulating the service load was of about 300 kN and it was applied to the specimens by means of metal cages filled with rocks. Hence specimens SF2, SF3 and SF4 were subjected to both creep (produced by the sustained load) and the time-dependent effects induced by shrinkage, while the response of sample SF1 was assumed to be affected by shrinkage only.

The load was applied by metal cages filled with stones which were placed on steel beams so as to distribute the load on the concrete slab surface (Fig. 4-2). For specimens SF2 and SF4, the metal cages were applied in three layers. Both the first and the second layer comprises of 6 metal cages (Fig. 4-2). Each metal cage has a nominal weight of 23.54 kN. The third layer consists of one metal cage with a nominal weight of 11.77 kN. The nominal total load applied is of about 294.3 kN. The load on specimen SF3 was applied along two longitudinal lines symmetric with respect to the steel web (Fig. 4-3). The load was applied in three layers (Fig. 4-3) by metal cages with a nominal weight of 16.68 kN. In order to evaluate the actual weight applied to the beam, each metal cage was weighed and its position onto the slab recorded. The actual loads applied on the specimens resulted of 305.03 kN for specimen SF2, of 286.20 kN for specimen SF3, and of 305.23 kN for specimen SF4.



Fig. 4-2: Loading specimen SF2

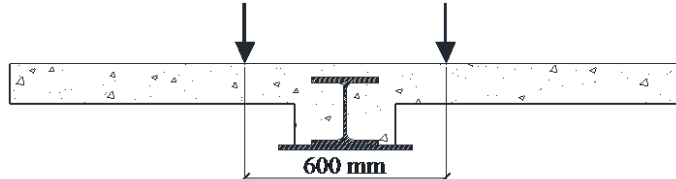


Fig. 4-3: Loading specimen SF3

The response of specimens SF1 and SF2 was monitored for a period of approximately 10 months. On the base of the results the loading period was reduced to 5 months for specimens SF3 and SF4. The measurement setup was designed to monitor the response of the mid-span section, the deflected shape of the beam and the steel-concrete slip at the beam ends (Fig. 4-4). At mid-span, LVDTs and strain gauges were installed allowed evaluating the deflection and the section deformation. Further LVDTs were installed at both the ends of the specimens to capture the concrete vs steel slippage at the heights of the steel flanges.

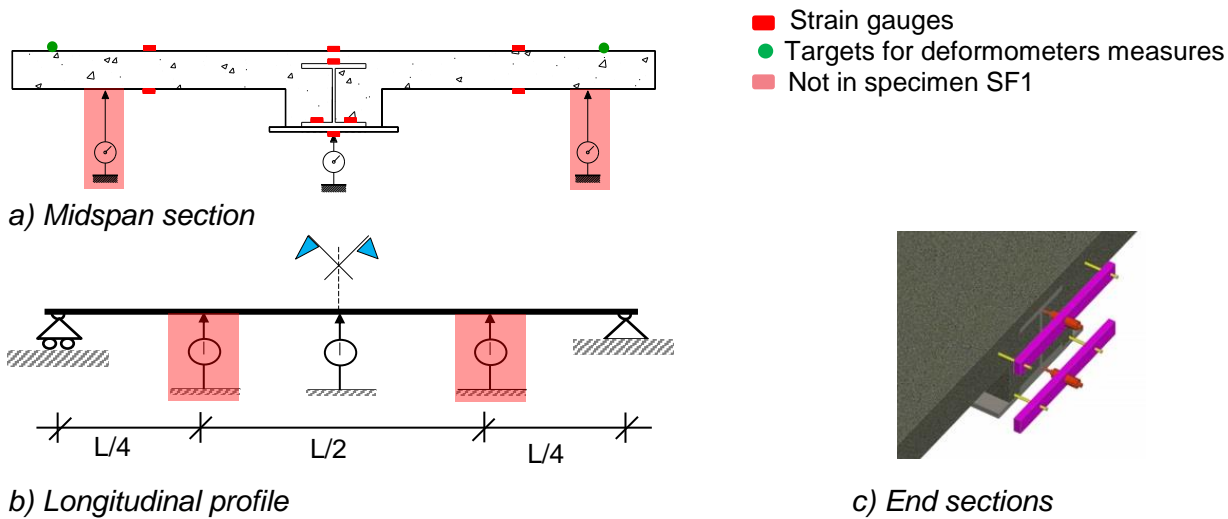


Fig. 4-4: The measurement set-up

4.2.2.3 Complementary tests on materials

As mentioned in the above, standard tests were planned in order to characterize the material properties of concrete. At this aim, it was planned to perform compression and tensile tests on concrete according to EN 12390-3:2009 [43] and EN 12390-6:2009 [44] respectively [9]. The modulus of elasticity of concrete was also evaluated according to the EN 12390-13:2009 [45]. The material properties of the steel beams, the steel bottom plate and of the rebars ø16mm were evaluated according to EN ISO 6892-1:2009 [46].

Fig. 4-5a) shows the preparation of concrete cylinders. The compression tests on cylinders were carried out at different times in order to get data consistent with the various phases of the test on the beams specimens. Cylinders were also used for determining the creep law. Further tests on concrete were designed to study the time effects on concrete. Fig. 4-5b) shows the shrinkage samples: their



a)



b)

Fig. 4-5: Preparation of a) concrete cylinders and of b) shrinkage specimens

dimensions were 900 x 900 x 120 mm to simulate the slab. These samples were unreinforced and were left unloaded.

The creep was appraised in accordance with specifications of the ASTM C512/C512M-15 standard [47]. An ‘ad hoc’ machine was designed and built-up (Fig. 4-6). Concrete cylinders were subjected to a compression sustained load equivalent to approximately 40% of the compressive resistance of concrete at the age of loading. In Fig. 4-6 the creep machine built-up in Trento and the cylinders under compression are shown. The cylinders were loaded in the machine the same day as the full-scale specimens and remained under load as long as the long-term tests on the full scale beam specimens.



Fig. 4-6: The creep test on concrete

4.2.2.4 Beam tests results

The main outcomes from the long-term beam tests are the evolution under the sustained load of the deflections, the strains at mid-span and the end-slip. A consistent general response was recorded among all four specimens, as apparent from [9].

Some data are presented here related to specimen SF2. The significant increase in deflection and the negligible slippage are apparent from Fig. 4-7 and Fig. 4-8.

Fig. 4-9 compares the increase of mid-span deflection for the three beams subject to sustained load. The trend is consistent. Beam SF3 is stiffer due to the different loading method, which leads to a higher effective width of the slab. The increase of the deformation at the end of the test was of 34.66 % for beam SF2, 26.93 % for beam SF3 and of 33.21 % for beam SF4.

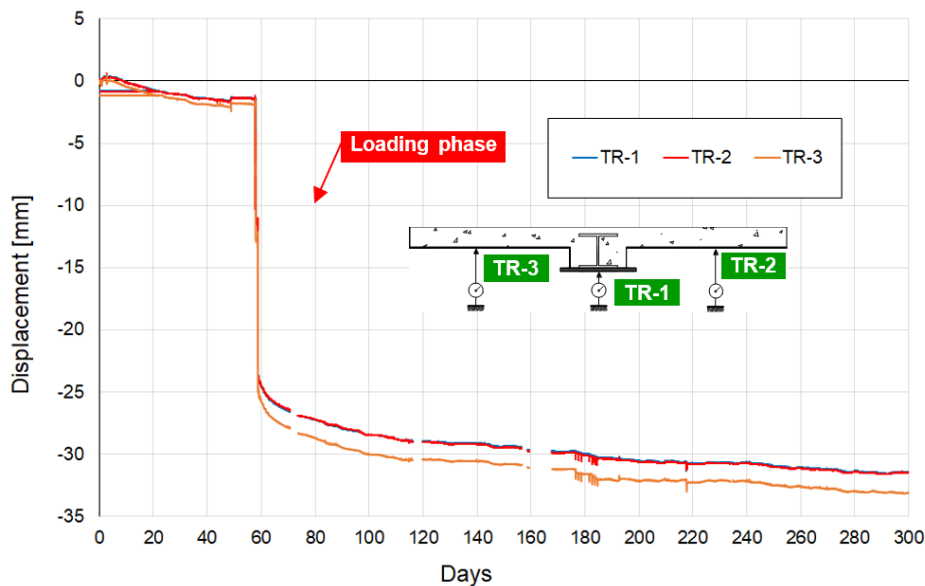


Fig. 4-7: Mid-span deflection in time for specimen SF2

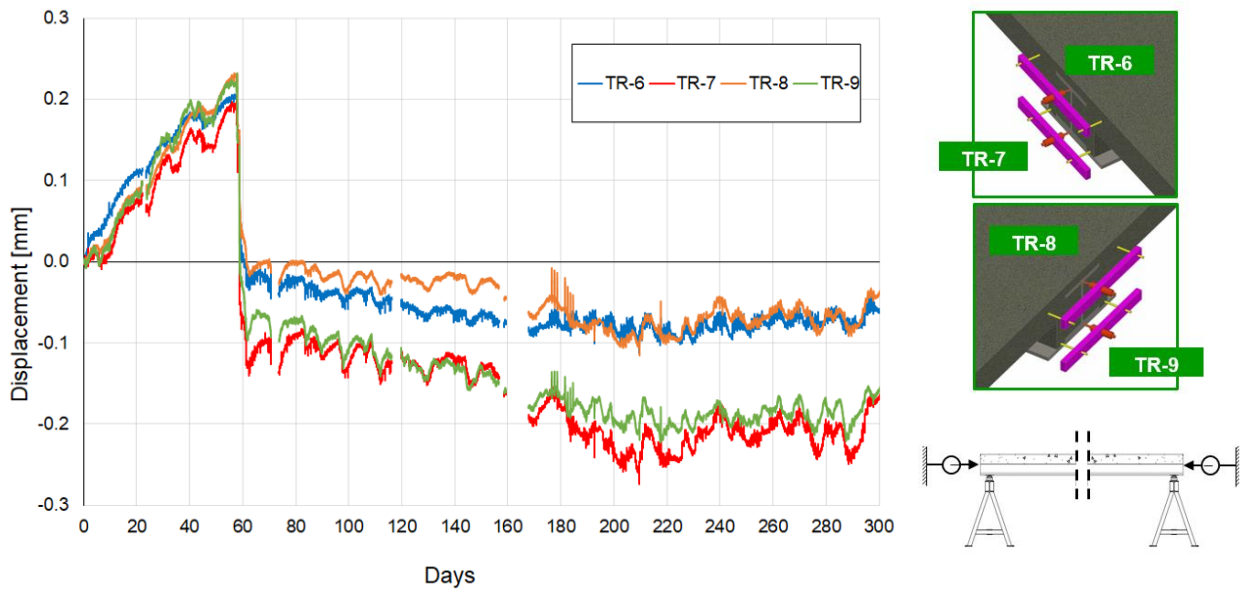


Fig. 4-8: End slippage in time

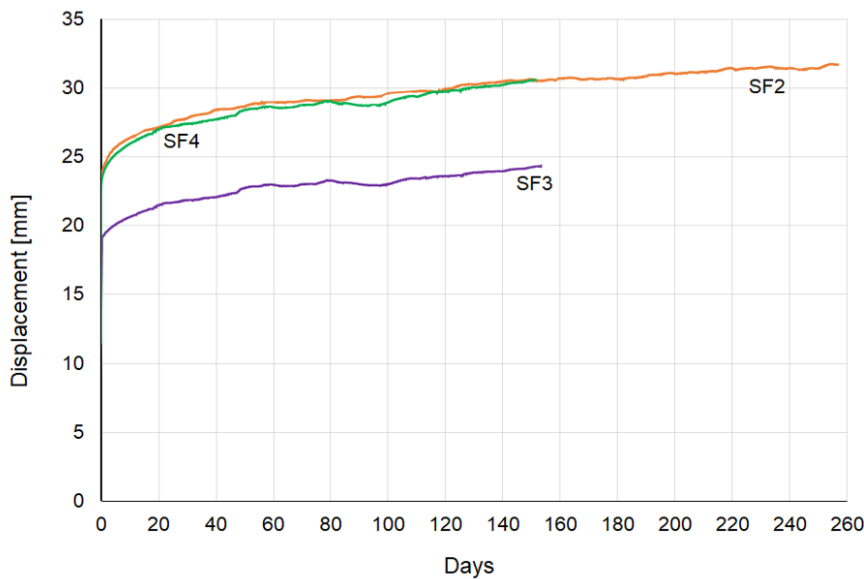


Fig. 4-9: Increase in time of the mid-span deflection due to time effects

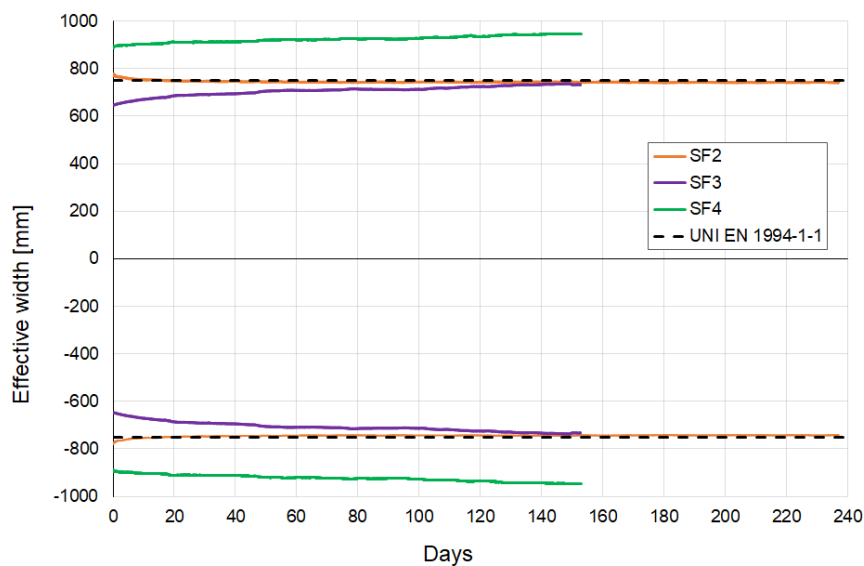


Fig. 4-10: Effective width in time

The strain readings on the concrete slab allowed computation of the effective width and of its evolution in time. The results are presented in Fig. 4-10. The value of $L/4$ recommended by EN 1994-1-1 [40] appears to be adequate for service calculations. The results seems to indicate that the effective width remains practically unchanged in time.

4.2.2.5 Material tests: creep and shrinkage

The tests aiming at appraising the creep-shrinkage behaviour of the concrete indicating there is a good agreement in average with the Eurocode 2 [48] model (Fig. 4-11).

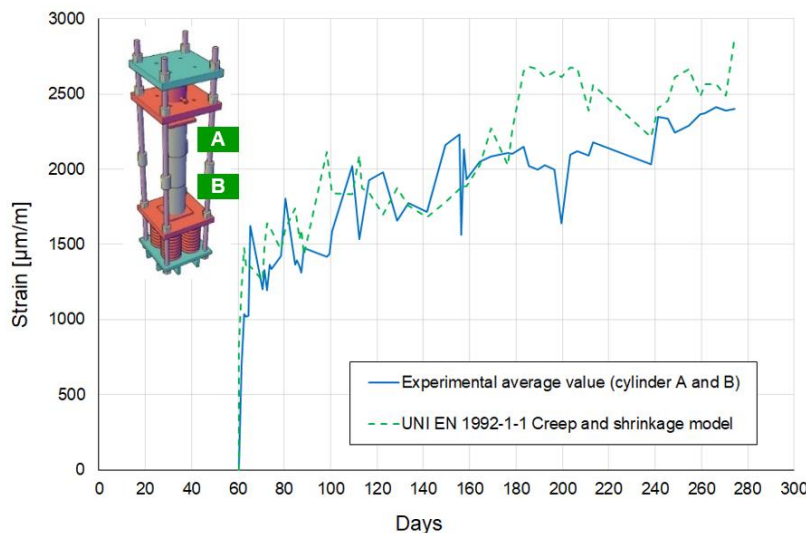


Fig. 4-11: Creep and shrinkage strain in time

The shrinkage tests allowed to assess the strains associated with this phenomenon only (Fig. 4-12). The maximum value of about $500 \mu\text{m}/\text{m}$ is higher than the value of $325 \mu\text{m}/\text{m}$ recommended by Annex C of EN 1994-1-1 [40].

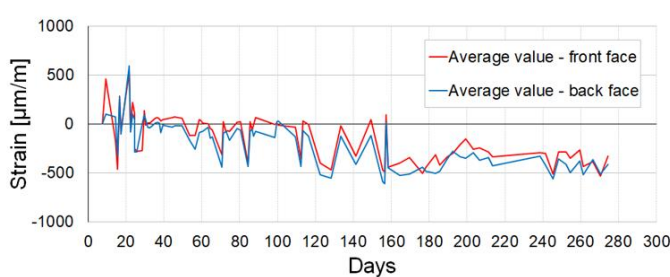


Fig. 4-12: Shrinkage strains in time

4.2.3 Beams failure tests

After long-term loading, the loading removal and the vibrational tests, the four investigated beams were loaded up to collapse. Two different loading set-ups were used consistently with the long-term tests. The loading set-up in Fig. 4-13a) refers to specimens SF1, SF2 and SF4. Beam SF3, for which the shear transfer is provided by friction at the steel-concrete interface, was loaded in four points eccentric with respect to the steel section's web (Fig. 4-13b)).

The load was applied by an actuator MOOG L085-759 with a stroke of 500 mm with a maximum capacity of $\pm 1 \text{ MN}$; the tests were carried in displacement control. In all the tests, the values of the vertical displacement at midspan were significant, and higher than the actuator's stroke. It was hence necessary to unload fully the beam allowing for inserting suitable shim plates. The load was then increased again up to collapse. The comparison between the beam responses is presented in Fig. 4-14 while the maximum loads reached in tests are collected in Tab. 4-1. Specimens SF1 and SF2 (which have a shear connection with 40mm holes and crossing $\varnothing 16\text{mm}$ rebars) showed a very ductile response. Fig. 4-15 points out the high deformation capacity of the shear connection for beam SF1.

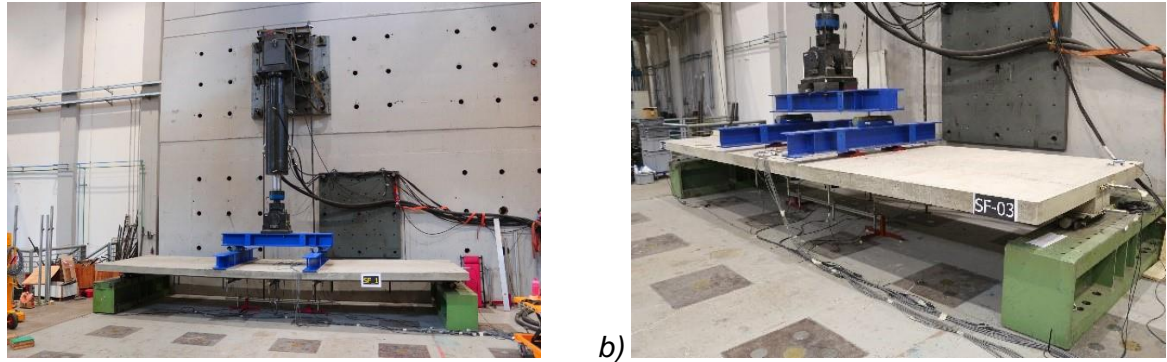


Fig. 4-13: The loading setup: a) Beams SF1, SF2 and SF4; b) Beam SF3

A similar behaviour was observed also for beam SF2. On the contrary, beams SF3 (no shear connector) and SF4 (80mm holes and no crossing rebar) showed a sudden and sharp load capacity reduction due to the unzipping failure of the shear connection.

Tab. 4-1: Summary of the collapse loads

Specimen	SF1	SF2	SF3	SF4
Collapse load [kN]	537.48	562.93	571.74	660.18

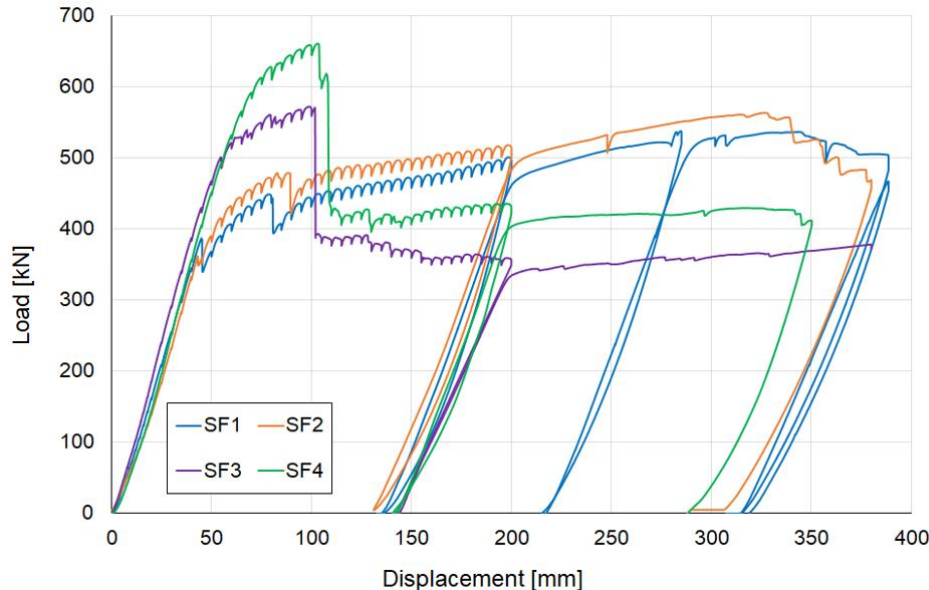


Fig. 4-14: The load-deflection curves

4.3 Vibration tests

In order to contribute to the appraisal of the floor dynamic response and of how this is affected by concrete time-dependent behaviour and cracking, and by the concrete-steel interface properties vibration tests were carried out on the four beam specimens. Dynamic tests on specimens SF1 and SF2 were performed at the end of the long-term tests only. Specimens SF3 and SF4 were tested just before and just after the long-term tests. A summary of the vibrational tests performed is presented in Tab. 4-2.

In order to obtain the complete modal response with respect to its vertical, torsional and transversal behaviour, 12 PCB 393C piezoelectric accelerometers of 1 V/g resolution were applied to the sample so as they were aligned in both the vertical and the transverse directions.

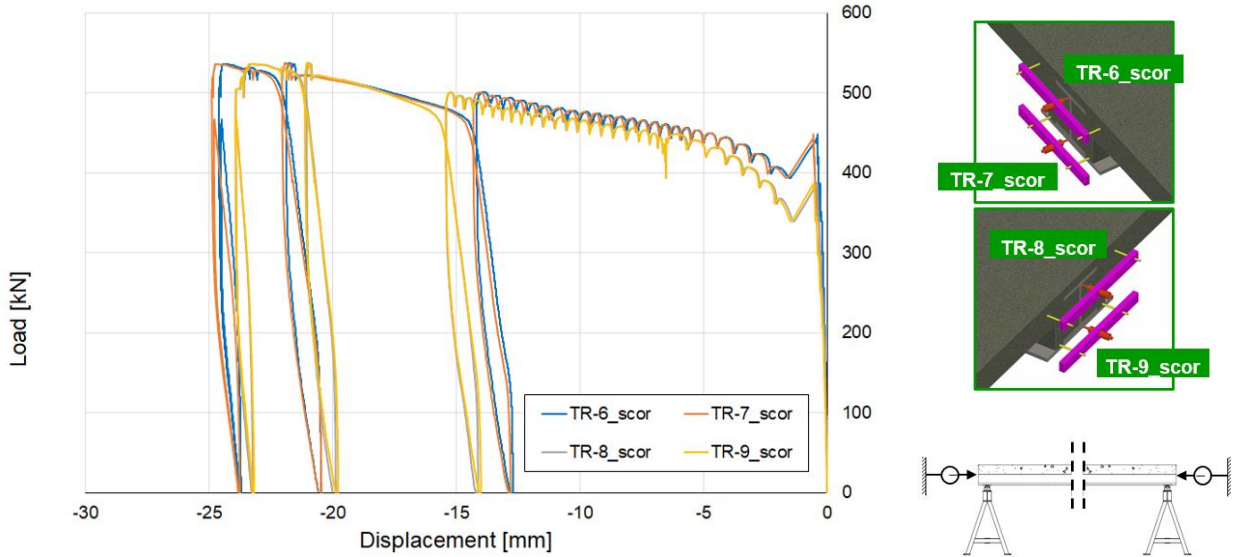
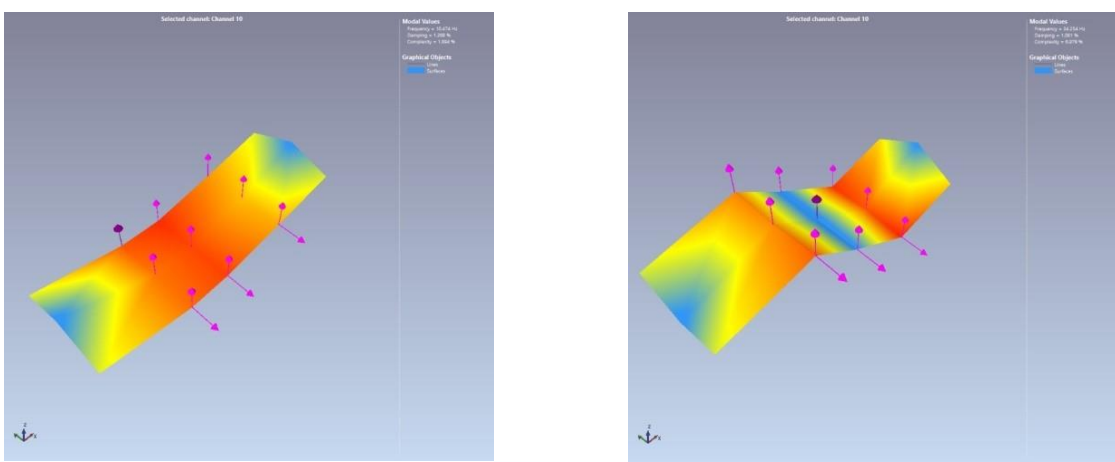


Fig. 4-15: End slippage in beam SF1

Tab. 4-2: Summary of the vibrational tests

Specimen	Vibrational test	
	Before long term test	After long term test
SF1	-	X
SF2	-	X
SF3	X	X
SF4	X	X

The main issue of this study is to investigate the structural behaviour with reference to the condition in issue; moreover, to detect any modal variation in the loaded specimen. In detail, the natural frequency and the modal damping of the vertical modes are of interest. To this aim, Ambient Vibration Tests were carried out exciting the structure with two persons randomly walking above the structure. Fig. 4-16 presents the first and second flexural modes, which are the ones of interest in slim-floor design.



a) First mode

b) Second mode

Fig. 4-16: First two flexural modes

Tab. 4-3 summarises the frequencies measured in the tests associated to the first and second flexural modes.

Tab. 4-3: Summary of the vibrational tests

Specimen	Weight [kN]	Vibrational mode	Frequency [Hz]	
			Before long term test	After long term test
SF1	44,542	1 st flexural mode	-	11.389
		2 nd flexural mode	-	35.712
SF2	44,957	1 st flexural mode	-	10.113
		2 nd flexural mode	-	33.685
SF3	46,737	1 st flexural mode	11.974	10.474
		2 nd flexural mode	37.480	34.254
SF4	46,877	1 st flexural mode	11.775	11.040
		2 nd flexural mode	37.728	36.220

4.4 Conclusions

The experimental work carried out in Trento leads to the following main conclusions:

- Time-dependent properties of concrete affect significantly the deflection of beams and cannot be neglected.
- All shear connections investigated did not show any end slippage of practical interest under the sustained load: service analyses may neglect this parameter.
- Failure tests indicated that the ductility of the flexural response is substantially enhanced by the presence of rebars crossing the web. For this reason, design recommendations shouldn't allow holes without rebars.
- The frequency values of the first two flexural modes of the slim-floor beams are fully consistent and their variation due to long-term effects is rather limited. In any case, these results show that natural frequency is sufficiently high to exclude any uncomfortable interference with pedestrian walking.

5 LIFE CYCLE ASSESSMENT AND DEVELOPMENT OF OPTIMIZED SLIM-FLOOR SOLUTIONS IN VIEW OF LCA ASPECTS

5.1 General

In the scope of the project, the normative framework for LCA is described in Fig. 5-1.

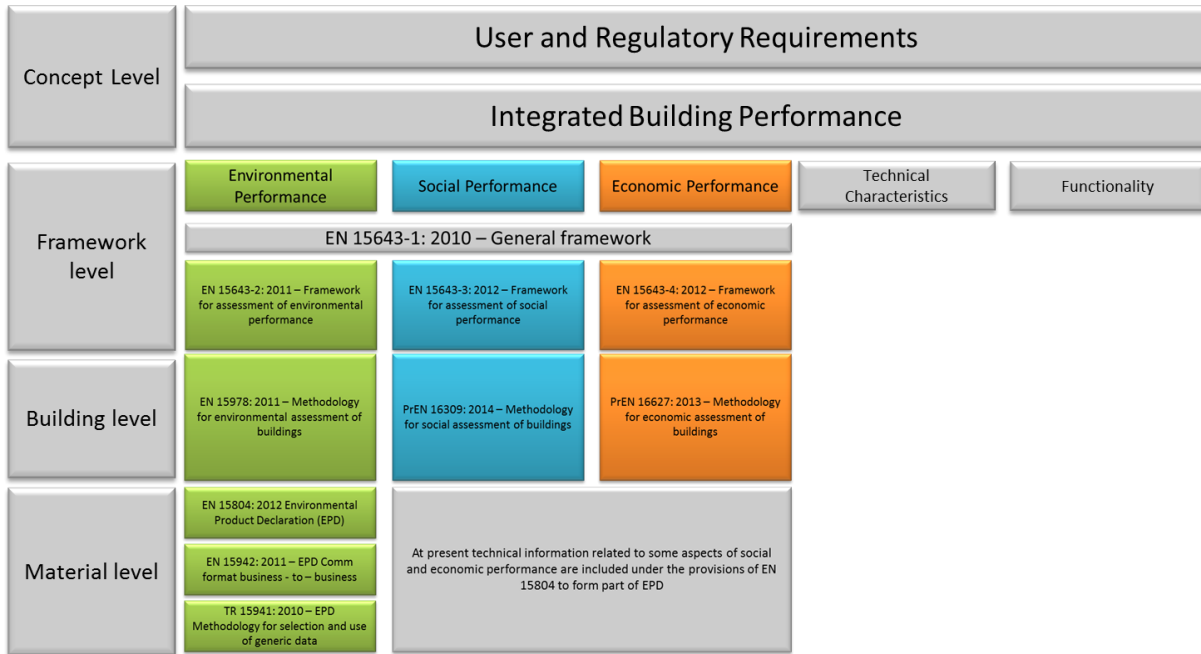


Fig. 5-1: Framework for assessing the sustainability of construction works

The environmental framework related to buildings and construction products includes:

- EN 15643-2: 2011 [49] - Framework for assessment of environmental performance
- EN 15978: 2011 [50] - Methodology for environmental assessment of buildings
- EN 15804: 2012 [51] - Core product category rules for environmental product assessment
- EN 15942: 2011 [52] - EPD Communication format business - to - business
- TR 15941: 2010 [53] - EPD Methodology for selection and use of generic data

The social and economic framework standards are published, but the standards on building and product level are still ongoing:

- EN 15643-3: 2012 [54] - Framework for assessment of social performance
- EN 15643-4: 2012 [55] - Framework for assessment of economic performance

The total integrated building performance incorporates environmental, social, and economic performance, as well technical and functional performance, each of which is intrinsically related to the other.

According to EN 15978, 2011 [50], the lifecycle analysis of a building consists of a consecutive and interlinked stages of the building's life:

PRODUCT stage	CONSTRUCTION PROCESS stage	USE stage	END-OF-LIFE stage	Benefits and loads beyond the system boundary
A1 Raw material supply A2 Transport A3 Manufacturing	A4 Transport A5 Construction – Installation process	B1 Use B2 Maintenance B3 Repair B4 Replacement B5 Refurbishment B6 Operational energy use B7 Operational water use	C1 Deconstruction demolition C2 Transport C3 Waste processing C4 Disposal	D Reuse- Recovery- Recycling- potential

Fig. 5-2: Information modules of a building lifecycle (EN 15978, 2011)

The indicators, needed to carry out the required LCA assessment, are grouped into three families:

- Environmental impact — indicators related to change to the environment, whether adverse or beneficial, wholly or partially resulting from environmental aspects,
- Economic impact — indicators related to change to the economic conditions, whether adverse or beneficial, wholly or partially resulting from economic aspects (aspect of construction works, part of works, processes or services related to their life cycle that can cause change to economic conditions),
- Social impact —indicators related to change to society or quality of life, whether adverse or beneficial, wholly or partially resulting from social aspects.

5.2 LCA - Validation of the methodology

The first task of WP5 requires defining a methodology that allows for the proper evaluation of sustainability of slim-floor solutions. The evaluation employs the life-cycle approach (LCA): product stage, construction process, use stage, and end-of-life stage (as shown in Figure 5-1). This type of assessment quantifies impacts and aspects for the environmental, social, safety and economic performance of buildings using quantitative and qualitative indicators, both of which are measured without value judgements.

In the past years, life cycle assessment methodologies have been developed by ArcelorMittal Maizières. The methodology was implemented into a user-friendly software AMECO, owned by ArcelorMittal. The LCA methodology of the first version of AMECO was peer reviewed by an independent organism (thinkstep, former PE International).

In the scope of RFCS LVS3 project [68], AMECO software has been put in line with EN 15804 [51] in terms of:

- Number of impacts: AMECO deals with 24 indicators such as environmental impacts, resources use & secondary materials and fuel, waste categories, output flows relative to reuse/recycling and recovery
- Distribution among the modules as defined in the standard, taking into account of the Module D (recyclability of the steel)

Within SlimAPP-project, additional features were implemented in order to be able to perform the LCA of slim-floor solutions. The LCA methodology, applicable to LCA of slim-floor systems identified in this project are described in a detailed specific deliverable, provided separately (Deliverable D5.1 Validation report of methodology).

5.3 LCA - Adaptation of AMECO software

In this paragraph, the adaptation of AMECO software [69] is summarized.

The functional specifications for adaptation of AMECO software [69] are:

New categories of slim-floor systems were implemented, according to the case studies to be analyzed in the scope of the project SlimAPP.

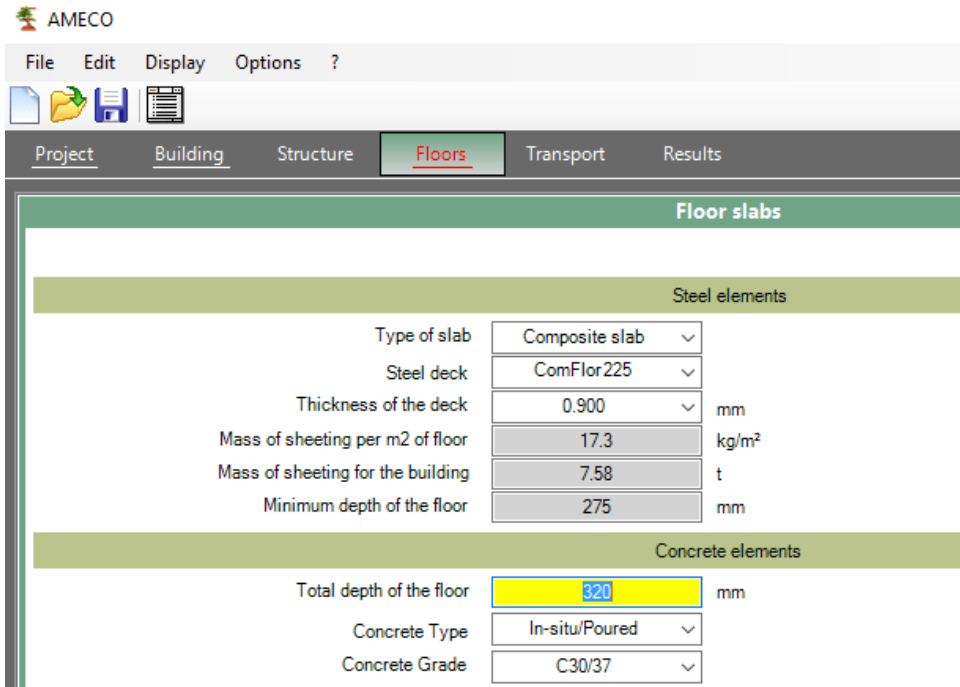


Fig. 5-3: AMECO3 interface: layout of the “Floors” window

This category comprises the following slim-floor systems:

- Cofradal 200/230 and 260 (steel sheet, rebars, rockwool and concrete)
- CofraPlus 220 (steel sheet, rebars, and concrete)
- Inodeck/Monodeck (hollow core, rebars, concrete screed, gypsum as fire protection material)
- Tata Steel solutions (Comfloor steel deckings, rebars and concrete)

In the previous version of AMECO 3, classical concrete flat slab floor system were already available: concrete C20/25 and C30/37. Various concrete classes were implemented (C25/30, C35/45, C45/55 and C50/60) in the scope of the current project.

- LCI datasets for Rockwool (included in the Cofradal systems) and associated LCA methodology;
- LCI datasets for Gypsum (used as fire protection material with Inodek Hollow core systems), and associated LCA methodology
- The Technical specifications document and User’s manual with additional data and functionalities;
- AMECO has been adapted to allow a comprehensive visualization and comparison of the results for the various typologies of slim-floor systems.

5.4 Life Cycle Analysis of slim-floor systems, examples of application – comparison

5.4.1 Introduction

In this task, the objective is to present the LCA calculation results of the case studies identified in the section 1. There also the design loads and design criteria are detailed, see also [14].

In summary, these assumptions are:

- Dead load:	Depends on slab system (to be added when fixed)
- Imposed loading	$q_i = 2.5 \text{ kN/m}^2 + 1 \text{ kN/m}^2$ partitions $q_i = 2.5 \text{ kN/m}^2$ for car parks
- Other loads	$q_d = 1.5 \text{ kN/m}^2$ for concrete screed $q_d = 0.7 \text{ kN/m}^2$ for raised floor and ceiling
- Vibration criteria	$f > 3.0 \text{ Hz}$ for offices and residential $f > 2.3 \text{ Hz}$ for car parks
- Deflection criteria	Total deflection $< L/200$ Imposed load deflection $< L/300$
- Fire resistance	6 store buildings: REI 90
- Floor depth, h_c	300 mm to 400 mm depending on beam depth
- Façades	Without façade: $q_i = 0 \text{ kN/m}$
- Building height	6 storeys (plus option of 1 underground level)
- Design:	Slim-floor: EN 1994-1-1: 2006 [40] /Technical approvals (Slim-floor)
- Concrete slab:	EN 1992-1-1: 2005 [48] (concrete slab)

The identified case studies are shared in 4 different scenarios, with variants for each scenario.

5.4.2 LCA - analysis

5.4.2.2 General

The complete structural design, which includes

- the fire protection materials, and
- the bill of materials of each case variant

are presented with the LCA comparison results. The details of the LCA analysis is reported in Deliverable 5.3 [14].

5.4.2.3 Case 1: Commercial/residential building

5 slim-floor variants:

- Concrete in-situ
- Concrete hollowcore
- Cofradal 260
- Cofraplus 220
- Comflor 225

Grid = (8.1m + 5.4m) x 8.1m

Column height: 3.50m

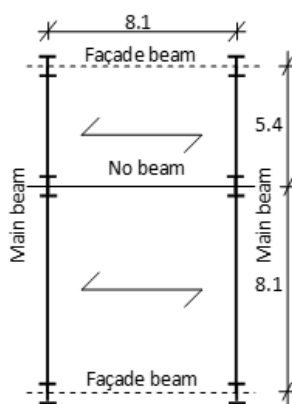


Fig. 5-4: floor layout of 6 floor commercial / residential building

According to the structural design, the bill of materials for the 5 variants are summarized in Tab. 5-1.

Tab. 5-1: Bill of material for commercial/residential building (case 1)

Floor system	in tons	Concrete	Inodek	Cofradal 260	Cofraplus 220	ComFlor 225	
Steel	Beams	-	3.302	0.727	1.268	1.478	
	Plates	-	1.292	0.622	0.668	0.757	
	Steel sheet	-	-	1.361	1.832	1.895	
	Reinforcement	2.92	0.29	1.436	1.14	1.215	
Concrete	Slab	In situ	Hollowcore	In situ	In situ	In situ	
		C30/37 t= 30 cm	C45/55 t=20 cm	C30/37 t= 26 cm	C30/37 t= 35 cm	C30/37 t= 32 cm	
	Screed	78.73	32.04	28.34	43.83	39.63	
		In situ C20/25 t= 8 cm		-	-	-	
		18.59					
Rockwool		-	-	0.765	-	-	
Gypsum		-	0.238	-	-	-	
Total weight	in tons	81.7	55.8	33.2	48.7	45	
Total weight in ton/m² of floor		0.75	0.51	0.30	0.45	0.41	

Note: No formwork is considered for concrete solutions

Note: Steel reinforcement is including dowels, slab rebars, and fire protection in Concrete, Cofradal, Cofraplus and Comflor solutions.

The LCA results (GWP Global Warming Potential) are given hereafter in Tab. 5-2, for different solution of steel decks and an in-situ concrete solution.

Tab. 5-2: Global Warming Potential of investigated solutions for commercial/residential building (case 1)

in tCO _{2eq}	Concrete	Inodek	Cofradal 260	Cofraplus 220
Module A	12.74	12.70	14.31	17.18
Module C	1.09	0.63	0.54	0.68
Module D	-0.45	-1.72	-3.96	-4.40
TOTAL A-C	13.8	13.3	14.9	17.9
TOTAL A-D	13.4	11.6	10.9	13.5
GWP (in kgCO_{2eq} per m²)				
TOTAL A-C	105	101	112	135
TOTAL A-D	101	88	82	102

The comparison as given in Tab. 5-3 show advantages for Inodek. This is also demonstrated in Fig. 5-5.

Tab. 5-3: Comparative results of the LCA (Case 1)

Comparative results	
Reference:	Cofradal 260
Concrete in-situ	+23%
Inodek:	+6%
Cofraplus 220:	+24%

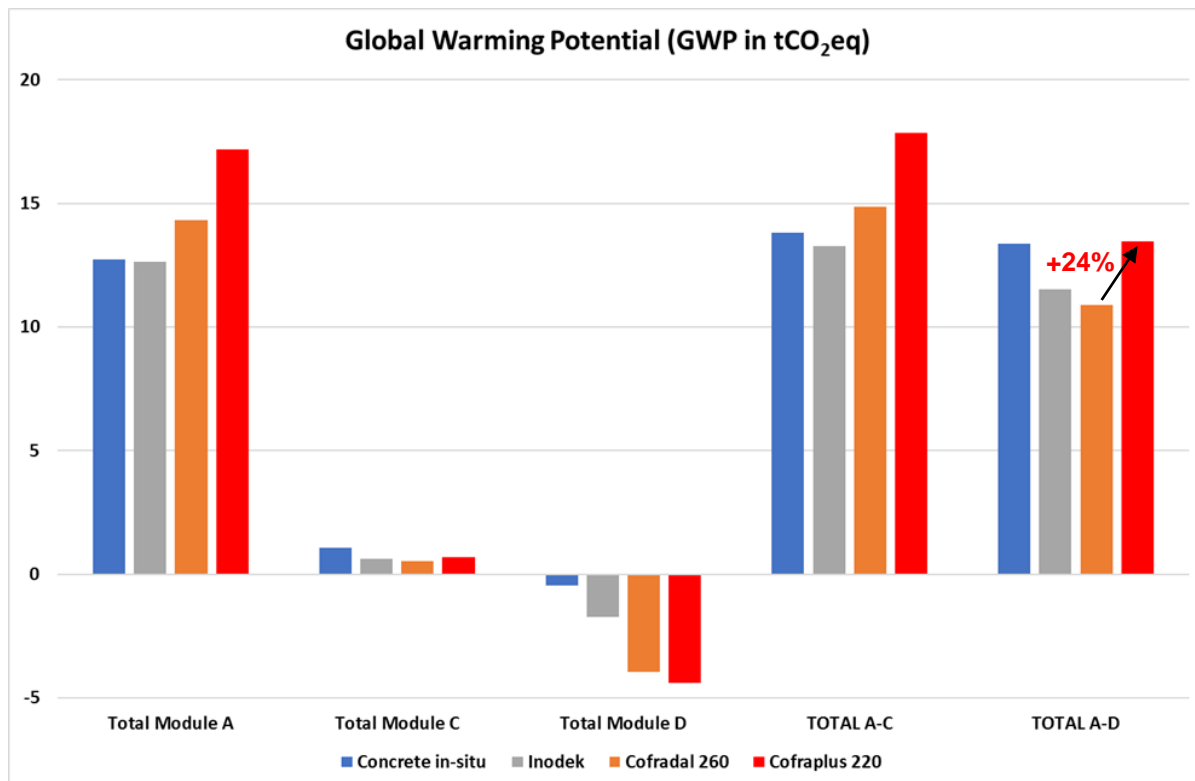


Fig. 5-5: Global warming potential of different variants (Case 1) regarding the different modules as given in Tab. 5-2.

5.4.2.4 Case 2: Commercial/residential building

4 slim-floor variants:

- Concrete hollowcore
- Cofradal 260
- Cofraplus 220
- Comflor 225

Grid= 10.8m x 8.1m

Column height: 3.50m

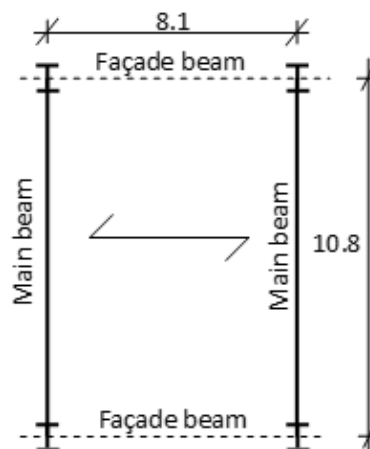


Fig. 5-6: Floor layout of 6 floor commercial/residential building

The bill of materials for the 4 variants is summarized in

Tab. 5-4.

Tab. 5-4: Bill of material for commercial/residential building (case 2)

Floor system	in tons	Inodek	Cofradal 260	Cofraplus 220	ComFlor 225
Steel	Beams	5.113	1.264	1.372	1.674
	Plates	1.155	0.763	1.272	0.636
	Steel sheet	-	1.089	1.465	1.516
	Reinforcement	0.219	1.223	0.978	0.978

Floor system	in tons	Inodek	Cofradal 260	Cofraplus 220	ComFlor 225
Concrete	Slab	Hollowcore C45/55 t=32 cm	In situ C30/37 t= 26 cm	In situ C30/37 t= 36 cm	In situ C30/37 t= 44 cm
		41.028	22.675	37.162	56.897
	Screed	In situ C20/25 t= 8 cm	-	-	-
		14.872			
Rockwool	-	0.612	-	-	-
Gypsum	0.248	-	-	-	-
Total weight	in tons	62.6	27.6	42.2	61.7
Total weight in ton/m² of floor		0.72	0.32	0.48	0.71

Note: Steel reinforcement: including dowels, slab rebars, and fire protection in Cofradal, Cofraplus and Comflor solutions

The LCA results (GWP Global Warming Potential) are given hereafter in Tab. 5-5, for different solution of steel decks.

Tab. 5-5: LCA results (Global Warming Potential)

in tCO _{2eq}	Inodek	Cofradal 260	Cofraplus 220	Comfloor 225
Module A	15.50	10.40	13.33	14.16
Module C	0.59	0.36	0.44	0.63
Module D	-2.19	-2.81	-3.90	-3.24
TOTAL A-C	16.1	10.8	13.8	14.8
TOTAL A-D	13.9	8.0	9.9	11.6

GWP in kgCO ₂ eq per m ²				
	Inodek	Cofradal 260	Cofraplus 220	Comfloor 225
TOTAL A-C	184	123	157	169
TOTAL A-D	159	91	113	132

The comparison as given in Tab. 5-6 show advantages for Cofraplus 220. This is also demonstrated in Fig. 5-7.

Tab. 5-6: Comparative results of the LCA (Case 2)

Comparative results	
Reference:	Cofradal 260
Inodek:	+ 75%
Cofraplus 220:	+ 24%
ComFlor 225:	+ 45%

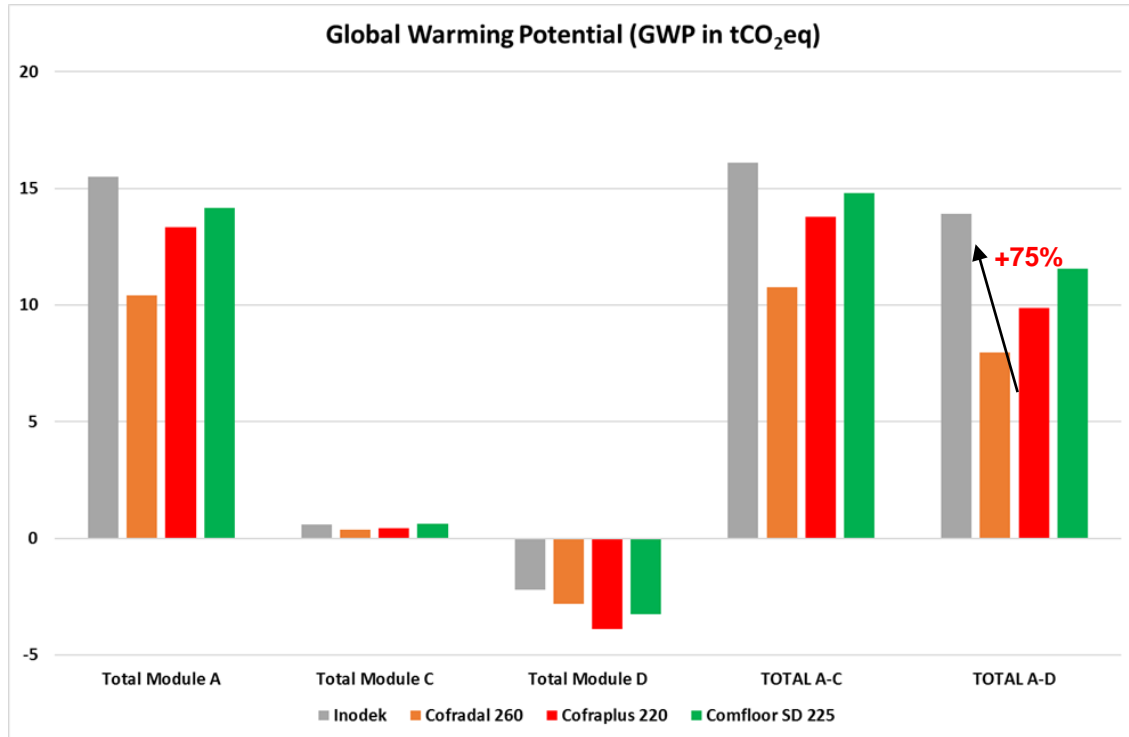


Fig. 5-7: Global warming potential of different variants (Case 2) regarding the different modules as given in Tab. 5-4.

5.4.2.5 Case 3: Below ground car park

4 slim-floor variants:

- Concrete in-situ
- Concrete hollowcore
- Cofradal 260
- Cofraplus 220

Grid = (4.1 m + 8.1 m + 4.1 m) x 8.1 m

Column height: 2.80 m

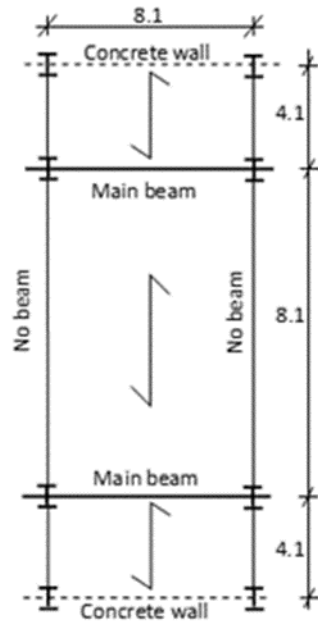


Fig. 5-8: floor layout below ground car park

The bill of materials for the 4 variants is summarized in Tab. 5-7.

Tab. 5-7: Bill of material for commercial/residential building (case 2)

Floor system	in tons	Concrete	Inodek	Cofradal 260	Cofraplus 220
Steel	Beams	-	2.543	0.992	1.581
	Plates	-	0.997	1.017	0.763
	Steel sheet	-	-	1.644	2.212
	Reinforcement	2.789	0.351	1.856	1.859
Concrete	Slab	In situ C30/37 t= 30cm	Hollowcore C45/55 t=20 cm	In situ C30/37 t= 26 cm	In situ C30/37 t= 36 cm
		95.062	38.685	34.222	56.086
	Screed	-	In situ C20/25 t= 8 cm	-	-
			22.445		
Rockwool		-	-	0.924	-
Gypsum		-	0.322	-	-
Total weight	in tons	97.9	65.3	40.7	62.5
Total weight in ton/m² of floor		0.74	0.49	0.31	0.47

Note: Steel reinforcement: including dowels, slab rebars, and fire protection in Concrete, Cofradal and Cofraplus solutions

The LCA results (GWP Global Warming Potential) are given in Tab. 5-8, for different solution of steel decks and an in-situ concrete solution.

Tab. 5-8: LCA results (Global Warming Potential) for Case 3

in tCO _{2eq}	Concrete	Inodek	Cofradal 260	Cofraplus 220
Module A	12.74	12.70	14.31	17.18
Module C	1.09	0.63	0.54	0.68
Module D	-0.45	-1.72	-3.96	-4.40
TOTAL A-C	13.8	13.3	14.9	17.9
TOTAL A-D	13.4	11.6	10.9	13.5

GWP (in kgCO _{2eq} per m ²)				
	Concrete	Inodek	Cofradal 260	Cofraplus 220
TOTAL A-C	105	101	112	135
TOTAL A-D	101	88	82	102

The comparison as given in Tab. 5-9 show advantages for Inodek. This is also demonstrated in Fig. 5-9.

Tab. 5-9: Comparative results of the LCA (Case 3)

Comparative results	
Reference:	Cofradal 260
Concrete in-situ	+ 23%
Inodek:	+ 6%
Cofraplus 220:	+ 24%

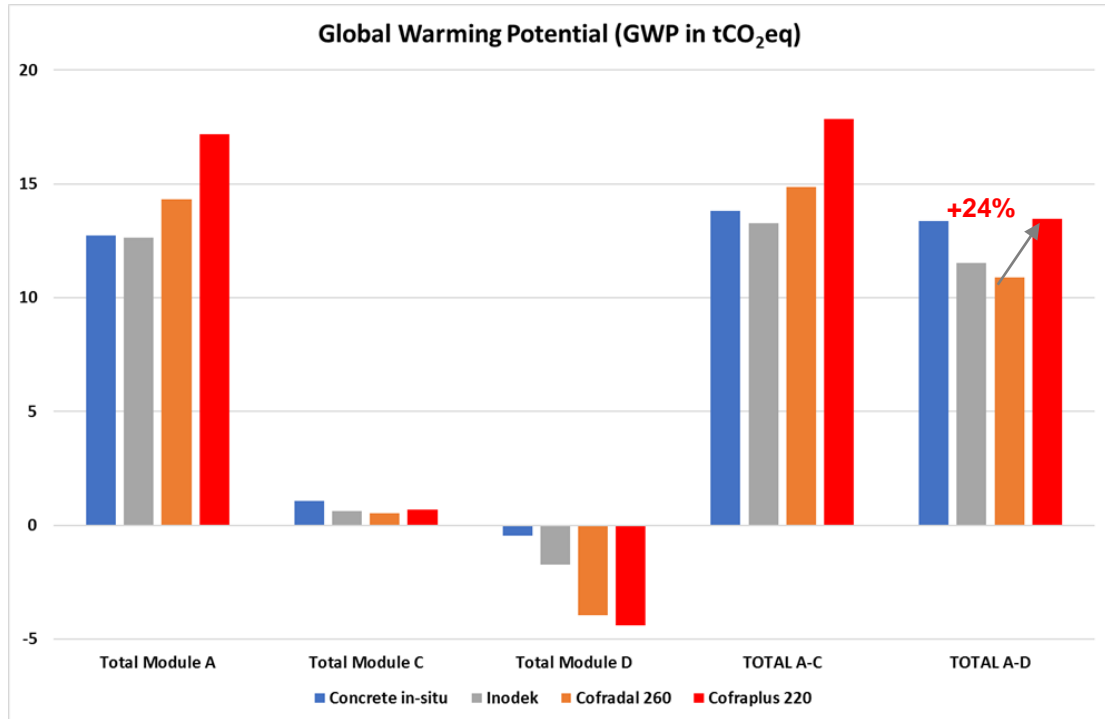


Fig. 5-9: Global warming potential of different variants (Case 3) regarding the different modules as given in Fig. 5-2.

5.4.2.6 Case 4: Below ground car park

2 slim-floor variants:

- Cofradal 260
- Comflor 225

Grid: 10.8 m x 8.1 m

Column height: 3.0 m

The beam distance was reduced to 5.0 m because it is a parking

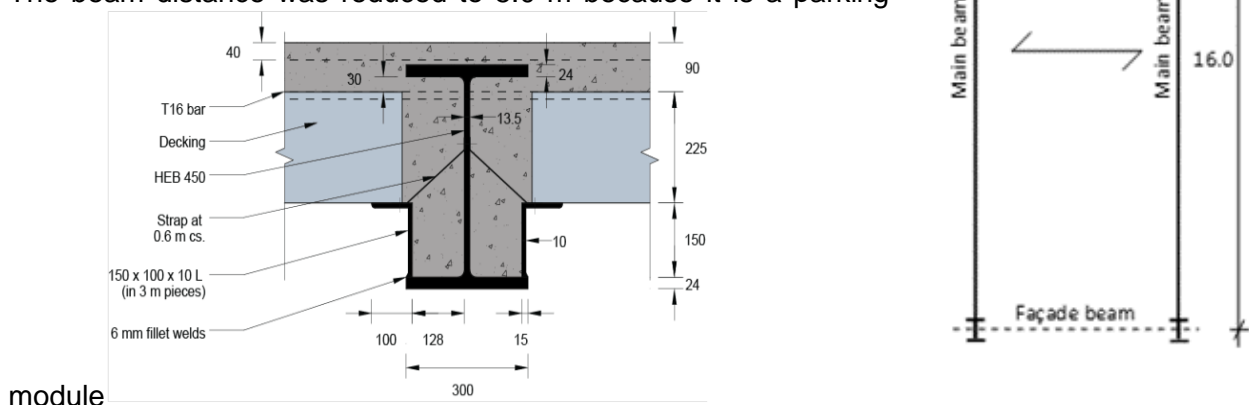


Fig. 5-10: Floor layout below ground car park

For variant b) "Long span beam", the deep decking solution proposed by SCI is used. In this system, the slab is supported by angles welded to the bottom flange of I-profile.

The bill of materials for the 2 variants is summarized in Tab. 5-10

Tab. 5-10: Bill of material for below ground car park (case 4)

Floor system	in tons	Comflor 225	Cofraplus 220
Steel	Beams	3.184	2.24
	Plates	0.69	1.57
	Steel sheet	1.386	1.34
	Reinforcement	1.414	1.138
Concrete	Slab	In situ C30/37 t=36 cm 36.672	In situ C30/37 t= 36 cm 33.984
Rockwool		-	-
Gypsum		-	-
Total weight in tons		43.3	40.3
Total weight in ton/m² of floor		0.54	0.50

Note: Steel reinforcement: including dowels, slab rebars, and fire protection for Cofraplus and Comflor solutions

The LCA results (GWP Global Warming Potential) are given in Tab. 5-11 for 2 different steel deck solutions.

Tab. 5-11: LCA results (Global Warming Potential) for Case 4

GWP (in tCO ₂ eq)	Comflor 225	Cofraplus 220
Total Module A	14.301	14.647
Total Module C	0.473	0.428
Total Module D	-3.295	-4.212
TOTAL A-C	14.8	15.1
TOTAL A-D	11.5	10.8
<hr/>		
GWP (in kgCO ₂ eq per m ²)		
TOTAL A-C	185	188
TOTAL A-D	143	136

The comparison as given in Tab. 5-12 show slight advantages for Cofraplus. This is also demonstrated in Fig. 5-11.

Tab. 5-12: Comparative results of the LCA (Case 4)

Comparative results	
Reference:	Cofraplus 220
Comflor 225	+ 6%

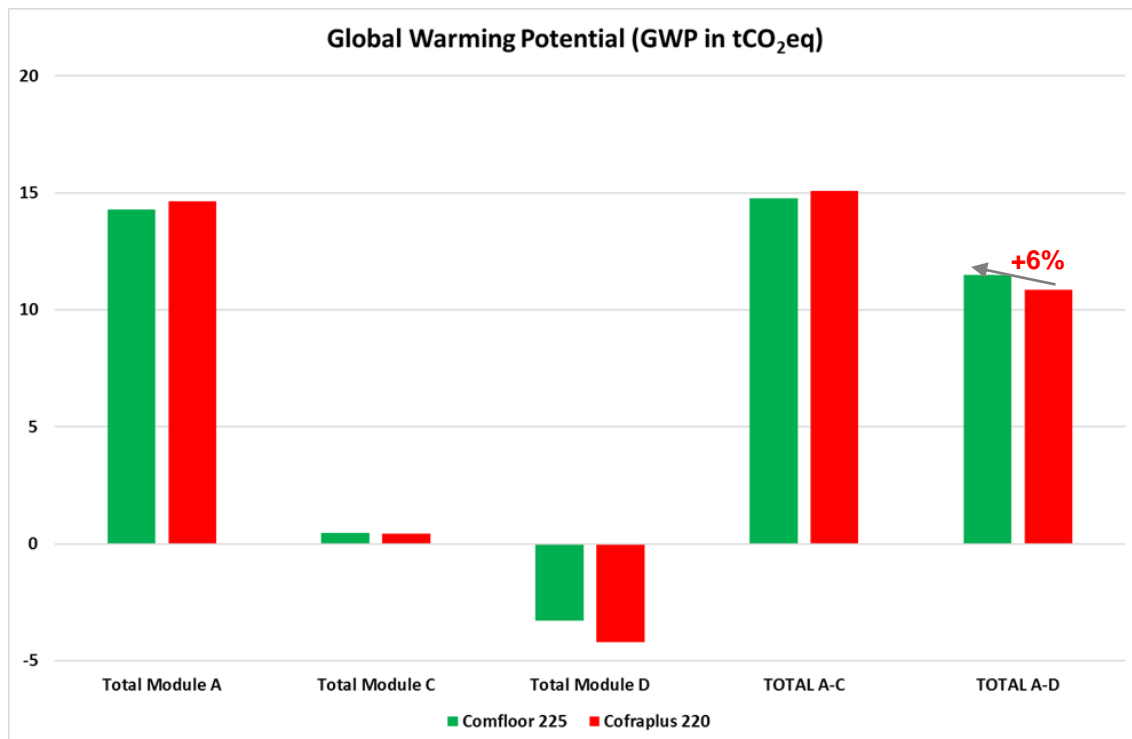


Fig. 5-11: Global warming potential of different variants (Case 4) regarding the different modules as given in Tab. 5-10.

5.4.3 Conclusion of the LCA - analysis

The comparison of results of all case studies performed in the scope of this project lead to the general conclusion that the lightest solution provides the best LCA solution, in all case studies.

The slim-floor systems with steel provide lower environmental impact in term of Global Warming Potential (CO₂ eq) than for concrete solutions. The gain obtained varies from 24% until 75%, depending of the selected case study.

5.4.4 LCP - Life cycle performance analysis of slim-floors systems

5.4.4.1 General

Regarding the social performance, the following parameters based on the slim-floor systems identified are:

- Acoustic behaviour of the slim-floor system
- Durability of the flooring
- Possibility of conversion of the flooring
- Integration of services in the floor zone.

5.4.4.2 Acoustic behaviour of the slim-floor system

Acoustic tests were performed on a 10-storey building comprising restaurants and shops on the ground floor and 120 apartments on the floors above. The apartments ranged from one bedroom studios to three bedroom apartments. The structural solution was a steel frame with composite floors using deep decking .The form of construction of the floors is shown in Fig. 5-12.

On-site acoustic testing was carried out to EN ISO 140: Parts 4 [61] and 7 [62] for airborne sound reduction and impact sound transmission. The Standard Weighted Level Difference $D_{hT,w}$, the Standard Weighted Impact Sound Pressure Level $L'_{nT,w}$ and the spectrum adaptation term C_{tr} were

calculated and the measured results for the 18 separating floors on different apartments are shown in Tab. 5-13. The

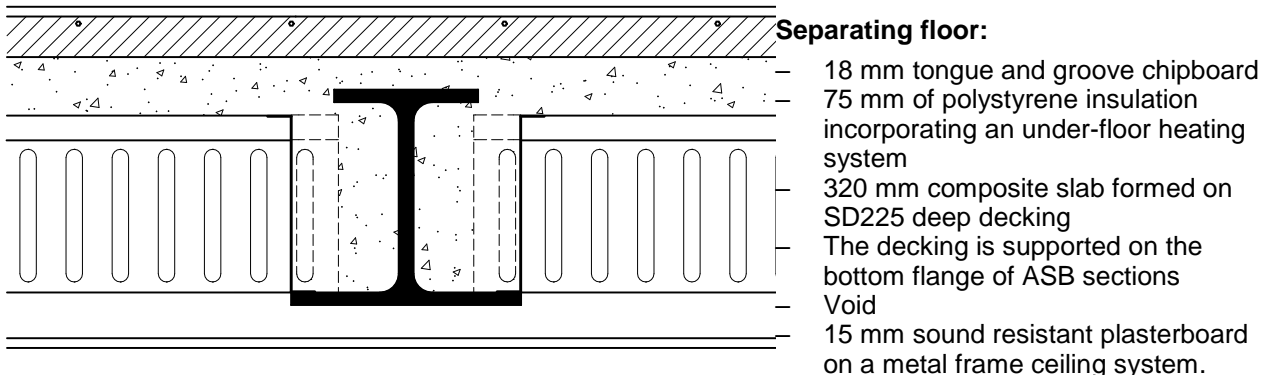


Fig. 5-12: Build-up of floor and its finishes

average airborne sound reduction was 10 dB better than the UK Building Regulations including the C_{tr} value. The average impact sound transmission was 19 dB less than the Regulations. It is concluded that the acoustic results of the *Slimdek* system are excellent.

Tab. 5-13: Acoustic test results measured on the completed building

Floor test results (18 tests)		Measured	Building Regulations
Airborne $(D_{nT,w} + C_{tr})$	Test Maximum	64 dB	
	Test Minimum	53 dB	
	Average	55 dB	≥ 45 dB
Floor test results (18 tests)		Measured	Building Regulations
Impact $(L'_{nT,w})$	Test Maximum	47 dB	≤ 62 dB
	Test Minimum	39 dB	
	Average	43 dB	≤ 62 dB

5.4.4.3 Service integration in slim floor construction

Slim floor systems provide the minimum floor depth so that services run underneath. However, there are opportunities to integrate services within the structural zone and especially between the ribs of the deep decking. Examples of service integration are:

- Circular or elongated openings through the webs of the slim floor beam shown in Fig. 5-13.
- Electrical ducts embedded in the top of the slab.
- Extract ducts and chilled beams located between the ribs of the decking, as shown in Fig. 5-13.
- Ceilings, electrical trays and ducts suspended from the decking ribs.

In the RFCS project BATIMASS [75] the passive cooling effect of the exposed deep deck flooring system was investigated in comparison to other forms of decking and to a flat concrete slab over a 24 h heating cycle. The maximum rate of heat transfer to the deep deck slab was 37 W/m²K in comparison to 24 W./m²K for an equivalent thickness of flat concrete slab, because of the greater exposed surface of the deep decking.

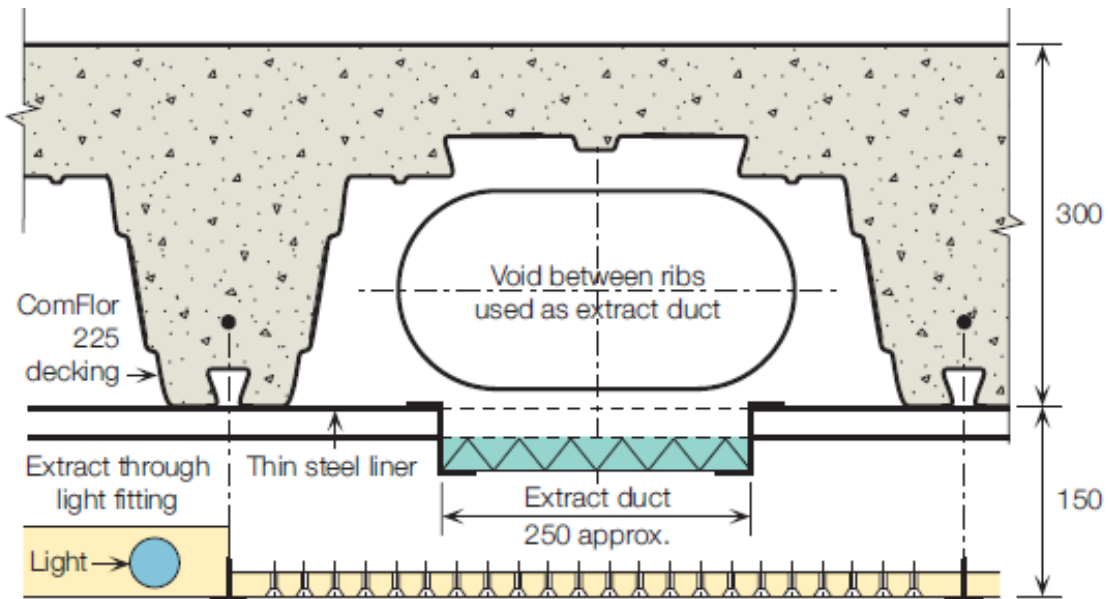


Fig. 5-13: Terminal units and chilled beams located between the deck ribs

5.4.4.4 Durability of slim floor systems

The durability of slim floor systems is dependent on three aspects of design:

- Protection to the exposed bottom plate or flange of the beam that may be subject to risk of corrosion
- The use of galvanised (zinc coated) decking or coated decking
- Risk of water ingress through the cracked concrete

Generally only the exposed bottom plate is protected if required by the environmental conditions. The steel decking is protected by its zinc coating (at 20 µm per face or 275 g/m² zinc) for exposure Classes 1 and 2, but an additional painted coating may be required for more severe environments. It is also possible to design the decking as 'formwork' and to use additional reinforcement rather than relying on composite action over the long term. An example of the use of coated decking in partially exposed car parks is shown in Fig. 5-14.

Water ingress through cracked concrete may be a risk in car parks or industrial structures. The minimum reinforcement area is typically 0.5% of the concrete topping area to the decking or precast concrete units, which equates to about 500 mm²/m.



Fig. 5-14: Use of colour coated composite decking in car parks

5.4.4.5 Conversion of slim floor systems

Slim floor systems provide an essentially flat floor and so it is easy to re-configure internal walls without down stand beams. Also slim floor systems are often used in the renovation of existing buildings where the minimum slab depth is required to conform to the fenestration pattern and floor to floor zone.

In the deep deck systems, openings of up to 300mm diameter may be drilled through the stab topping between the deck ribs for services. Because the beams are partially encased in the slab, no additional fire protection is required for 60 minutes fire resistance which assists in building conversions

6 DEVELOPMENT OF APPLICATION RULES IN EUROCODES

6.1 General

In this section of the report, guidance for the design of slim-floor beams for both the normal stage and the construction (non-composite) stage is given.

6.2 Rules for the Ultimate Limit State (ULS)

6.2.1 Construction stage

6.2.1.2 Actions

This section gives a brief description of the basis of design with particular emphasis to the steel profile of the slim-floor beam configuration should be designed to support the loads that occur during the construction phase, which depend on whether the beam is propped or unpropped during construction. The actions for which the steel profile is designed are:

- The self-weight of the slab and the steel section;
- Temporary actions due to the operatives placing the concrete and the additional weight of concrete locally. This is taken as a construction imposed load applied over the loaded area (refer to EN 1991-1-6 [57] and the relevant National Annex for characteristic value, at least 0.75 kN/m² recommended). Construction loads are treated as variable actions.

The relevant standards for actions and structural design in the construction phase are:

- EN 1991-1-1 [56] for actions on structures and EN 1991-1-6 [57], for actions during execution (construction stage);
- EN 1993-1-1 [42] for general rules for steel structures;
- EN 1993-1-3 [58] or technical approvals for profiled steel sheeting

6.2.1.3 Section classification

The section class of the steel profile determines whether plastic or elastic properties may be used for the beam design at the construction stage. In a slim-floor beam, the HE or UC steel profile is welded to a bottom plate. Therefore the resulting slim-floor beam profile is asymmetric in shape. The plastic neutral axis depth is therefore low in the section and so the web may be almost fully in compression. The section class depends also on the web as well as the flange.

The dimensional limits for Class 2 sections are:

- Compression flange:
$$c \leq 10 \cdot t_f \cdot \varepsilon; \quad (6-1)$$

- Web in compression:
$$y_w \leq 38 \cdot t_w \cdot \varepsilon; \quad (6-2)$$

where

c	flange outstand dimension
t_f	flange thickness
t_w	web thickness
y_w	depth of web in compression taking account also of the root radius for rolled profiles
ε	$= (235/f_y)^{0.5}$

If these dimensional properties are not satisfied then elastic properties should be used. Because the (span/depth)-ratio of slim-floor beams is often in the range of 25 to 30, the control of deflections is often the critical design condition.

It is not generally practical for the top flange of the HE profile to extend above the final level of the slab, but the top of the beam may be placed level with the top of the slab. In this case, the section class of the top flange is partially affected by its bond with the concrete. In general for rolled sections, Class 2 properties may be used in the final design stage.

6.2.1.4 Design situations for internal and edge beams

There are two distinct stages for the design of internal beams in the construction stage, which are depicted in Fig. 6-1:

- Self-weight and construction loads applied to the supported area, which causes the maximum bending moment and shear force acting on the steel profile.
- Self-weight and construction loads applied to one side of the beam to cause the maximum torsional moment acting on the steel profile.

The beams are usually designed as simply supported beams that connect directly to columns or in some cases to other beams. Because of the need to resist torsional effects, end plate connections are generally used rather than fin plates or angle cleats. If some benefit from continuity is required, extended end plate connections may be used.

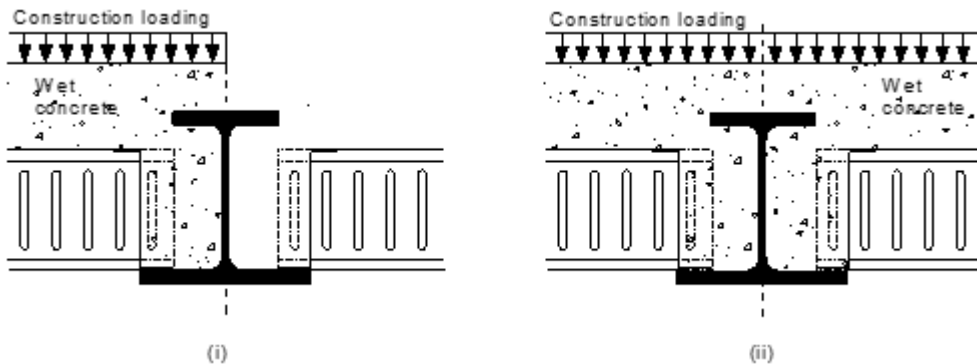


Fig. 6-1: Design situations during the construction stage

For slim-floor edge beams, only one situation with all the loads (self-weight and construction) present needs to be considered.

For these situations, the following resistances should be verified:

- Bending resistance of cross- section;
- Shear resistance of cross- section;
- Resistance of the beam to lateral torsional buckling;
- Resistance to combined bending and torsion.

6.2.1.5 Bending resistance

The bending resistance of a cross- section is given by EN 1993-1-1 [42], 6.2.5 as:

$$M_{c,Rd} = \frac{W_y \cdot f_y}{\gamma_{Mo}} \quad (6-3)$$

where

W_y is the section modulus for bending about the y-y axis:
 for Class 1 and 2 cross-sections, $W_y = W_{pl,y}$;
 for Class 3 cross-sections, $W_y = W_{el,y}$;

	for Class 4 cross-sections, $W_y = W_{\text{eff},y}$;
$W_{pl,y}$	plastic section modulus about the y-y axis;
$W_{el,y}$	elastic section modulus about the y-y axis;
$W_{\text{eff},y}$	effective section modulus about the y-y axis;
f_y	yield strength of structural steel;
γ_{M0}	= 1.0, as given by EN 1993-1-1 or the relevant National Annex.

6.2.1.6 Vertical shear resistance

The vertical shear resistance of the steel section is determined in accordance with EN 1993-1-1 [42], 6.2.6(2) as follows:

$$V_{\text{pl,Rd}} = \frac{A_v \cdot f_y}{\sqrt{3} \cdot \gamma_{M0}} \quad (6-4)$$

where

A_v is the shear area, which may be calculated from EN 1993-1-1 [42], 6.2.6(3).

If the section has web openings, the shear resistance at a web opening position should be determined from sec. 6.4.

The interaction between bending and shear should be accounted for in accordance with EN 1993-1-1 [42], 6.2.8.

6.2.1.7 Resistance to lateral torsional buckling

In the construction stage the top flange of the section is laterally unrestrained and therefore the section should be verified against lateral torsional buckling (LTB) in accordance with EN 1993-1-1 [42], 6.3.2.1.

Due to the welding of the bottom plate, which may increase imperfections, a slim-floor beam is not expected to behave as well as a rolled beam of equivalent shape which can use LTB curves a or b according to EN 1993-1-1 [42], 6.3.2.2. A conservative approach is the use of curve c be used, which corresponds to an initial imperfection parameter of $a_{LT} = 0.49$. If justified, a less conservative curve may be used.

The elastic critical moment for LTB, which is required for the calculation of the non-dimensional slenderness, is given for a section that is symmetric about its minor axis loaded through its bottom plate as:

$$M_{\text{cr}} = C_1 \cdot \frac{\pi^2 \cdot EI_z}{L^2} \left[\sqrt{\frac{I_w}{I_z} + \frac{L^2 \cdot GI_T}{\pi^2 \cdot EI_z} + (C_3 \cdot z_j)^2} + C_3 \cdot z_j \right] \quad (6-5)$$

where

I_T	St. Venant torsional constant;
I_w	warping constant;
I_z	second moment of area about the minor axis;
G	shear modulus;
C_1, C_3	factors depending on the loading and end restraint conditions (see Tab. 6-1);

k_z, k_w are effective length factors referring to end rotation conditions on plan and end warping, respectively (they vary from 0.5 for full restraint at both ends to 1.0 for no restraint at each end, with 0.7 for one end fixed and one end free);

$$z_j \cong \psi_f h_s / 2;$$

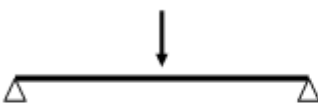
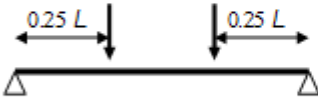
$$\psi_f = (I_{fc} - I_{ft}) / (I_{fc} + I_{ft});$$

I_{fc} second moment of area of the compression flange about the minor axis of the section;

I_{ft} second moment of area of the tension (compound) flange about the minor axis of the section.

h_s Distance between the shear centres of the compression flange and the tension (compound) flange

Tab. 6-1: Values of factors C_1 and C_3

Loading conditions	C_1	C_3
	1.35	0.411
	1.04	0.562
	1.12	0.525

6.2.1.8 Resistance to lateral torsional buckling in the presence of torsion

The resistance of non-composite slim-floor beams to combined bending and torsion is carried out in accordance with a modified form of the interaction criterion in Annex A of EN 1993-6 [59].

$$\frac{M_{y,Ed}}{\chi_{LT} \cdot M_{y,Rd}} + C_{mz} \cdot \frac{M_{z,Ed}}{M_{z,Rd}} + k_w \cdot k_{zw} \cdot k_a \cdot \frac{M_{w,Ed}}{M_{w,Rd}} \leq 1 \quad (6-6)$$

where

C_{mz} equivalent uniform moment factor for bending about the minor axis according to EN 1993-1-1 [42], Table B3;

$$k_w = 0.7 - 0.2 \cdot M_{w,Ed} / M_{w,Rd};$$

$$k_{zw} = 1 - M_{z,Ed} / M_{z,Rd};$$

$$k_a = 1 / (1 - M_{y,Rd} / M_{cr}).$$

However, $M_{z,Ed} = 0$ due to the restraining effect of the attached decking and therefore the above criterion becomes:

$$\frac{M_{y,Ed}}{\chi_{LT} \cdot M_{y,Rd}} + k_w \cdot k_a \cdot \frac{M_{w,Ed}}{M_{w,Rd}} \leq 1 \quad (6-7)$$

6.2.1.9 Local transverse bending of plate

Biaxial bending of the bottom flange plate has to be considered, due to the way the loads (wet concrete and construction loads) are applied at the construction stage (through the decking resting on the plate) which means that the plate is also subject to local transverse bending stresses. The

interaction between the longitudinal stress and these local transverse bending stresses is accounted for in accordance with the following approximate formulae [73] which is based on the Von Mises yield criterion:

$$f_{ybt} \cong f_y \cdot \left[1 - 0.52 \cdot \left(\frac{M_{ybt,Ed}}{M_{ybt,Rd}} \right) - 0.48 \cdot \left(\frac{M_{ybt,Ed}}{M_{ybt,Rd}} \right)^2 \right]^{0.5} \quad (6-8)$$

where

- f_{ybt} is the reduced yield strength of the bottom flange plate to be used in subsequent calculations of the design resistance moment;
- f_y is the nominal yield strength of the bottom flange plate;
- $M_{ybt,Ed}$ is the local bending moment per unit length of plate caused by an eccentric force at a distance (lever arm) taken between the centre of bearing of the decking onto the plate and midway the weld fillet (or the root radius);
- $M_{ybt,Rd}$ is the bending resistance of the plate, taken as 1.2 times the elastic resistance ($= 1.2 \cdot t_{bt}^2 \cdot f_y / 6$) instead of the full plastic resistance, in order to limit the extend of irreversible (plastic) deformation under serviceability loads.

6.2.2 Normal stage

6.2.2.1 Shear connection

When headed stud connectors are used, their design shear resistance should be determined from EN 1994-1-1 [40], 6.6.3.1. The relevant requirements of EN 1994-1-1, 6.6.1.1, 6.6.1.3, 6.6.5.2 and 6.6.5.5 to 6.6.5.8 should also be satisfied, as appropriate.

The design shear resistance per reinforcing bar through a circular opening in the web of the steel section should be determined from:

$$P_{Rd} = \frac{P_{conc} + P_{dowel}}{\gamma_v} \quad (6-9)$$

where

$$P_{conc} = \frac{30 \cdot (f_{ck} \cdot t_w \cdot h_o)^{1/3}}{(1-\rho)^2} \text{ (in kN)}$$

$$P_{dowel} = 2V_{pl,r} = \frac{2A_r f_{sk}}{\sqrt{3}} \text{ (in kN)}$$

$$\rho = \frac{A_r}{A_o} = \frac{\phi^2}{h_o^2}$$

$$\gamma_v = 1.25$$

f_{ck} concrete compressive strength in kN/cm²

t_w width of the steel profile web in cm

h_o diameter of the holes in the steel profile web in cm

$A_r = \frac{\phi^2 \pi}{4}$ - section area of the reinforcement bar in cm²

f_{sk} characteristic tensile strength of the reinforcement bar in kN/cm²

$A_r = \frac{h_o^2 \pi}{4}$ - area of the hole in the web of the steel profile in cm²

This model is valid for concrete grades C25/30 up to C55/67, web openings between 40 mm and 80 mm and bar diameters between 12 mm and 20 mm.

Note: The above design model is semi-empirical and was partly fitted to the push-out test results of this project. A similar model was obtained by Braun [71]. The difference with that model in terms of formulation is found in the concrete term. Also, the validity of that model was reportedly limited to 12 mm diameter bars.

The push-out test results of this project suggest that the bar diameter has a significant effect on the resistance and the stiffness of the connection. This is demonstrated in Fig. 2-3 by comparing the results of POT 3b vs POT 6 for example, but also POT 2 vs POT 7 (the concrete strength was also different but only slightly, i.e. average values of 38.5 N/mm² and 42.1 N/mm² were obtained for POT 2 and POT 7, respectively).

The good agreement of the model against the push out test results of this project and also those reported in [71] is demonstrated in Fig. 6-2. The tests are excluded, where failure of the concrete support occurred first. The set of points in the lower left corner is for POT 4 (no reinforcing bar) and therefore the predicted value was obtained only from the concrete term of the presented resistance model.

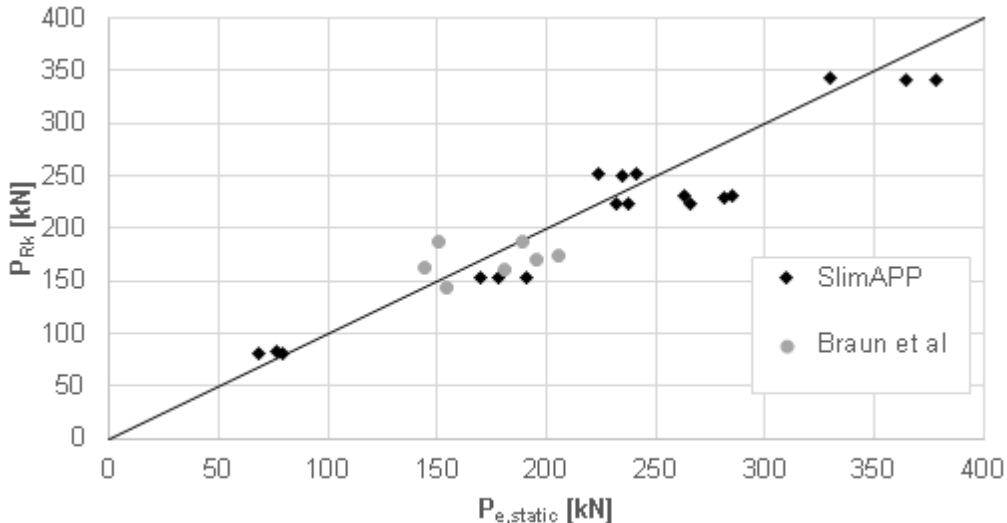


Fig. 6-2: Concrete dowel resistance predicted using Eq. (6-9) against push-out test results of section 2.2 and those reported in [71]

Back-analysis of the beam tests was also carried out. Shear connection is significantly enhanced due to friction effects. Therefore, if the degree of shear connection is calculated only by taking account of the connectors (headed studs or concrete dowels) and ignoring friction will be significantly underestimated. This, in combination with the high ductility exhibited by both types of connectors in the tests, suggests that adoption of the current minimum degree of shear connection rules of EN 1994-1-1 [40] would be conservative. Instead, a minimum degree of shear connection of 40% is recommended, provided that partial shear connection is also accounted for in the calculation of deflections at serviceability. However, more research is required in order to verify this.

6.2.2.2 Moment resistance

Plastic resistance moment

The plastic resistance moment of the composite slim-floor beam may be determined using plastic cross-section analysis (stress blocks).

The effective width is taken as that given in EN 1994-1-1 [40], 5.4.1.2(5), i.e. for an internal beam this is equal to span/4, limited by the actual distance between beam centres. However, the degree of shear connection has to be accounted for in the calculations by limiting the compression resistance to the longitudinal shear force N_q that can be transferred to the concrete by the shear

connectors (partial shear connection case). Full shear connection is achieved when the longitudinal shear force available is equal to or greater than the compression resistance of the concrete.

The position of the plastic neutral axis (PNA) should be determined by taking into account equilibrium in the section. Concrete in tension is neglected. For the typical case of having a highly asymmetric steel section, which could result by welding a plate to the bottom flange of an I or H shaped steel beam and partial shear connection through concrete dowels, the following two scenarios are considered, namely PNA in the lower part of the web and PNA in the bottom flange of the steel beam. Design equations are developed for these two cases and are presented here. Although these cases are expected to occur more frequently, other cases are possible, depending on the asymmetry of the steel section, the depth of concrete and also the degree of shear connection (full or partial shear connection). However, formulae for these cases may be derived in the same manner.

Case 1 PNA in lower part of web (below the opening)

$$N_p + N_{fb} + N_{wb2} > N_{wb1} + N_{wt} + N_{ft} + N_q \text{ and } N_q \leq N_c \quad (6-10)$$

where

N_q longitudinal shear force available ($= n \cdot P_{Rd}$)

n number of shear connectors between the point of maximum bending and a point of zero moment

P_{Rd} Design resistance of one shear connector

N_c compression resistance of the concrete flange ($= 0.85 \cdot f_{cd} \cdot b_{eff} \cdot h_c$)

Depth is taken equal to the depth of concrete above the steel deck h_c (no contribution from the concrete encasement between the steel decks)

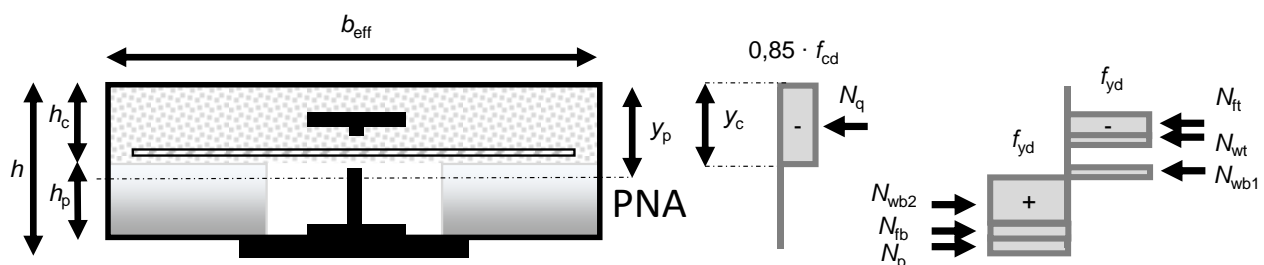


Fig. 6-3: Stress blocks for calculation of moment resistance (PNA in lower part of web)

With reference to Fig. 6-3:

$$y_p = h_{cc} + t_{ft} + h_{wt} + h_o + \frac{N_p + N_{fb} + N_{wb2} - (N_{wb1} + N_{wt} + N_{ft} + N_q)}{2 \cdot f_y \cdot t_w} \quad (6-11)$$

where

h_{cc} concrete cover above the steel section;

y_c depth of concrete in compression ($N_q / (0.85 \cdot f_{cd} \cdot b_{eff})$).

The plastic resistance moment of the composite section is:

$$\begin{aligned}
 M_{pl,Rd} = & N_p \cdot \left(h_s - y_p + \frac{t_p}{2} \right) + N_q \cdot \left(y_p - \frac{y_c}{2} \right) + N_{ft} \cdot \left(y_p - h_{cc} - t_{ft}/2 \right) \\
 & + N_{wt} \cdot \left(y_p - h_{cc} - t_{ft} - h_{wt}/2 \right) + N_{fb} \cdot \left(h_s - y_p - \frac{t_{fb}}{2} \right) + N_{wb2} \cdot \\
 & + (h_s - y_p - t_{fb})/2 + N_{wb1} \cdot (y_p - h_o - h_{wt} - t_{ft} - h_{cc})/2
 \end{aligned} \quad (6-12)$$

Case 2 PNA in bottom flange

$$N_p + N_{fb} > N_{wb} + N_{wt} + N_{ft} + N_q \text{ and } N_q \leq N_c \quad (6-13)$$

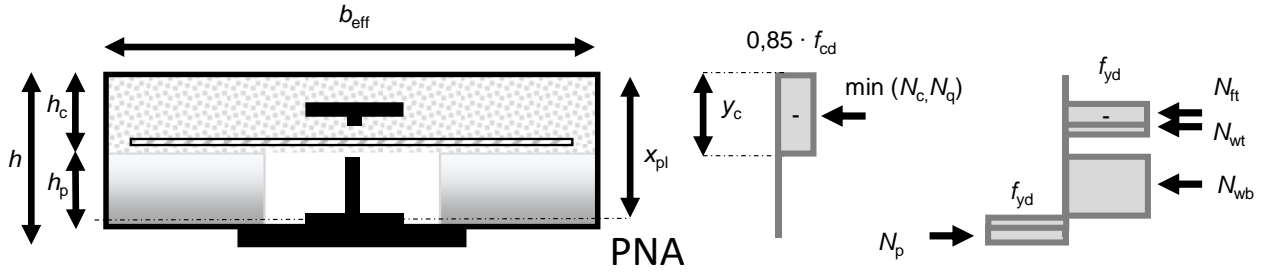


Fig. 6-4: Stress blocks for calculation of moment resistance (PNA in bottom flange)

With reference to Fig. 6-4:

$$y_p = h_c + h_p - t_{fb} + \frac{N_p + N_{fb} - (N_{wb} + N_{wt} + N_{ft} + N_q)}{2 \cdot f_y \cdot b_{fb}} \quad (6-14)$$

and the plastic resistance moment of the composite section (ignoring any contribution from the bottom flange for simplicity) is:

$$\begin{aligned}
 M_{pl,Rd} = & N_p \cdot (h_s - y_p + t_p/2) + N_q \cdot (y_p - y_c/2) + N_{ft} \cdot (y_p - h_{cc} - t_{ft}/2) \\
 & + N_{wt} \cdot \left(y_p - h_{cc} - t_{ft} - \frac{h_{wt}}{2} \right) + N_{wb} \cdot (y_p - h_{cc} - t_{ft} - h_{wt} - h_o - h_{wb}/2)
 \end{aligned} \quad (6-15)$$

Strain based resistance moment

A strain-based method of design was also formulated and comparisons were carried out with plastic design for a number of cases. These comparisons identified cases where the plastic resistance moment may not be reached and yielding of the steel section may be preceded by the strain in the concrete reaching the limiting value of 3.5 %. For such cases, the calculated plastic resistance may be unconservative. Full shear connection (strain compatibility) was assumed for the purposes of these comparisons, which is a conservative assumption. Although research is ongoing, Fig. 6-5 presents a proposed reduction factor β to the plastic resistance moment plotted against the depth of the plastic neutral axis x_{pl} relative to the total depth of the composite section h . Similar findings were reported by others [74]. Currently, EN 1994-1-1 [40] limits plastic design only for steel grades S420 and S460.

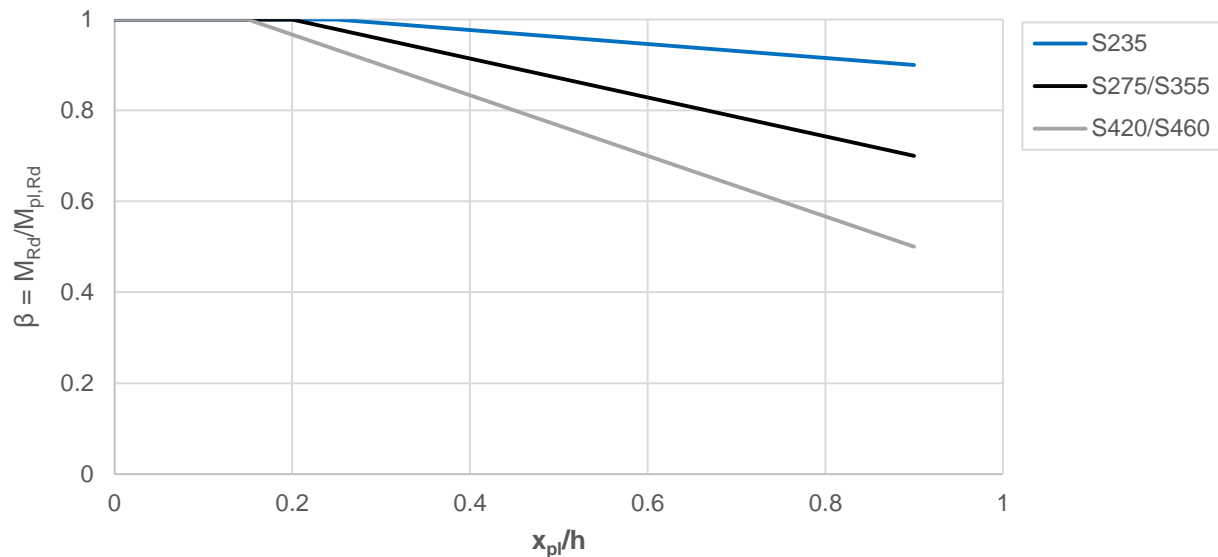


Fig. 6-5: Reduction factor β to the plastic resistance moment plotted against the depth of the plastic neutral axis x_{pl} relative to the total depth of the composite section h [15]

6.2.2.3 Longitudinal shear resistance

It is required to ensure that the compressive force in the concrete can be distributed across the effective width without failure of one of the assumed shear surfaces shown in Fig. 6-6. The design shear strength of the concrete flange should be determined in accordance with the strut-and-tie model of EN 1992-1-1 [48], 6.2.4.

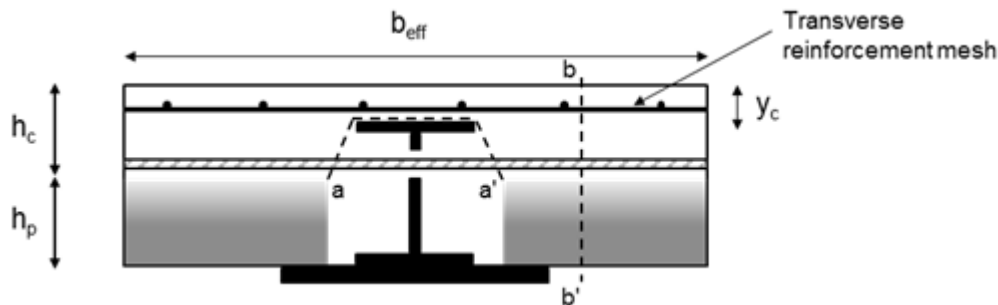


Fig. 6-6: Critical surfaces for longitudinal shear failure

The longitudinal shear stress ν_{Ed} , at a critical shear surface is given by:

$$\nu_{Ed} = \frac{\Delta F_d}{h_f \cdot \Delta x} \quad (6-16)$$

where

ΔF_d change in the force in the concrete over the length Δx

h_f length of the shear surface as defined in EN 1994-1-1 [40], 6.6.6.2 and 6.6.6.4 (for shear plane b-b')

Δx length being considered

Considering the length between two connectors (headed studs or reinforcing bars through web openings, i.e. $\Delta x = s$), the change in the force is equal to the longitudinal shear resistance of the connector ($\Delta F_d = P_{Rd}$).

The required transverse reinforcement area per unit length may then be determined from:

$$\frac{A_{sf} \cdot f_{yd}}{s_f} \geq \nu_{Ed} \cdot \frac{h_f}{\cot \theta_f} \quad (6-17)$$

where

- A_f area of each bar
- s_f spacing of the reinforcement bars
- f_{yd} design yield strength of the reinforcement
- θ_f angle of dispersion of the force from the connector, taken as $26.5^\circ \leq \theta_f \leq 45^\circ$

The effective reinforcement to be considered for each of the shear surfaces of Fig. 6-6 is given in Tab. 6-2.

Tab. 6-2: Effective transverse reinforcement

Failure type	A_{sf}/s_f
a-a'	$2A_b$
b-b'	$A_t + A_b$

The minimum area of transverse reinforcement as a proportion of the concrete area is determined in accordance with EN 1992-1-1 [48], 9.2.2(5) and the ratio:

$$\rho_{w,min} \geq \frac{0.08 \cdot \sqrt{f_{ck}}}{f_{yk}} \quad (6-18)$$

Therefore, the minimum area of transverse reinforcement is obtained from:

$$\frac{A_{sf}}{s_f} = \rho_{w,min} \cdot h_f \quad (6-19)$$

6.2.2.4 Transverse shear resistance

The transverse shear resistance of the composite slim floor section is conservatively taken as the resistance provided by the steel section as calculated in 6.2.1.6, ignoring any contribution from the concrete.

Note: It is expected that the concrete contributes significantly to the transverse shear resistance, particularly in the case of slim floor beams. This is also supported by research findings [70]. The current version of EN 1994-1-1 [40] ignores any contribution of the concrete slab for downstand beams. However, this may change in the future as the Eurocodes are currently being revised.

6.3 Rules for the Serviceability Limit State (SLS)

In addition to rules and principles given in Section 7 of EN 1994-1-1 [40], it should be assured that the stresses at any point in the steel section do not exceed the yield strength, taking into account transversal bending. Calculation of stresses shall be done in accordance with Section 7.2, EN 1994-1-1 [40].

The shear lag may be taken into account according to clause 5.4.1.2 of EN 1994-1-1 [40], or by available refined methods [64].

6.3.1 Serviceability limit state – construction stage

In the case of unpropped construction, the design of steel slim floor beams should be carried out in accordance with EN 1993-1-1 [42]. Construction loads should be specified in accordance with EN 1991-1-6 [57] and based on the details of expected construction procedure. Deflections due to loading applied to the steel member alone should be calculated in accordance with EN 1993-1-1 [42].

In propped construction, the design of the slim floor beam should be performed as a composite member based on the design rules provided in the following section for the in-service stage. In this case, the concrete properties should be determined at the times relevant to the design (and this should include the time of unpropping) and the design loads should be evaluated as specified in EN 1991-1-6 [57] and EN 1994-1-1 [40] for composite floor beams.

6.3.2 Serviceability limit state – in-service stage

6.3.2.2 General

A structure with composite members shall be designed and constructed such that all relevant serviceability limit states are satisfied according to the Principles of 3.4 of EN 1990 [60].

The verification of serviceability limit states should be based on the criteria given in EN 1990 [60], 3.4(3).

Serviceability limit states of floor slabs supported by the slim-floor beams and cast on either prefabricated components or on profiled steel sheeting should be verified in accordance with EN 1992-1-1 [48] and EN 1994-1-1 [40]. The vertical deformation of the slab supporting steel plate of the shallow cross-section due to the local load introduction should be verified and considered for the design of the slab.

6.3.2.3 Deformations in buildings

Deflections due to loading applied to the composite member should be calculated using elastic analysis in accordance with Section 5 of EN 1994-1-1 [40].

The reference level for the sagging vertical deflection of un-propped beams is the underside of the composite beam. Only where the deflection can impair the appearance of the building should the underside of the beam be taken as reference level.

The effects of partial shear connection should be included in the calculation of the deflection of the slim floor beam δ based on the following expressions [76]:

- for propped construction

$$\delta = \delta_c + 0.5 \cdot \left(1 - \frac{n}{n_f}\right) (\delta_s - \delta_c) \quad (6-20)$$

- for un-propped construction

$$\delta = \delta_c + 0.3 \cdot \left(1 - \frac{n}{n_f}\right) (\delta_s - \delta_c) \quad (6-21)$$

where:

δ_c deflection of the composite member with complete interaction

δ_s deflection of the steel member

n number of shear connectors provided

n_f number of shear connectors determined for full shear connection

Appropriate allowance shall be made for the effects of creep and shrinkage of concrete.

Creep and shrinkage effects shall be accounted for by satisfying the requirements set in EN 1994-1-1 [40] for composite beams.

The degree of shear connection defined as $\eta = n/n_f$ should be equal or greater than 0.4 unless a smaller value is justified through a design by testing approach [60].

6.3.2.4 Vibration

The dynamic properties of slim floor beams should satisfy the criteria in EN 1990 [60], A1.4.4.

6.3.2.5 Cracking of concrete

Cracking in the concrete components should be controlled in accordance with EN 1992-1-1 [48] and EN 1994-1-1 [40] so that structural performance, durability and appearance of the structure are not compromised.

6.4 Additional rules for web openings in slim-floor beams

6.4.1 General

The design of slim-floor beams with circular web openings is based on the transfer of shear and bending at the critical cross-section. Generally openings up to 40% of the beam depth have a small effect on the bending resistance and stiffness of the beam and so verification of the shear resistance of the reduced section is sufficient. For larger web openings, the transfer of shear by *Vierendeel* bending is the controlling aspect of the design.

The diameter of circular openings, h_o , can be up to 80% of the beam depth, but for forming of the openings, the minimum depth of the Tee section is equal to the flange depth plus 30 mm, so typically 50 mm. This means that the maximum opening diameter in an HE 300 section is 200 mm.

Openings may be widely or closely spaced and the definition of closely spaced is when the edge to edge spacing s_o , of the openings is less than their diameter. Openings may also be elongated by cutting of two circular openings, in which case, the opening length a_o , is generally less than 1.5x opening depth.

Often the openings are not placed on the centre-line of the beam in which case, the eccentricity is defined as distance e_o , of the centre-line of the opening from the centre-line of the steel section, which is positive when the centre-line of the opening is above the centre-line of the section and is negative below the centre-line of the section. The web-post is the web that remains between the openings and the end-post is the web-post next to a support.

6.4.2 Design verifications

The design of the slim-floor beams with web openings should be checked for the overall requirements of EN 1993-1-1 [42].The following additional verifications are required at web opening positions:

- Global bending resistance;
- Shear resistance;
- Combined *Vierendeel* bending resistance of the Tees reduced for axial forces and shear;
- Web-post shear, bending and buckling.

The following additional verifications are required for beams with web openings:

- Lateral torsional buckling in the construction phase;

- Additional deflections caused by the openings;
- Checks on connections and load introduction points at or near to the openings, which may require separate checks.

6.4.3 Section classification

For bending resistance in the construction stage, the section classification of the beam may be based on the cross-section at the web opening. The classification of the flanges or the web may be taken as in EN 1993-1-1 [42], 7.5 (Table 7.2). Where the flange is Class 1 or 2, the unsupported Class 3 web outstand at the opening may be classified as Class 2 by taking the depth as equal to Class 2 limit in pure compression. Where the flange is Class 1 to 3, the unsupported Class 4 web outstand at the opening may be classified as Class 3 by taking the depth as equal to the Class 3 limit in pure compression.

For local verification of the *Vierendeel* bending resistance, the section class of unstiffened outstand of the web of the Tee is determined by taking account of the variation of moment across the length of the opening. The outstand may be classified depending on the ratio of the effective length of the Tee at the opening, a_{eff} , to the outstand depth d_t . For rolled profiles, the outstand d_t is measured from the root radius. The effective length of the Tee at the opening is defined as:

$$\begin{aligned} a_{\text{eff}} &= 0.7 \cdot h_o && \text{for circular openings} \\ a_{\text{eff}} &= a_0 - 0.3 \cdot h_o && \text{for elongated circular openings} \end{aligned}$$

Class 3 web outstands of depth, d_t may be treated as Class 2 for *Vierendeel* bending when $a_{\text{eff}} > 32 \cdot t_w \cdot \varepsilon$ and:

$$d_t \leq \frac{10 \cdot t_w \cdot \varepsilon}{\sqrt{1 - \left(\frac{32 \cdot t_w \cdot \varepsilon}{a_{\text{eff}}} \right)^2}} \quad (6-22)$$

All Class 3 web outstands may be treated as Class 2 when $a_{\text{eff}} \leq 32 \cdot t_w \cdot \varepsilon$. For circular openings, this leads to a Class 2 limit of $h_o \leq 45 \cdot t_w \cdot \varepsilon$, which is always satisfied for rolled HE sections.

6.4.4 Shear resistance at web opening positions

For local checks at each web opening, the plastic shear resistance of the Tees may be used. The shear force at the centre-line of the opening should satisfy:

$$V_{\text{Ed}} \leq V_{\text{pl,Rd}} - \frac{h_o \cdot t_w \cdot f_y}{\sqrt{3} \cdot \gamma_{M0}} \quad (6-23)$$

where

- V_{Ed} shear force at the centre of the opening;
- $V_{\text{pl,Rd}}$ plastic shear resistance of the solid web cross-section from EN 1993-1-1 [42], 8.2.6;
- f_y steel yield strength.

The yield strength of the shear area of the Tees should be reduced due to the combination of high vertical shear, moment and normal force according to EN 1993-1-1 [42], 8.2.8 (4).

6.4.5 Bending resistance of beam with web openings

The bending resistance of the steel beam at the opening position $M_{o,\text{Rd}}$, should exceed the applied moment, M_{Ed} , at the centre of the opening. The bending resistance of the steel section may be given conservatively by:

$$M_{o,\text{Rd}} = (h - z_b - z_t) \cdot A_{tT} \cdot f_y \quad (6-24)$$

where:

- A_{tT} cross-sectional area of the top Tee;
- A_{bT} cross-sectional area of the combined bottom Tee and plate (if present);
- z_b, z_t are the elastic neutral axis distances of the bottom and top Tees from the bottom and top of the section, respectively.

6.4.6 Resistance of the Tees in Vierendeel bending

The shear resistance to *Vierendeel* bending is obtained from the combined bending resistances of the Tees divided by the equivalent opening length, a_{eq} in Tab. 6-3. The bending resistances of the top and bottom Tees may be different, which influences the development of a web-post moment for closely spaced openings in section 2.7.

Tab. 6-3: Equivalent rectangular opening dimensions for verification of Vierendeel bending

Shape of opening	Equivalent opening length, a_{eq}	Equivalent opening height, h_{eq}
Circular	$0.45 \cdot h_o$	$0.9 \cdot h_o$
Elongated	$a_o - 0.55 \cdot h_o$	$0.9 \cdot h_o$

The shear resistance to *Vierendeel* bending at the opening position should satisfy:

$$V_{Ed} \leq \frac{2 \cdot M_{NV,bT,Rd} + 2 \cdot M_{NV,tT,Rd}}{a_{eq}} \quad (6-25)$$

For Class 1 and 2 sections, the bending resistances of the Tees are reduced due to axial tension and compression, according to the following approximate formulae:

$$M_{NV,Rd} = M_{pl,Rd} \cdot \left[1 - \left(N_{Ed} / N_{pl,Rd} \right)^2 \right] \quad (6-26)$$

where:

- $M_{NV,Rd}$ bending resistance of the Tee section reduced due to axial force and shear;
- $M_{pl,Rd}$ plastic bending resistance of the Tee section including the effective yield strength with the depth of its web taken as the lesser of the actual depth and the limit for a Class 2 web outstand determined in 2.3.2;
- $N_{pl,Rd}$ compression resistance of the Tee including the effective yield strength with the depth of its web taken as the lesser of the actual depth and the limit for a Class 2 web determined in 2.3.2;
- N_{Ed} design value of the normal force due to the global bending acting on a Tee at the centre-line of the opening.

6.4.7 Web buckling next to openings

In the construction stage, web-post buckling next to the opening need not be checked for rolled sections if $h_o \leq 25 \cdot t_w \cdot \varepsilon$ for circular and elongated openings. This will cover practical cases of use of HE beams. In normal conditions, the web is stabilised by the concrete encasement.

For asymmetric sections, or where the centre of the opening is eccentric to the mid-height of the web, the distribution of shear force acting on the Tees, $V_{t,Ed}$ and $V_{b,Ed}$, may lead to development of an in-plane web-post moment, $M_{wp,Ed}$, between closely spaced openings.

The web-post moment at the centre-line of the opening is given by:

$$M_{wp,Ed} = 0.5 \cdot (V_{t,Ed} - V_{b,Ed}) \cdot s + V_{wp,Ed} \cdot e_o \quad (6-27)$$

where

$V_{b,Ed}$; $V_{t,Ed}$ shear forces resisted by the Tees based on their shear areas;

$V_{wp,Ed}$ web-post horizontal shear which is given by $V_{Ed} \cdot s / (h - z_h - z_t)$.

$M_{wp,Ed}$ can be positive or negative depending on the asymmetry of the section. The vertical shear forces may be distributed between the upper and lower Tees to minimize the web-post moment.

The shear resistance of the web-post should exceed $V_{wp,Ed}$ and is given by:

$$V_{wp,Rd} = \frac{s_o \cdot t_w \cdot f_y}{\sqrt{3} \cdot \gamma_{M0}} \quad (6-28)$$

where s_o is the edge to edge spacing of the openings.

The elastic bending resistance of the web-post should exceed $M_{wp,Ed}$, and is given by:

$$M_{wp,Rd} = \frac{s_o^2 \cdot t_{w,min} \cdot f_y}{6 \cdot \gamma_{M0}} \quad (6-29)$$

The web-post buckling model between closely spaced openings is based on an effective length of the compressed web-post, illustrated in Fig. 6-7. This applies only for steel slim-floor beams in the construction stage as the concrete encasement restrains the web-post in normal conditions.

For the purposes of this verification, the compressive force acting on the web-post, $N_{wp,Ed}$, is represented by the effective horizontal shear force, given by $N_{wp,Ed} = V_{wp,Ed}$. For web-posts subject to an in-plane moment, $M_{wp,Ed}$, web-post buckling may be analysed by considering an effective horizontal force in the web-post, $N_{wp,Ed}$, given by:

$$N_{wp,Ed} = V_{wp,Ed} + 2 \cdot M_{wp,Ed} / h_o \quad (6-30)$$

where $M_{wp,Ed}$ is determined from Equation 6-26 using the positive or negative value of the moment.

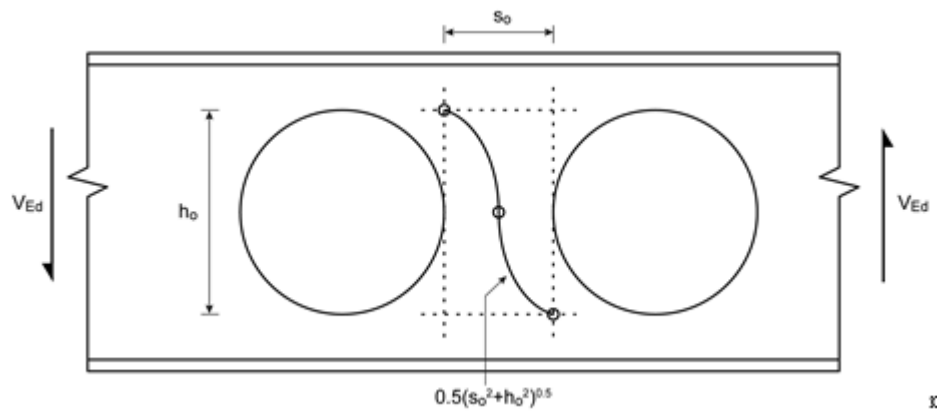


Fig. 6-7: Model for buckling of web-post between closely spaced circular openings

The web-post buckling resistance is given by:

$$N_{wp,Rd} = s_o \cdot t_{w,min} \cdot \chi_{wp} \cdot f_y / \gamma_{M1} \quad (6-31)$$

where χ_{wp} is determined from buckling curve a in EN 1993-1-1, 8.1.1.3 for steel grades up to S460 using the relative slenderness of the web-post given by:

$$\bar{\lambda}_{wp} = \frac{1.75 \cdot \sqrt{s_o^2 + h_o^2}}{t_w} \frac{1}{\lambda_1} \leq \frac{2.4 \cdot h_o}{t_w} \frac{1}{\lambda_1} \quad (6-32)$$

6.4.8 Alternative method for Vierendeel bending (circular openings)

This alternative method is based on equilibrium of the radial stresses around circular openings. The overall bending and shear resistance of the beam should be checked at the centre of the opening as in 2.4 and 2.5 (section a-a in Fig. 6-6).

The effects of *Vierendeel* moments should be checked on a radial plane around the opening (see section b-b in Fig. 6-6). The critical angle ϕ corresponding to the critical section b-b should be determined by increments of 5°. At the critical angle for the effects of *Vierendeel* moments, the internal force, $N_{\phi,Ed}$, and moment, $M_{\phi,Ed}$, on section b-b should satisfy the following criterion:

$$\frac{N_{\phi,Ed}}{N_{\phi,Rd}} + \frac{M_{\phi,Ed}}{M_{\phi,Rd}} \leq 1.0 \quad (6-33)$$

where

$N_{\phi,Ed}$ axial force perpendicular to the section b-b;

$N_{\phi,Rd}$ resistance to axial force of the section b-b;

$M_{\phi,Ed}$ bending moment in the section b-b;

$M_{\phi,Rd}$ moment resistance of the section b-b.

The internal forces and moments on section b-b should be determined by considering the equilibrium of the segment between sections a-a and b-b. The design resistances $N_{\phi,Rd}$ and $M_{\phi,Rd}$ should be determined allowing for the effects of the shear force V_{ϕ} according to EN 1993-1-1 [42], 8.2.6.

The design resistances $N_{\phi,Rd}$ and $M_{\phi,Rd}$ should be determined according to the class of the section on the radial plane of the opening.

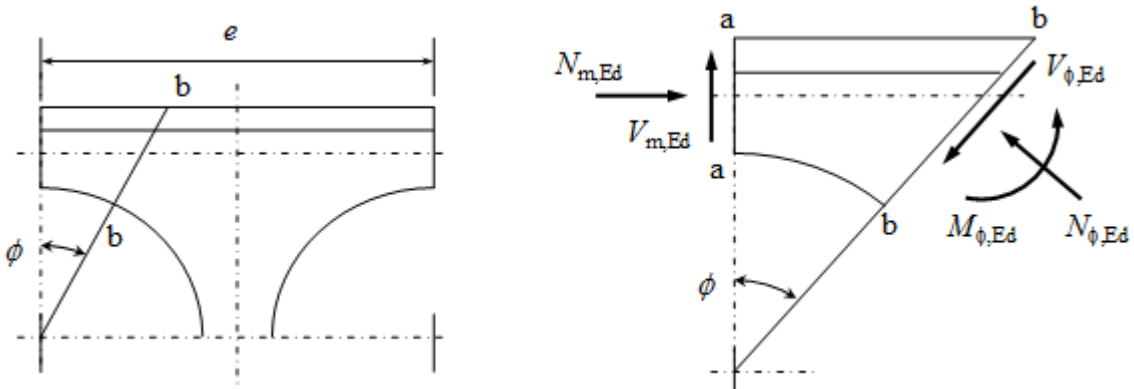


Fig. 6-8: Internal forces and moments at the critical section around an opening

7 DESIGN RECOMMENDATIONS FOR EC4 AND GUIDELINES FOR PRACTICE

7.1 Recommendations for Eurocode 4

7.1.1 Introduction

The following recommendations for future Eurocode 4 consider only slim-floor beams. In order to avoid uncertainties a definition for slim-floor beams must be given.

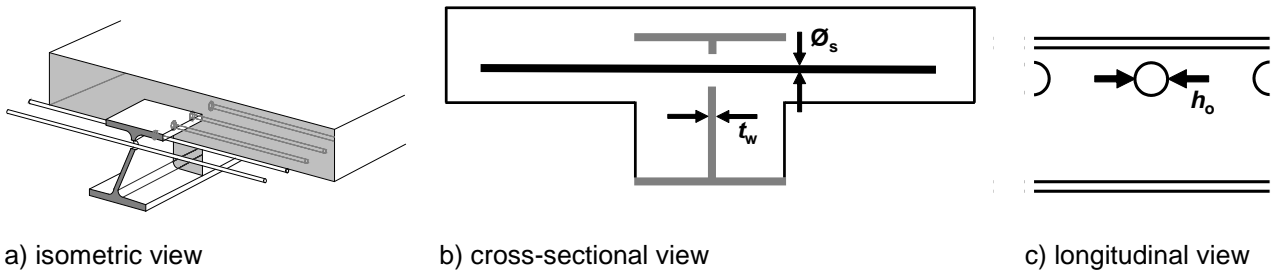
"A beam acting compositely with a slab. The slab may be precast concrete or in-situ concrete, with or without metal decking, where the concrete extends from the top of the bottom flange to at least the underside of the top flange". [72]

Design recommendations for ultimate limit state and for serviceability limit state are given hereafter based on the findings of this project.

7.1.2 Ultimate Limit state

Concrete dowel shear connectors

(1) The design shear resistance of concrete dowel shear connectors P_{Rd} as shown in Fig. 7-1 should be determined from eq. (7-1).



a) isometric view

b) cross-sectional view

c) longitudinal view

Fig. 7-1: Concrete dowel shear connectors system – Geometrical parameters

$$P_{Rd} = \frac{P_{\text{conc}} + P_{\text{dowel}}}{\gamma_v} \quad (7-1)$$

where

$$P_{\text{conc}} = \frac{30 \cdot (f_{ck} \cdot t_w \cdot h_o)^{1/3}}{(1-\rho)^2} \quad (\text{in kN}) \quad (7-2)$$

$$P_{\text{dowel}} = 2 \cdot V_{pl,r} = \frac{2 \cdot A_r f_{sk}}{\sqrt{3}} \quad (\text{in kN}) \quad (7-3)$$

and

$$\rho = \frac{A_r}{A_o} = \frac{\varnothing_s^2}{h_o^2}$$

γ_v = 1.25 - partial factor

\varnothing_s diameter of the reinforcement bar in cm

f_{ck} $1.2 \text{ cm} \leq \varnothing_s \leq 2 \text{ cm}$

f_{ck} characteristic concrete compressive strength in kN/cm^2

	$2.5 \text{ kN/mm}^2 \leq f_{ck} \leq 5.5 \text{ kN/cm}^2$
t_w	width of the steel profile web in cm
	$0.75 \text{ cm} \leq t_w \leq 1.55 \text{ cm}$
h_o	diameter of the holes in the steel profile web in cm
	$4 \text{ cm} \leq h_o \leq 8 \text{ cm}$
A_r	$= \frac{\phi^2 \pi}{4}$ - section area of the reinforcement bar in cm^2
f_{sd}	characteristic tensile strength of the reinforcement bar in kN/cm^2
A_r	$= \frac{h_o^2 \pi}{4}$ - area of the hole in the web of the steel profile in cm^2

7.1.3 Serviceability limit state

Deflections considering partial shear connection

(1) The effects of partial shear connection should be included in the calculation of the deflection of the slim floor beam δ based on the following expressions [76]:

- for propped construction

$$\delta = \delta_c + 0.5 \cdot \left(1 - \frac{n}{n_f}\right) (\delta_s - \delta_c) \quad (7-4)$$

- for un-propped construction

$$\delta = \delta_c + 0.3 \cdot \left(1 - \frac{n}{n_f}\right) (\delta_s - \delta_c) \quad (7-5)$$

where:

δ_c	deflection of the composite member with complete interaction
δ_s	deflection of the steel member
n	number of shear connectors provided
n_f	number of shear connectors determined for full shear connection

Appropriate allowance shall be made for the effects of creep and shrinkage of concrete.

(2) Creep and shrinkage effects shall be accounted for by considering the requirements set in sec. 5.4.2.2 for composite beams.

(3) The degree of shear connection defined as $\eta = n/n_f$ should be equal or greater than 0.4 unless a smaller value is justified through a design by testing approach [60].

7.2 Design rules and guidelines for the practice

State-of-the-art guidelines and recommendations have been developed within the project and comprised in a Handbook [18]. This type of guidelines offer help for designers and practical engineers interpreting the rules in Eurocodes. Additional practical and technical information are given, that are not part of the rules provided by Eurocode.

The Handbook comprises the following aspects for slim-floor beam design:

– Connections design	Shear connector design for a sufficient transfer of longitudinal shear load, partial shear connection, usage of innovative shear connector systems, etc.
– Ultimate Limit state design	ULS design in construction and In-service stage, moment resistance, shear resistance, etc.
– Serviceability Design	SLS design in construction and In-service stage, deformations, deflections, vibrations as well as cracking in the concrete, etc.
– Fire Design	Temperature distribution in protected and unprotected slim-floor beams, recommendations for resistance calculation under fire
– Joint Design	Efficient joint design supporting reducing deformations due to bending of the beam.

Based on the pilot projects described in sec. 1.4 design examples are provided focusing on the principles of the structural behaviour.

7.3 Workshop and dissemination

A workshop with experts has been conducted at the end of the project (June 2018) a Workshop in Valencia, Spain during “Advances in Steel-Concrete Composite Structures (ASCCS 2018)” conference (see Fig. 7-2).

The flyer is divided into several sections:

- Venue:** Universitat Politècnica de Valencia, Building 1G, Room 2, room 211, Camino de Vera s/n, 46022 Valencia.
- In the frame of the workshop the presentation of results of the pilot work will give a deeper insight into the project.**
- Project Sponsors:** Research Fund for Coal and Steel, European Union.
- Partners:** University of Stuttgart (Germany), SCI Steel Knowledge, ArcelorMittal, UNIVERSITY OF BRADFORD, ASTRON.
- SlimAPP Workshop:**
 - Content:** The RFCS-CT-2015-00020 project SlimAPP aims to increase the competitiveness of steel in buildings by developing a holistic approach for slim-floor solutions. This approach leads to efficient design also in view of sustainable constructions, which especially takes into account the connection between steel slab and concrete floor slab in normal conditions.
 - Program:**
 - 10:00 – 10:10 University of Stuttgart: Slim-floors: recent developments and trends. Rules in view of improved safety, functionality and LCA for practicing engineers.
 - 10:10 – 10:30 Novel connections for slim-floor beams - Experimental observation and conclusions.
 - 10:40 – 11:10 University of Bradford: Flexural behaviour of slim-floor beams - Experimental observations and conclusions.
 - 11:40 – 12:00 University of Vienna: Deflection and vibration behaviour of slim-floor beams - Experimental observation and conclusions.
 - 12:00 – 12:30 University of Bradford: Ultimate limit state design - Development of application rules.
 - 13:30 – 13:00 Christian-Albrechts-Universität zu Kiel: Lifecycle assessment of slim-floor solutions - Example calculations and presentation of software tool.
 - 13:00 – 13:30 University of Stuttgart: Built examples and optimization by improved solutions.
 - Registration:** Includes fields for Name, First Name, Company, Position, Address, City, Zip Code, and E-Mail. A note states: "The participation is free of charge. Registration requested up to 1st of June 2018".

Fig. 7-2: Workshop-Flyer

During the workshop following presentations have been held by the partners:

- Slim-floors: recent developments and trends - Rules in view of improved safety, functionality and LCA for practicing engineers
- Flexural behaviour of slim-floor beams - Experimental observations and conclusions
- Deflection and vibration behaviour of slim-floor beams - Experimental observation and conclusions
- Ultimate limit state design - Development of application rules
- Lifecycle assessment of slim-floor solutions - Example calculations and presentation of software tool
- Built examples and optimization by improved solutions

A number of experts attended the workshop giving valuable feedback to the work conducted within the project.

Several papers and presentations result from the work conducted within the scope of the project. A corresponding list can be found under Publications and in the Reference list. Also a number of bachelor and master thesis promoted the knowledge and application of slim-floor beams to the next generation.

8 SUMMARY & OUTLOOK

8.1 Summary & Conclusions

Slim-floor beams integrate steel profiles into concrete slabs to reduce the overall height of the floor structure in buildings. Characteristic for the load-bearing behaviour is a close interaction between the steel profile and concrete. The concrete slab itself contributes to the bending capacity. Precast or in-situ concrete deck, with or without metal decking are conceivable solutions.

“Slim-Floor Beams - Preparation of Application rules in view of improved safety, functionality and LCA (SlimAPP)” aimed to increase the competitiveness of steel in buildings by developing a holistic approach for slim-floor beams. All aspects of efficient design in view of sustainable constructions are considered. The approach especially took into account the composite shear connection between steel beam and concrete floor slab in normal conditions. The focus was on application rules for slim-floor solutions, which are currently not covered by Eurocode 4. The aim of the project was to achieve improved behaviour in view of safety (ULS), functionality (SLS) and lifecycle assessment.

Slim-floor constructions currently have spans of up to 11 m. Promising new types were developed using different strategies to activate additional load-bearing effects, speeding up the construction process and minimising the self-weight of the floor slab. Partial fixity between beam and columns reduces deflections and increases the natural frequency of slim-floor beams. By taking advantage of the described opportunities spans of up to 16 m are possible.

A compilation of authorities’, industries’ and designers’ needs highlights the advantages of slim-floor beams and give a broad view of possible applications. On these findings the partners defined different case studies, grouped into 3 cases in function of building type and span. These case studies represent commonly used floor layouts for slim-floor solutions guaranteeing practical applications of the research. Furthermore, these layouts were used for the lifecycle assessment analysis.

The load-bearing behaviour of slim-floor beams depends on the characteristics of the shear connectors. Therefore, push-out- and shear beam tests to investigate the shear connection, flexural beam tests and subsequent numerical analyses were carried out. Investigating the load-bearing behaviour of innovative concrete dowel shear connector systems with reinforcement bar going through a hole in the steel profile web, 30 push-out tests have been conducted. Within the tests the influence of concrete grade, reinforcement bar diameter and diameter of the hole in the web of the steel profile was determined. The investigated shear connectors are highly suitable for slim-floor beams due to its space saving design and the combined ductile and high load capacity. The load-bearing behaviour comprises concrete compression at the rounding of the steel-profile holes. The distribution of load in the concrete slab leads to bending of the reinforcement accompanied with activation of the surrounding concrete and bracing of developing concrete struts at the flanges of the steel profile.

The major influences including the diameter of the reinforcement combined with a sufficient concrete grade are contained in a developed analytical model to estimate the load capacity of the shear connector system.

Friction and clamping have – due to the integration of the steel profile – major effects on the load-bearing behaviour and cannot be neglected. Eight shear beam tests investigated these effects. Integrating the steel profile into the concrete slab leads to a remarkable degree of shear connection. Furthermore, clamping action is ensured by a sufficient concrete cover. Clamping action results from a force couple in transverse direction developed by the reinforcement mesh over the steel profile and the compression strut clamping the web of the steel profile. That effect increases significantly the shear capacity of the system. Furthermore, an enlarged size of the concrete filled hole provides significant shear resistance.

The shear connector capacity in slim-floor beams therefore benefits from friction and clamping, added to the pure shear connector capacity.

Flexural beam tests with differing degrees of shear connection and subsequent numerical analysis have been conducted. Furthermore, the type of shear connectors as well as the loading (concentric-eccentric) have been investigated determining its effect on the bending behaviour of slim-floor beams.

The degree of shear connection strongly influences the load-bearing behaviour of slim-floor constructions. Increasing degree of shear connection leads to increasing load capacities as well as increasing initial stiffness. The latter is decisive for slim-floor constructions, because their design is often driven by serviceability limit states. Low degrees of shear connection also lead to increasing end-slip in the interconnection joint. Therefore, increased requirements regarding the deformation capacity of shear connectors are needed. Comparable welded shear connectors – horizontally lying studs – provide more stiffness, leading to less deformation and higher capacities. So far rules for shear connectors concerning partial shear connection provided by Eurocode 4 imply not more than 6 mm deformation, limiting the usage of highly ductile types of shear connectors. Using a specific type of shear connector therefore requires understanding of the load deformation behaviour and its effect on the load-bearing of slim-floor beams.

Eccentric loading causes higher load capacities than concentric loading, confirming that the clamping effect influences the load-bearing behaviour of slim-floor beams.

Four long-term beam tests were conducted over a couple of months investigating the influence of shear connectors on the long-term load-bearing behaviour. Accompanying material tests quantified creep and shrinkage of the concrete. Tests on vibration determined the natural frequency of slim-floors, also after long-term loading.

Creep and shrinkage of the concrete slab lead to increasing deformation of the tested slim-floor beams. Therefore, these effects must be taken into account. The variation of frequency values due to long-term effects on the investigated beams of 6m was rather limited. So for this typical case, the natural frequency was sufficiently high, excluding any uncomfortable interference with pedestrian walking.

Based on the presented investigations and evaluations application rules for ultimate limit state have been developed. These rules consider the construction as well as the normal stage, edge and internal beams. Rules for moment resistance, resistance against combined bending and torsion, local transverse bending and transverse shear resistance have been proposed. Additionally rules for web openings in down-stand beams are presented.

According to the application rules, recommendations for EC4, design rules and guidelines for practice have been developed and comprised in a handbook. The handbook addresses connections design, ultimate limit state, serviceability limit state design, fire design and joint design.

Lifecycle Assessment analysis (LCA) confirms that slim-floor beams provide lower environmental impact on the Global Warming potential than equivalent concrete solutions. The developed pilot project layouts served for comparison. Four different slim-floor solutions and two concrete slabs were compared.

“Slim-Floor Beams - Preparation of Application rules in view of improved safety, functionality and LCA (SlimAPP)” successfully enlarged the understanding of slim-floor beams. The provided rules will support the development of the second generation of Eurocode 4. The recommendations and guidelines will help designers to construct slim-floor beams and understand the load-bearing behaviour more easily. In terms of sustainability slim-floor solutions contribute to a cleaner environment than similar concrete solutions.

8.2 Outlook

SlimAPP addresses the load-bearing behaviour of slim-floor constructions with focus on the shear connector behaviour.

The transverse shear capacity of slim-floor beams should also be investigated. The transverse shear capacity according to Eurocode 4 only takes into account the capacity of vertical steel sections, e.g.

steel profile webs. The transverse shear capacity of the concrete slab is being neglected. For composite beams of normal height this assumption is sufficient. However, as has been shown by some research [70] the concrete slab in slim-floor beams usually carries up to 70 % of the implied loading. Neglecting this loading capacity of the concrete slab does neglect existing reserves which may be interesting for slender steel profiles, high point load and in fire. Therefore, additional research is needed, developing design rules reproducing the transverse shear load capacity more realistically.

The mid-span deflection of slim-floor beams can be reduced by taking into account the continuity of slim-floor beams over two or more spans. The design of slim-floor beams is mainly driven by deformation under service beams with smaller construction height. Available rules should be investigated by further tests and prepared for application in the frame of Eurocode 4.

The current safety concept for composite beams just superimposes the partial factors of steel design and concrete design and is not based on an integrated reliability approach. Such an integrated approach can take into account that there are 2 materials which act together and where the weaknesses of each of the material can be balanced by the other. Individual composite beam parts are multiplied by a partial factor: concrete, constructional steel and shear connector. An appropriate concept including the individual characteristics of specific composite structures could be a huge effort, allowing a more appropriate and economic construction. The design of such a concept should be done in future research also in view of new recent concepts of overall reliability including also the loading site.

Composite beams and especially slim-floor beams are suitable for conversion. Re-usable shear connectors permit an easy separation of concrete slab and steel beam. Reconstruction the composite beam at another site is therefore easy to handle and of advantage for life cycle considerations. Similar approaches are conceivable for joints.

8.3 Acknowledgement

The authors thank the Research Fund for Coal and Steel for the financial support of the "Slim-Floor Beams - Preparation of Application rules in view of improved safety, functionality and LCA (SlimAPP)".

ABBREVIATIONS

AMBD	ArcelorMittal Belval and Differdange S.A.
AMECO	Software for LCA-Studies by AMBD
CoSFB	Composite Slim-floor Beam
GWP	Global warming potential
LCA	Life Cycle Assessment
LCC	Life Cycle Costing
LCP	Life Cycle Performance
LVDT	Linear variable differential transformer
PNA	Plastic Neutral Axis
POT	Push-out test
RC	Reinforced concrete
SBT	Shear beam test
SCI	Steel Construction Institute
SG	Strain Gauge
SF	Longterm test
SLS	Serviceability Limit State
UBRAD	University of Bradford
UDL	Uniform distributed load
ULS	Ultimate Limit State
USTUTT	University of Stuttgart
UTRENTO	University of Trento
WP	Work package

LIST OF FIGURES

Fig. 1-1: Prefabricated floor cassettes using C sections supported on the bottom plate	14
Fig. 1-2: Slab supported by UPN sections welded to the bottom plate	15
Fig. 1-3: Slab supported by profiled bottom plate	15
Fig. 1-4: Slab supported by angles welded to the bottom flange of HEB 450	16
Fig. 1-5: Hybrid slim-floor concept using a welded half cell	16
Fig. 1-6: Slim-floor beams in free-standing car park	21
Fig. 1-7: Slim-floor beams in below ground car park	21
Fig. 1-8: Slim-floor beams spanning along and across the building - medium spans.....	21
Fig. 1-9: Slim-floor beams spanning along and across the building - long spans.....	22
Fig. 2-1: Push-out tests - Test setup	24
Fig. 2-2: Extensometers	24
Fig. 2-3: Load-slip curves - One specimen of each series	25
Fig. 2-4: Influence of the rebar diameter on the load-bearing behaviour of the CoSFB dowels depending on concrete grade.....	25
Fig. 2-5: Push-out-test model-led in ABAQUS	26
Fig. 2-6: Verification of load-slip-curve	26
Fig. 2-7: Details of specimen SBT1b.....	27
Fig. 2-8: Details of specimen SBT2.....	27
Fig. 2-9: Relationship between load and mid-span deflection for shear beam specimens	28
Fig. 2-10: Test specimen in test-rig	29
Fig. 2-11: Shear cracks in concrete.....	29
Fig. 2-12: Relationship between load and top flange strain	30
Fig. 2-13: Relationship between load and bottom flange strain	30
Fig. 2-14: Relationship between load and concrete strain	31
Fig. 2-15: FE model and assembly of a typical tested specimen (SBT5)	32
Fig. 2-16: Comparison of end-slips obtained from FE prediction and test observation	33
Fig. 2-17: Comparing predicted concrete slab crack/damage pattern and composite beam end-slip <i>with those observed.</i>	33
Fig. 2-18: Comparison of shear beam with different web dowel hole-diameter (with rebar T16)...	35
Fig. 2-19: Comparison of shear beam with different web dowel hole-diameter (without rebar)	35
Fig. 2-20: Comparison of loading capacity of composite beam with different dowel hole-diameters at 30/60 mm mid-span deflection	35
Fig. 2-21: Load vs mid span deflection and end-slip of beam systems with different rebar diameters (the dowel hole-diameter 100mm).....	36
Fig. 2-22: Effect of rebar diameter on the load-bearing capacity (the dowel hole-diameter 100mm)	36
Fig. 2-23: Load-mid span deflection/end-slip curves of SBT5 with varying concrete strength.....	37
Fig. 2-24: Effect of concrete strength on the load capacity of different specimens at 30mm and 60mm mid-span deflection	37

Fig. 2-25: Shear beam tests – Load - Mid-span deflection	38
Fig. 2-26: Push-Out tests - Load-slip behaviour	38
Fig. 2-27: End-slip in shear beam tests	39
Fig. 2-28: Push-Out tests - Load-slip behaviour	39
Fig. 2-29: Discretization and distribution of membrane and bending state for a one span girder [64]	39
Fig. 2-30: M- κ -curve for positive bending [64]	39
Fig. 2-31: M- κ -curve for different elements according to their position [36]	40
Fig. 2-32: Recalculation of beam test 3 (BT 3) assuming rigid shear connection [36].....	40
Fig. 3-1: Typical beam cross-section.....	41
Fig. 3-2: Specimen BT3 at beginning of test: (a) Test-specimen in rig; (b) LVDT underneath to measure vertical deflection; (c) LVDT to measure end-slip	42
Fig. 3-3: Relationship between moment and mid-span deflection	43
Fig. 3-4: Cracking in concrete for specimen BT3.....	43
Fig. 3-5: Relationship between moment and end-slip.....	44
Fig. 3-6: Strains measured in top flange at loading point.....	45
Fig. 3-7: Strains measured in bottom plate at loading point.....	45
Fig. 3-8: Influence of degree of shear on (a) bending moment; (b) end-slip for slim-floor beams in flexure.....	46
Fig. 3-9: FE-model in SOFiSTiK of slim-floor beam test BT3 [7].....	47
Fig. 3-10: Spring-curves derived from push-out tests.....	48
Fig. 3-11: Validation of the load-mid-span deflection of Beam test 3 (BT3)	49
Fig. 3-12: BT3 – Load - end-slip.....	49
Fig. 3-13: Analysis of the load-bearing behaviour, test BT4	50
Fig. 3-14: Point A - Concrete uncracked, linear-elastic behaviour of the slim-floor	50
Fig. 3-15: Point B - Concrete started cracking.....	50
Fig. 3-16: Point C - Linear-elastic material behaviour of the steel section ($f_y < 420 \text{ N/mm}^2$)	50
Fig. 3-17: Point D, Transition of the steel section to the plastic range ($f_y > 420 \text{ N/mm}^2$).....	50
Fig. 3-18: Point D - Plastic load-bearing capacity of the steel section not completely reached....	51
Fig. 3-19: Longitudinal shear force in correspondence with the mid-span deflection	51
Fig. 4-1: Typical beam cross-section (measures in mm)	53
Fig. 4-2: Loading specimen SF2	54
Fig. 4-3: Loading specimen SF3	55
Fig. 4-4: The measurement set-up	55
Fig. 4-5: Preparation of a) concrete cylinders and of b) shrinkage specimens.....	55
Fig. 4-6: The creep test on concrete	56
Fig. 4-7: Mid-span deflection in time for specimen SF2.....	56
Fig. 4-8: End slippage in time.....	57
Fig. 4-9: Increase in time of the mid-span deflection due to time effects	57
Fig. 4-10: Effective width in time	57

Fig. 4-11: Creep and shrinkage strain in time.....	58
Fig. 4-12: Shrinkage strains in time.....	58
Fig. 4-13: The loading setup: a) Beams SF1, SF2 and SF4; b) Beam SF3	59
Fig. 4-14: The load-deflection curves	59
Fig. 4-15: End slippage in beam SF1	60
Fig. 4-16: First two flexural modes	60
Fig. 5-1: Framework for assessing the sustainability of construction works.....	63
Fig. 5-2: Information modules of a building lifecycle (EN 15978, 2011)	64
Fig. 5-3: AMECO3 interface: layout of the “Floors” window	65
Fig. 5-4: floor layout of 6 floor commercial / residential building	66
Fig. 5-5: Global warming potential of different variants (Case 1) regarding the different modules as given in Tab. 5-2.	68
Fig. 5-6: Floor layout of 6 floor commercial/residential building	68
Fig. 5-7: Global warming potential of different variants (Case 2) regarding the different modules as given in Tab. 5-4.	70
Fig. 5-8: floor layout below ground car park	70
Fig. 5-9: Global warming potential of different variants (Case 3) regarding the different modules as given in Fig. 5-2.	72
Fig. 5-10: Floor layout below ground car park	72
Fig. 5-11: Global warming potential of different variants (Case 4) regarding the different modules as given in Tab. 5-10.	74
Fig. 5-12: Build-up of floor and its finishes	75
Fig. 5-13: Terminal units and chilled beams located between the deck ribs	76
Fig. 5-14: Use of colour coated composite decking in car parks.....	76
Fig. 6-1: Design situations during the construction stage	80
Fig. 6-2: Concrete dowel resistance predicted using Eq. (6-9 against push-out test results of section 2.2 and those reported in [71]	84
Fig. 6-3: Stress blocks for calculation of moment resistance (PNA in lower part of web).....	85
Fig. 6-4: Stress blocks for calculation of moment resistance (PNA in bottom flange)	86
Fig. 6-5: Reduction factor β to the plastic resistance moment plotted against the depth of the plastic neutral axis x_{pl} relative to the total depth of the composite section h [15].	87
Fig. 6-6: Critical surfaces for longitudinal shear failure	87
Fig. 6-7: Model for buckling of web-post between closely spaced circular openings	93
Fig. 6-8: Internal forces and moments at the critical section around an opening	94
Fig. 7-1: Concrete dowel shear connectors system – Geometrical parameters	94
Fig. 7-2: Workshop-Flyer	97

LIST OF TABLES

Tab. 1-1: Typical slim-floor beam spans for three HEB sections with welded bottom plate	13
Tab. 1-2: Typical long span slim-floor beam spans and their span capabilities for offices.....	17
Tab. 2-1: Overview of the conducted push-out testing programme.....	24
Tab. 3-1: Differences mid-span deflection between test and FE-model, BT3 [kN, mm]	49
Tab. 4-1: Summary of the collapse loads	59
Tab. 4-2: Summary of the vibrational tests	60
Tab. 4-3: Summary of the vibrational tests	61
Tab. 5-1: Bill of material for commercial/residential building (case 1)	67
Tab. 5-2: Global Warming Potential of investigated solutions for commercial/residential building (case 1).....	67
Tab. 5-3: Comparative results of the LCA (Case 1).....	67
Tab. 5-4: Bill of material for commercial/residential building (case 2)	68
Tab. 5-5: LCA results (Global Warming Potential).....	69
Tab. 5-6: Comparative results of the LCA (Case 2).....	69
Tab. 5-7: Bill of material for commercial/residential building (case 2)	71
Tab. 5-8: LCA results (Global Warming Potential) for Case 3.....	71
Tab. 5-9: Comparative results of the LCA (Case 3).....	71
Tab. 5-10: Bill of material for below ground car park (case 4).....	73
Tab. 5-11: LCA results (Global Warming Potential) for Case 4.....	73
Tab. 5-12: Comparative results of the LCA (Case 4)	73
Tab. 5-13: Acoustic test results measured on the completed building	75
Tab. 6-1: Values of factors C_1 and C_3	82
Tab. 6-2: Effective transverse reinforcement.....	88
Tab. 6-3: Equivalent rectangular opening dimensions for verification of Vierendeel bending.....	92

LIST OF REFERENCES

Own references as outcome of the project

Deliverables

- [1] Tibolt, M.; Lawson, M.; Aggelopoulos, E.: "New developments in long span slim-floor and shear connector systems", "Scope for new application rules for steel and composite design", "Definition of innovative use of slim-floor systems, selected pilot project and case studies, calculation example.", Deliverable D1.1, D1.2, D1.3, ArcelorMittal Belval et Diverdange, Luxembourg, 2017
- [2] Kuhlmann, U.; Schorr, J.: Test report push-out tests, Deliverable D2.1a, University of Stuttgart, Germany, 2018
- [3] Lam, D.; Sheehan, T.; Dai, X.: Test report on shear beam tests, Deliverable D2.1b, University of Bradford, UK, 2018.
- [4] Schorr, J.; Kuhlmann, U.: Numerical investigations on push-out tests, Deliverable D2.2a, University of Stuttgart, UK, 2018
- [5] Dai, X.; Sheehan, T.; Lam, D.: Numerical investigations on slim-floor composite shear beams, Deliverable D2.2b, University of Bradford, UK, 2018
- [6] Aggelopoulos, E.; Schorr, J.; Sheehan, T.: Shear connection systems for composite action of slim floor beams, Deliverable D2.3, Steel Construction Institute, UK, 2018
- [7] Lam, D.; Sheehan, T.; Dai, X.: Test report including all detailed experimental data gathered during each beam test, University of Bradford, UK, 2018.
- [8] Schorr, J.: Numerical investigations on flexural beams, Deliverable D3.2, University of Stuttgart, Germany, 2018
- [9] Zandonini, R.; Baldassino, N.: Service deflection and vibration behaviour of slim-floor systems with innovative shear connections - Test report, Deliverable 4.1a & 4.1b, University of Trento, Italy, 2018.
- [10] Zandonini, R.; Baldassino, N.: Service behaviour of slim floor systems with innovative shear connections - Report on numerical methods, Deliverable D4.2, University of Trento, 2018
- [11] Zandonini, R.; Baldassino, N.: Analysis of vibration test results, Deliverable D4.3, University of Trento, 2018
- [12] Labory, F.; Tibolt, M.: Validation report of LCA methodology, Deliverable D5.1, ArcelorMittal Belval et Diverdange, Luxembourg, 2018
- [13] Labory, F.; Tibolt, M.: AMECO software adapted for slim floor solutions, Deliverable D5.2, ArcelorMittal Belval et Diverdange, Luxembourg, 2018
- [14] Labory, F.; Tibolt, M.: Case study report, ArcelorMittal Belval et Diverdange, Luxembourg, 2018
- [15] Aggelopoulos, E.; Lawson, R.M.; Couchman, G.H.: Design guidance for the ultimate limit state, Deliverable D6.1, Steel Construction Institute, UK, 2018
- [16] Zandonini, R.; Baldassino, N.: Design guidance for serviceability limit state, Deliverable D6.2, University of Trento, 2018
- [17] Lawson, R.M.; Aggelopoulos, E.: Special rules for web openings, Deliverable D6.3, Steel Construction Institute, UK, 2018
- [18] Kuhlmann, U.; Schorr, J.; Aggelopoulos, E.; Lam, D.; Sheehan, T.; Dai, X.; Zandonini, R.; Baldassino, N.; Tibolt, M.; Oly, R.; Design recommendation and guideline for practice - handbook, Deliverable D7.1 & D7.2, 2018
- [19] Tibolt, M.: Design Template, Deliverable D7.3, ArcelorMittal Belval et Diverdange, Luxembourg, 2018

Papers

- [20] Schorr, J.; Kuhlmann, U.; Hauf, G.: Slim-Floor Constructions - Deformation and Load Carrying Behaviour, In: 8th International Conference on Composite Construction in Steel and Concrete, Jackson Hole, Wyoming, USA, 30.07.2017-02.08.2017
- [21] Sheehan, T.; Lam, D.; Dai, X.: Experimental studies of composite slim-floor beams, In: 8th International Conference on Composite Construction in Steel and Concrete, Jackson Hole, Wyoming, USA, 30.07.2017-02.08.2017
- [22] Schorr, J.; Kuhlmann, U. : Slim-Floor Deckenkonstruktionen. In: Wolfgang Breit, Wolfgang Kurz, Matthias Pahn, Hamid Sadegh-Azar, Jürgen Schnell und Catherina Thiele (Hg.): Beiträge zur 5. DAfStb-Jahrestagung mit 58. Forschungskolloquium. 58. Forschungskolloquium. Kaiserslautern, Deutschland, 20.09.2017-21.09.2017, S. 259-270.
- [23] Lam, D., Sheehan, T. and Dai, X. (2018) Innovative flooring system for steel-concrete composite construction, Keynote paper for 13th International Conference on Steel, Space and Composite Structures, Perth, Australia, 31st Jan – 2nd February.
- [24] Schorr, J. : Push-Out Tests and Analysis on CoSFB Shear Connector, IABSE Young Engineers Colloquium Munich 2018, 2018
- [25] Kuhlmann, U. ; Eggert, F. ; Schorr, J. : Einfluss der Verdübelung auf das Tragverhalten von Verbundträgern unter Berücksichtigung unterschiedlicher Bauweisen, In: Festschrift Prof. Jörg Lange, 2018
- [26] Sheehan, T., Dai, X, Yang, J., Zhou, K and Lam D (2018) Flexural behaviour of composite slim floor beams. Proceedings of the 12th International Conference on Advances in Steel-Concrete Composite Structures, Valencia, Spain 27th – 29th June, pp 137-144.
- [27] Schorr, J. : Influence of shear-connector-behaviour on load-carrying of slim-floors beams, IABSE Future of Design Conference 2018, 19th of November 2018, London, UK
- [28] Sheehan, T., Dai, X, Yang, J., Zhou, K and Lam D.: (2018) Flexural behaviour of composite slim floor beams. Extended paper, submitted to Structures. Under review
- [29] Baldassino, N.; Roverso, G.; Ranzi, G.; Zandonini, R.: Service and Ultimate Behaviour of Slim Floor Beams: An Experimental Study, Structures, Volume 17, February 2019, Pages 74-86
- [30] Kuhlmann, U. ; Lam, D. ; Zandonini, R. ; Aggelopoulos, E. ; Tibolt, M. ; Sheehan, T. ; Baldassino, N. ; Labory, F. , Schorr, J. ; Anwendungsregeln für Slim-Floor-Träger unter Berücksichtigung von Sicherheit, Funktionalität und Nachhaltigkeit, Stahlbau - Special Issue: Slim-Floor, 2019
- [31] Kuhlmann, U.; Lam, D.; Zandonini, R.; Sheehan, T.; Baldassino, N.; Schorr, J. Experimentelle Untersuchungen an Slim-Floor-Trägern, Stahlbau - Special Issue: Slim-Floor, 2019
- [32] Schorr, J. ; Kuhlmann, U. : Design of slim-floors and their connections between steel and concrete, The 14th Nordic Steel Construction Conference, September 18-20, 2019, Copenhagen, Denmark
- [33] Dai, X., Lam, D., Sheehan, T., Yang, J. and Zhou, K. (2019) Numerical modelling analysis and parametric study of slim-floor composite shear beams (in progress)
- [34] Sheehan, T., Dai, X., Yang, J., Zhou, K. and Lam, D. (2019) Shear behaviour of slim floor composite beams (in progress)

Master- and Bachelortheses

- [35] W. Knecht, Development of a numerical model for the representation of the load capacity of slim-floor beams, Stuttgart: University of Stuttgart, Institute of Structural Design, 2019.
- [36] F. Rinke, Recalculation of slim-floor-girders with the model of the M-kappa-curve taking partial interaction into account, Stuttgart: University of Stuttgart, Institute of Structural Design, 2019.
- [37] Sigler, Sebastian: Advancement of an FE-Model for Push-out tests of CoSFB slim-floor beams and investigations on the shear connection behaviour, as well as subsequent parameter studies, Master-Thesis, Institute of Structural Design, University of Stuttgart, No. 2017-1X, 2017
- [38] Fritsch, Daniel: Development of an Excel-Tool for Slim-Floor-constructions and subsequent parametrical studies, Bachelor-Thesis, Institute of Structural Design, University of Stuttgart, No. 2018-11X, 2018

- [39] Guhl, Felix: Comparative calculation and limit analysis of slim-floor-constructions with and without composite action, Bachelor-Thesis, Institute of Structural Design, University of Stuttgart, 2019

Standards

- [40] EN 1994-1-1, *Eurocode 4: Design of composite steel and concrete structures - Part 1-1: General rules and rules for buildings*, CEN - European Committee for Standardization, 2010.
- [41] EN 1994-1-2, *Eurocode 4: Design of composite steel and concrete structures - Part 1-2: General rules - Structural fire design*, CEN - European Committee for Standardization, 2010.
- [42] EN 1993-1-1, *Eurocode 3: Design of steel structures - Part 1-1: General rules and rules for buildings*, European Committee for Standardization (CEN), 2005.
- [43] EN 12390-3, *Testing hardened concrete - Part 3: Compressive strength of test specimens*, European Committee for Standardization (CEN), 2009.
- [44] EN 12390-6, *Testing hardened concrete - Part 6: Tensile splitting strength of test specimens*, European Committee for Standardization (CEN), 2009.
- [45] EN 12390-13, *Testing hardened concrete - Part 13: Determination of secant modulus of elasticity in compression*, European Committee for Standardization (CEN), 2013.
- [46] EN ISO 6892-1, *Metallic materials - Tensile testing - Part 1: Method of test at room temperature (ISO 6892-1:2016)*; EN ISO 6892-1:2016, ISO - International Organization for Standardization, 2016.
- [47] ASTM C512/C512M-15, *Standard Test Method for Creep of Concrete in Compression*, West Conshohocken, PA: ASTM International, 2015.
- [48] EN 1992-1-1, *Eurocode 2: Design of concrete structures - Part 1-1: General rules and rules for buildings; German version EN 1992-1-1:2004 + AC:2010*, CEN - European Committee for Standardization, 2010.
- [49] EN 15643-2: *Sustainability of construction works - Assessment of buildings - Part 2: Framework for the assessment of environmental performance*, CEN - European Committee for Standardization, 2011.
- [50] EN 15978: *Sustainability of construction works - Assessment of environmental performance of building - Calculation methods*, CEN - European Committee for Standardization, 2011.
- [51] EN 15804: *Sustainability of construction works - Environmental product declarations - Core rule for the product category of construction products*, CEN - European Committee for Standardization, 2012.
- [52] EN 15942: *Sustainability of construction works - Environmental product declarations - Communication format business-to-business*, CEN - European Committee for Standardization, 2012.
- [53] TR 15941, *Sustainability of construction works - Environmental product declarations - Methodology for selection and use of generic data*; CEN/TR 15941:2010, CEN - European Committee for Standardization, 2010.
- [54] EN 15643-3: *Sustainability of construction works - Assessment of buildings - Part 3: Framework for the assessment of social performance*, CEN - European Committee for Standardization, 2012.
- [55] EN 15643-4: *Sustainability of construction works - Assessment of buildings - Part 4: Framework for the assessment of economic performance*, CEN - European Committee for Standardization, 2012.
- [56] EN 1991-1-1, *Eurocode 1: Actions on structures - Part 1-1: General actions - Densities, self-weight, imposed loads for buildings*; European Committee for Standardization (CEN), 2002.
- [57] EN 1991-1-6, *Eurocode 1: Actions on structures - Part 1-6: General actions, Actions during execution*, European Committee for Standardization (CEN), 2005.

- [58] EN 1993-1-3, *Eurocode 3: Design of steel structures - Part 1-3: General rules - Supplementary rules for cold-formed members and sheeting*, European Committee for Standardization (CEN), 2006.
- [59] EN 1993-6, *Eurocode 3: Design of steel structures - Part 6: Crane supporting structures; German version EN 1993-6:2007 + AC:2009*, European Committee for Standardization (CEN), 2010.
- [60] EN 1990: Eurocode: Basis of structural design, European Committee for Standardization (CEN), 2005
- [61] EN ISO 140-4: Acoustics - Measurement of sound insulation in buildings and of building elements - Part 4: Field measurement of airborne sound insulation between rooms (ISO 140-4:1998), European Committee for Standardization (CEN), 1998
- [62] EN ISO 140-7: Acoustics - Measurement of sound insulation in buildings and of building elements - Part 7: Field measurements of impact sound insulation of floors (ISO 140-7:1998), European Committee for Standardization (CEN), 1998

Further References

- [63] DIBt Z-26.4-59: Allgemeine bauaufsichtliche Zulassung - ArcelorMittal Belval & Differdange S.A., CoSFB-Betondübel, Berlin, 2014.
- [64] G. Hauf, Trag- und Verformungsverhalten von Slim-Floor-Trägern unter Biegebeanspruchungen, Dissertation, Stuttgart: University of Stuttgart, Mitteilung des Instituts für Konstruktion und Entwurf No. 2010-2, 2010.
- [65] ABAQUS 6.13-5 Handbook, SIMULIA, 2013.
- [66] SOFISTIK, Software Version 2016-5, SOFISTIK-AG, 2016.
- [67] P. Lade, "Failure Criterion for Frictional Materials," in *Mechanics of Engineering Materials*, New York, Wiley, 1984, pp. 385-402.
- [68] J.-F. Demonceau, O. Vassart, K. Jarmai, P. García, L. Cascini, M. Netušil, V. Ungreanu, M. Piasecki, M. Founti, P. Elguezabal, P. Može, I. Talvik, B. Åstedt, P.-O. Martin, J.-P. d. Hollander, V. Huet and Ger, "Large valorisation on sustainability of steel structures (LVS3)," Directorate-General for Research and Innovation (European Commission), Brussels, Belgium, 2016.
- [69] ArcelorMittal, *AMECO v.3.00 User Manual*.
- [70] Kuhlmann, U.; Hauf, G.: Querkrafttragfähigkeit von Slim-Floor Trägern, DASt/AiF-Research project No. 15639 N, Institute of Structural Design, University of Stuttgart, No. 2010-59X, 2010.
- [71] Braun, M.: Investigation of the load-bearing behaviour of CoSFB-Dowels, Phd-thesis, University of Luxembourg, 2018
- [72] CEN/TC 250/SC 4: Scope and Definitions from Project team SC4.T5 for "Development of rules covering shallow floor construction, and other flooring types using precast concrete", N 1885, European Committee for Standardization (CEN), 2018
- [73] Mullet, D.L.: Slim floor design and construction (P110), The Steel Construction Institute, 1992
- [74] Schäfer, M.: Limits of plastic design for composite beams – Requirements for slim and compact composite sections, EUROSTEEL 2017, September 13-15, 2017, Copenhagen, Denmark
- [75] Chuter, R.; Vassart, O.; Gilbert, J.; Feldmann, M.; Chica, J.; Ogden, R.; Nieminen, J.: Building in active thermal mass into steel structures (BATIMASS), Directorate-General for Research and Innovation (European Commission), Brussels, Belgium, 2016.
- [76] Johnson, R.P.; May, I.M. (1975) *Partial-interaction design of composite beams*, The Structural Engineer 53 (No. 8), pp. 305-311

European Commission
Research Programme of the Research Fund for Coal and Steel
Technical Group: TGS 8

Slim-Floor Beams - Preparation of Application rules in view of improved safety, functionality and LCA

SlimAPP

University of Stuttgart
Pfaffenwaldring 7, 70569 Stuttgart, Germany
The Steel Construction Institute
Silwood Park, Ascot, Berks, SL5 7QN, United Kingdom
ArcelorMittal Belval and Differdange S.A.
L-4008 Esch-Belval and L-4503 Differdange, Luxembourg
University of Bradford
Richmond Road, BD7 1DP Bradford, United Kingdom
University of Trento
Via Calepina 14, 38122 Trento, Italy
LINDAB SA
Route d Ettelbruck, 9230, Diekirch, Luxembourg

RFSR-CT-2015-00020
1st July 2015 - 30th June 2018

Final Technical report

Getting in touch with the EU

In person

All over the European Union there are hundreds of Europe Direct information centres. You can find the address of the centre nearest you at:
https://europa.eu/european-union/contact_en

On the phone or by email

Europe Direct is a service that answers your questions about the European Union. You can contact this service:

- by freephone: 00 800 6 7 8 9 10 11 (certain operators may charge for these calls),
- at the following standard number: +32 22999696 or
- by email via: https://europa.eu/european-union/contact_en

Finding information about the EU

Online

Information about the European Union in all the official languages of the EU is available on the Europa website at: https://europa.eu/european-union/index_en

EU publications

You can download or order free and priced EU publications at: <https://publications.europa.eu/en/publications>. Multiple copies of free publications may be obtained by contacting Europe Direct or your local information centre (see https://europa.eu/european-union/contact_en).

EU law and related documents

For access to legal information from the EU, including all EU law since 1951 in all the official language versions, go to EUR-Lex at: <https://eur-lex.europa.eu>

Open data from the EU

The EU Open Data Portal (<https://data.europa.eu/euodp/en/home>) provides access to datasets from the EU. Data can be downloaded and reused for free, for both commercial and non-commercial purposes.

This is the final technical report of the RFCS-project SlimAPP describing the activities carried out under contract RFSR CT 2015-00020 during the period July 1st 2015 to June 30th 2018.

The aim of this project was to increase the competitiveness of steel in buildings by developing a holistic approach for slim-floor systems, considering all aspects of efficient design (in view of sustainable construction). The shear connection between the steel beam and the concrete floor slab in normal conditions is taken into account explicitly. In particular the focus is on the application rules for slim-floor solutions that are not currently covered by Eurocode 4 [40] in order to achieve improved behaviour in view of safety (ULS), functionality (SLS) and Lifecycle assessment.

The practical application of the research is demonstrated by defining typical pilot projects which are used as benchmark cases throughout the project.

A holistic testing program was conducted providing further insight into the load-bearing behaviour of slim-floor systems. Tests focused on shear connector behaviour, effect of shear connector performance on the load-bearing behavior of beams and the influence of partial shear connection. Furthermore, the effect of long-term service loads was investigated in terms of deflections, vibrations and long-term behaviour.

Evaluation according to LCA calculation methods considering the environmental impacts of the products and technology, including raw material, production, use and final disposal but also the transport and energy efficiency was realized for benchmark examples. Newly improved software tools allowed to compare different solutions in view of costs as well as the lifecycle assessment.

Recommendations and guidelines for efficient slim-floor beam design were developed giving sufficient background information for practical engineers but also for a possible transfer of rules into Eurocode 4. Design templates and examples provide further information and guidance for experts for the improved use of slim-floor beams in buildings.

